# Scalable electrocatalyzed formation of C–O bonds using flow reactor technology

Michael Prieschl,[a] David Cantillo,[a,b] C. Oliver Kappe,[a,c] Gabriele Laudadio[a,c]*

[a] Institute of Chemistry, University of Graz, NAWI Graz, Heinrichstrasse 28, 8010 Graz, Austria.

[b] School of Chemistry and Molecular Biosciences, The University of Queensland, Brisbane, Queensland 4072, Australia.

[c] Center for Continuous Flow Synthesis and Processing (CCFLOW), Research Center Pharmaceutical Engineering GmbH (RCPE), Inffeldgasse 13, 8010 Graz, Austria.

Correspondence to *gabriele.laudadio@uni-graz.at

# Supplementary Information

# Table of contents

# 1. General Experimental Information

For preparative and automated experiments, all reactions were carried out under an inert argon atmosphere with dry solvents under anhydrous conditions unless stated otherwise. Solvents and reagents were purchased of the highest commercial quality and used without further purification, unless stated otherwise.

**$^{1}$H- and $^{13}$C NMR** spectra were recorded on a Bruker Avance III 300 MHz instrument at ambient temperature, in $CDCl_3$ or DMSO-$d_6$ as solvent, at 300 MHz and 75 MHz, respectively. Chemical shifts (δ) are reported in ppm using TMS as internal standard. Coupling constants are given in Hz units. The letters s, d, t, q, and m are used to indicate singlet, doublet, triplet, quadruplet, and multiplet, respectively.

**HPLC Analysis**

| Shimadzu LC20 **HPLC** | | |
|---|---|---|
| C-18 column (150 mm x 4.6 mm / particle size 5 µm) | | |
| 37 °C | | |
| A: $H_2O$:MeCN 90:10 (v/v) + 0.1 % $CF_3COOH$ | | |
| B: MeCN + 0.1 % $CF_3COOH$ | | |
| 1.5 mL/min | | |
| Gradient program for mobile phase B in A (% v/v) | | |
| | time line | Increase of mobile phase B |
| HPLC method 2 | 0 > 3 min | 3 > 5 % B |
| | 3 > 7 min | 5 > 30 % B |
| | 7 > 10 min | 30 > 100 % B |
| | 10 > 12 min | 100 % B |
| | 12 > 12.5 min | 100 > 3 % B |
| | 12.5 > 15 min | 3 % B |

**LC-MS** analysis was carried out on a Shimadzu instrument using a C18 reversed-phase (RP) analytical column (150 mm × 4.6 mm, particle size 5 µm using mobile phases A ($H_2O$/MeCN 90:10 (v/v) + 0.1% HCOOH) and B (MeCN + 0.1 % HCOOH) at a flow rate of 0.6 mL/min. The following gradient was applied: hold at 5% solvent B until 2 min, increase to 20% solvent B until 8 min, increase to 100% solvent B until 16 min and hold until 22 min at 100% solvent B. Low resolution mass spectra were obtained on a Shimadzu LCMS-QP2020 instrument using electrospray ionization (ESI) in positive or negative mode.
Chromatographic purifications were done using a Biotage Isolera One system with Biotage Sfaer columns. All reagents and solvents were used as purchased without further purification. Solid reagents were stored in a desiccator over $CaCl_2$.

**High resolution mass spectrometry** (**HRMS**) was carried out with an Agilent 6230 TOF mass spectrometer, after injection on an Agilent 1260 Infinity Series HPLC system. The injection volume was set to 0.5 µL and the flow rate to 0.3 mL/min of a mixture of 40% $H_2O$ (0.1% 5 M ammonium formate) and 60% MeCN/$H_2O$ (5:1+0.1% 5 M ammonium formate). The HRMS module comprises an electrospray ionization source (Dual AJS ESI) and uses nitrogen as the nebulizer (15 psig) and the drying gas (5 L/min). ESI experiments were performed using the positive ionization mode (Gas Temp. = 300 °C, Fragmentor = 150 V, Skimmer = 65 V, OCT 1 RF Vpp = 750 V,Vcap = 1400, Nozzle Voltage = 2000 V, Reference Masses = 121.050873 and 922.009798, Acquisition = 100-1100 m/z, 1 spectra/s).

**Electrolysis cells:**

*1. Batch Synthesis*

Batch reactions were carried out in 5 mL vials (IKA Electrasyn 2.0). The electrodes were purchased from IKA and pretreated via ultrasonication in acetone/pentane and then dried in the over at 100°C. Geometry and electrode distance are according to the manufacturer. For supply of electricity either the commercial Electrasyn 2.0 (IKA) or a commercial power supply (BK Precision BK1739) was used. All reactions were conducted at room temperature under constant conditions.

*2. Parallel Plate Flow Reactor*

Flow electrolysis was performed in a homemade parallel-plate reactor. As shown in Figure S1 the cell has 4 fluidic inlets ($A_1$-$A_4$) that are compatible with standard fluidic fittings. There are also two connectors to attach electrical connections (B). Graphite plates with holes for fluidic in- and outlets were used as current collectors (C). Carbon Felt electrodes (CeTech GFC020) with a 2D surface area of (7.85 $cm^2$) were used as cathode and anode (D). PTFE gaskets were used to hold the electrodes in place (E). The two electrodes were electrically insulated from each other using 4 sheets of PTFE mesh. Since the separators were permeable to solvent, the cell is undivided and the reaction mixture is in contact to both the electrodes.

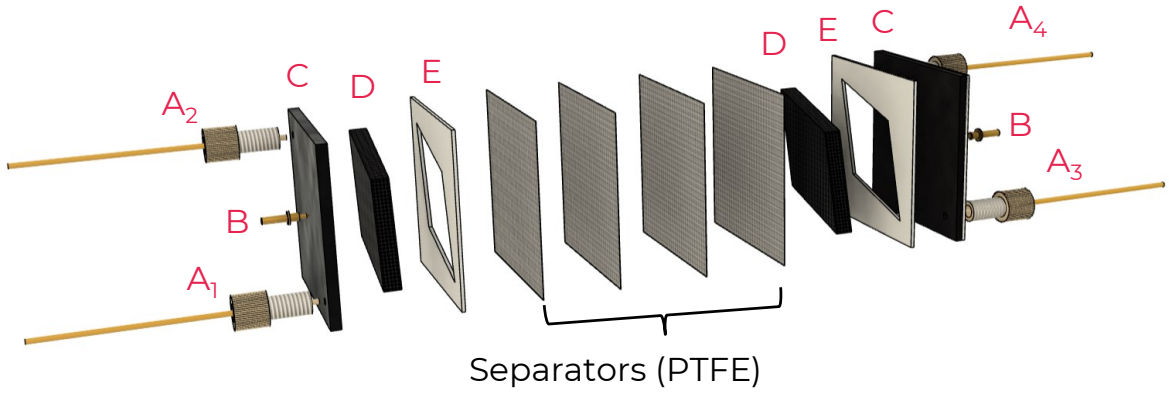


**Figure S1:** $A_{1\text{-}4}$: Fluidic inlets, B: pogo pins for current collection, C: Graphite current collectors, D: Carbon Felt electrodes, E: PTFE gaskets to keep electrodes in place.

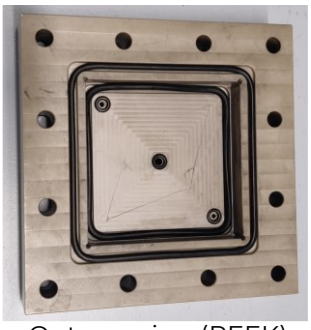
Outer casing (PEEK) with O-rings (FKM)

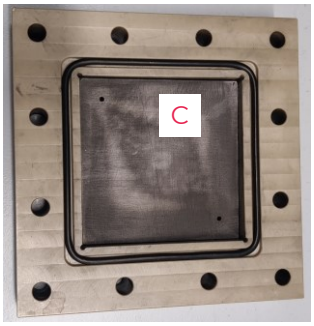

Current Collector **C**

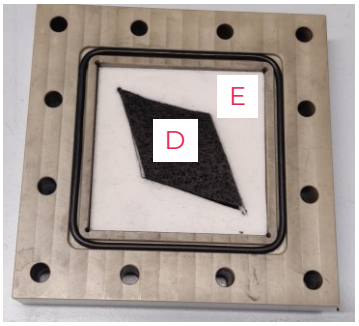

C-Felt electrode (**D**) & PTFE casing (**E**)

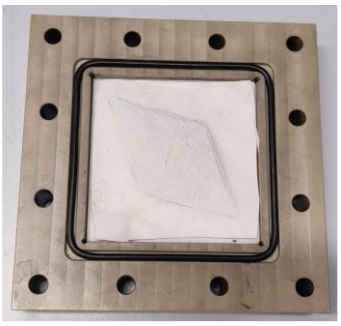
Separator (PTFE)

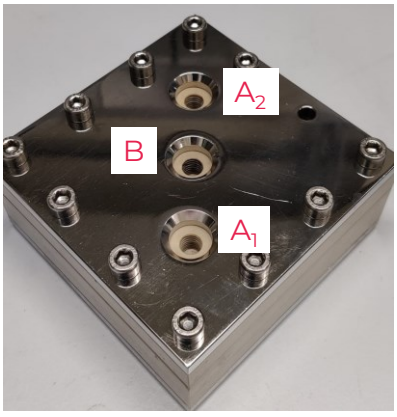


**Figure S2:** Top: Reactor assembly. Bottom: Assembled plate reactor with fluidic inlets $A_{1\text{-}2}$ and inlet B for current connection.

# 2. Experimental Procedures

## 2.1 Synthesis of $Ni(dtbbpy)_3Cl_2$

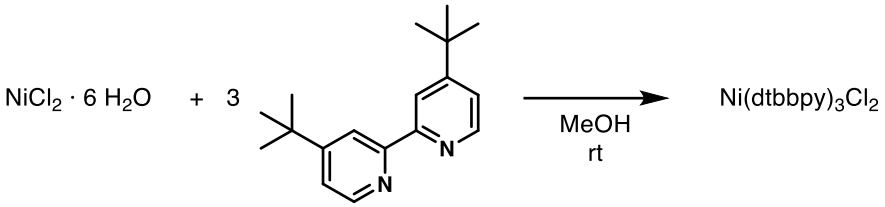


The synthesis of the catalyst was performed according to literature.[1]
4.03 g of 4,4'-di-tert-butyl-2-2'-bipyridine was placed into a 50 mL round-bottom flask. The solid was suspended in 10 mL methanol. 1.19 g $NiCl_2 \cdot 6\ H_2O$ were added. The color of the mixture changed from a white suspension to a deep red solution. After 15 minutes all solids were dissolved, and the reaction was considered finished. Solvent was evaporated under vacuum. The mixture was washed 3x with ~20 mL acetone and again concentrated under vacuum. After drying under vacuum at 40 °C, the product was isolated as a pale pink solid in quantitative yield (4.7 g).

## 2.2 General Batch Procedure

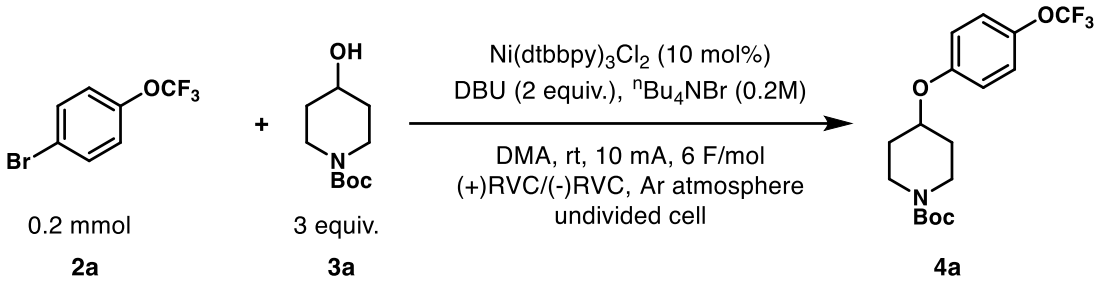


To an oven dried 5 mL ElectraSyn 2.0 vial (IKA), $Ni(dtbbpy)_3Cl_2$ (18.7 mg, 0.02 mmol, 0.1 equiv.), *N*-boc-4-hydroxypiperidine **3a** (120.8 mg, 0.6 mmol, 3.0 equiv.) and tetrabutylammonium bromide (TBAB, 193.4 mg, 0.06 mmol, 3.0 equiv.) were added directly and dissolved in 3 mL of dry *N,N*-dimethylacetamide (DMA). 1-bromo-4-(trifluoromethoxy)benzene **4a** (29.8 µL, 0.2 mmol, 1 equiv.) and 1,8-Diazabicyclo[5.4.0]undec-7-en (DBU, 59.7 µL, 0.4 mmol, 2 equiv.) were added. The reaction vessel was closed, and an argon balloon was attached to keep the reaction mixture under inert atmosphere. Before applying current the reaction mixture was stirred for 30 minutes. 10 mA of constant current were applied using a power supply (ElectraSyn 2.0 or BK Precision BK1739). Reactions were usually stopped after 6 F/mol (3h 13 min). The reaction mixture was analyzed using HPLC assay using biphenyl as standard.

Further electrochemical parameters:
Reactions were performed with an electrode area of 1.5 $cm^2$ in contact with reaction solution. This corresponded to a current density of 6.66 mA $cm^{-2}$ for a current of 10 mA.

## 2.3 General Flow Procedure

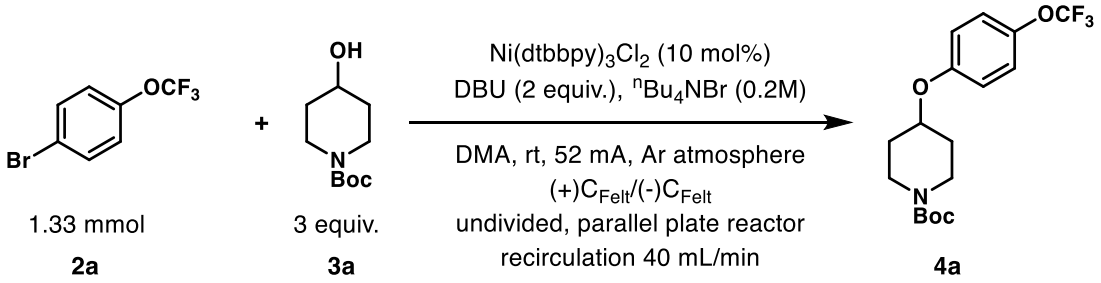


$Ni(dtbbpy)_3Cl_2$ (124.3 mg, 0.133 mmol, 0.1 equiv.), *N*-boc-4-hydroxypiperidine **3a (**804.9 mg, 4 mmol, 3 equiv.) and TBAB (1.29 g, 4 mmol, 3 equiv.) were added to a 20 mL volumetric flask. Dry DMA (10 mL) was added to dissolve the solid components. 1-bromo-4-(trifluoromethoxy)benzene **2a** (198.3 µL, 1.33 mmol, 1 equiv.) and DBU (398 µL, 2.67 mmol, 2 equiv.) were added. The volumetric flask was brought up to volume with dry DMA. The flask was closed with a rubber septum. Argon was bubbled through the mixture continuously using an argon line. Before starting recirculation and applying current the mixture was stirred for 30 min. The mixture was recirculated at 40 mL/min using a peristaltic pump (Masterflex L/S, easy load II pump head). 52 mA of constant current were applied using a power supply (BK precision BK1739). Samples were analyzed using a HPLC assay using biphenyl as standard.

*Workup (column chromatography):*
The reaction mixture was diluted with $H_2O$ (200 mL) and then extracted 3x with isopropyl acetate (*i*PrOAc, 100 mL). The combined organic phases were washed 3x with HCl (1M aq., 100 mL) and 1x with brine (100 mL). The organic phase was dried over $Na_2SO_4$ and purified by column chromatography (petrol ether/ethyl acetate).

Standard configuration of the flow cell:
Flow from $A_1$ to $A_4$ diagonally through the cell from bottom to top. Two CeTech GF020 carbon felt electrodes with an electrode area (2D) of 7.85 $cm^2$ were used. Operation under constant current with 52 mA leads to a current density of 6.62 $mA \cdot cm^{-2}$. This current density was chosen to be as close as possible to the current density in batch (6.66 mA $cm^{-2}$)

## 2.4 Scale-up Flow Procedure

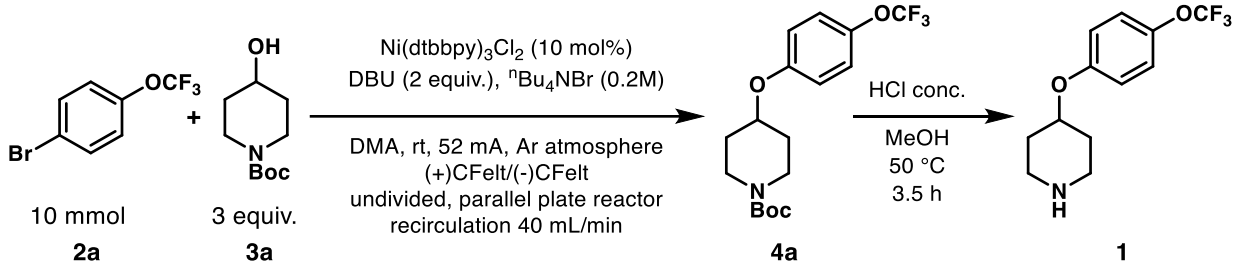


$Ni(dtbbpy)_3Cl_2$ (934.7 mg, 1.0 mmol, 0.1 equiv.), *N*-boc-4-hydroxypiperidine **3a** (6.04 g, 30 mmol, 3 equiv.) and TBAB (9.67 g, 30 mmol, 3 equiv.) were added to a 100 mL volumetric flask. Dry DMA (50 mL) was added to dissolve the solid components. 1-bromo-4-(trifluoromethoxy)benzene **2a** (1.49 mL, 10 mmol, 1 equiv.) and DBU (2.99 mL, 20 mmol, 2 equiv.) were added. The volumetric flask was brought up to volume with dry DMA. The flask was closed with a rubber septum. Argon was bubbled through the mixture continuously using an argon line. Before starting recirculation and applying current the mixture was stirred for 30 min. The mixture was recirculated at 40 mL/min using a peristaltic pump (Masterflex L/S, easy load II pump head). 52 mA of constant current were applied using a power supply (BK precision BK1739). Samples were analyzed using a HPLC assay using biphenyl as standard. The reaction was stopped when full conversion of **2a** was reached after 18 h (3.5 F/mol)

*Workup:*
The reaction mixture was diluted with $H_2O$ (500 mL) and then extracted 3x with isopropyl acetate (*i*PrOAc, 250 mL). The combined organic phases were washed 3x with HCl (1M aq., 500 mL) and 1x with brine (500 mL). The organic phase was reduced to dryness. MeOH (50 mL) and of HCl (conc., 5 mL) were added. The mixture was heated to 50 °C for 3.5 h until full conversion of **4a** to **1** was achieved.

After complete deprotection $H_2O$ (500 mL) was added. The mixture was 3x extracted with isopropyl acetate (250 mL). The aqueous phase was basified with NaOH until pH 9-10 was reached. The aqueous phase was subsequently extracted 2x with iPrOAc (250 mL). The resulting organic phases were combined and dried over $Na_2SO_4$. The product was isolated after evaporation of solvents. 1.754g of product were obtained as an off-white to yellow solid (63% yield considering 95% purity).

# 3. Batch Optimization

## 3.1 Preliminary Experiments

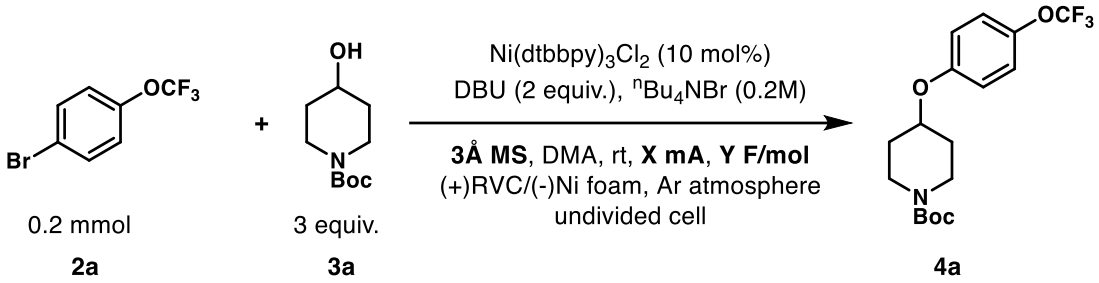


**Table S1:** Results of the first round of batch optimization reactions.

| Entry | Charge (F/mol) | Current (mA) | Pre-stirring (min) | Molecular-Sieves (mg) | **2a** (%)[a] | **4a** (%)[a] |
|---|---|---|---|---|---|---|
| 0[b] | 0 | 0 | 0 | - | >99 | <1 |
| 1 | 6 | 4 | 10 | 300 | <1 | 48 |
| 2 | 6 | 10 | - | 300 | <1 | 32 |
| 3 | 6 | 10 | 10 | 300 | 11 | 49 |
| 4 | 6 | 10 | 10 | - | <1 | 50 |
| 5 | 6 | 10 | 30 | - | <1 | 55 |
| 6 | 6 | 10 | 60 | - | <1 | 38 |
| 7 | 6 | 20 | 30 | - | <1 | 8 |
| 8a | 2 | 10 | 30 | - | 56 | 5 |
| 8b | 4 | 10 | 30 | - | 21 | 32 |
| 8c | 6 | 10 | 30 | - | <1 | 50 |
| 9[c] | 6 | 10 | 30 | - | 22 | 27 |

[a] Determined using calibrated HPLC analysis against biphenyl as standard. [b] Control reaction without any current. Stirred for 3 h at room temperature. [c] DBU added to reaction mixture by syringe after pre-stirring period.

First optimization results showed that current could be increased to 10 mA (decreased yield at higher values), molecular sieves were not needed, and 30 min pre-stirring was the optimal time. Full conversion was reached after 6 F/mol. Control reactions showed that no reaction occurs without current (entry 0) and that DBU was necessary during pre-stirring (entry 9).

**Pictures of Pre-stirring**

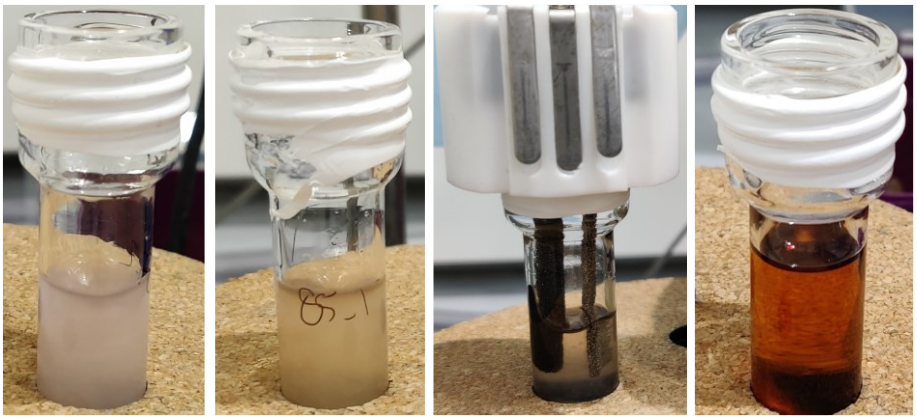


**Figure S3:** Pictures of the reaction mixture at different stages of the reaction.

## 3.2 HPLC Traces

### Blank reaction

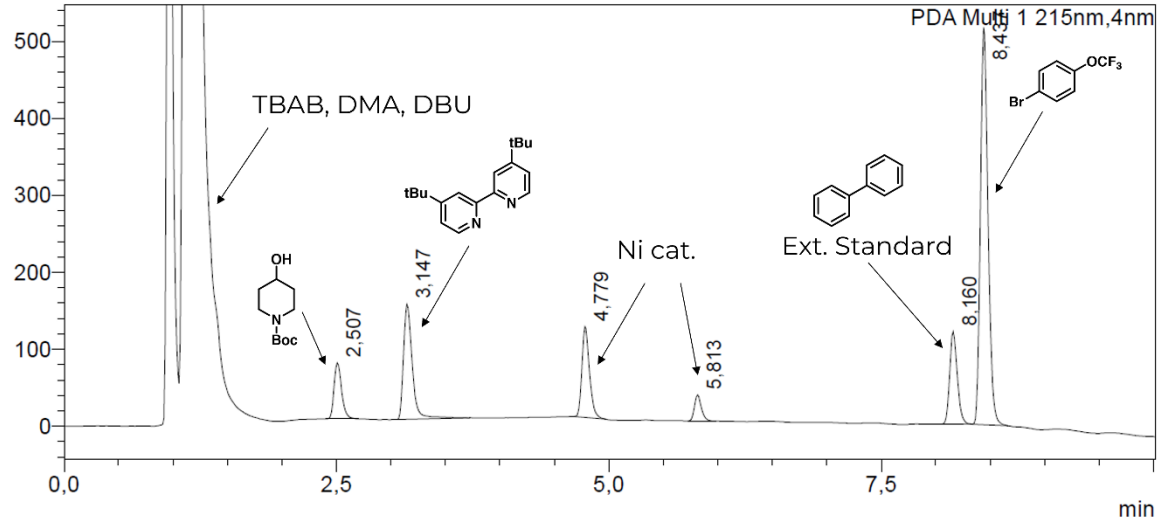


**Figure S4:** HPLC trace of a reaction mixture before any current was applied.

Without any current passed, no reaction occurred, full recovery of substrates.

### HPLC trace of reaction after 6F/mol

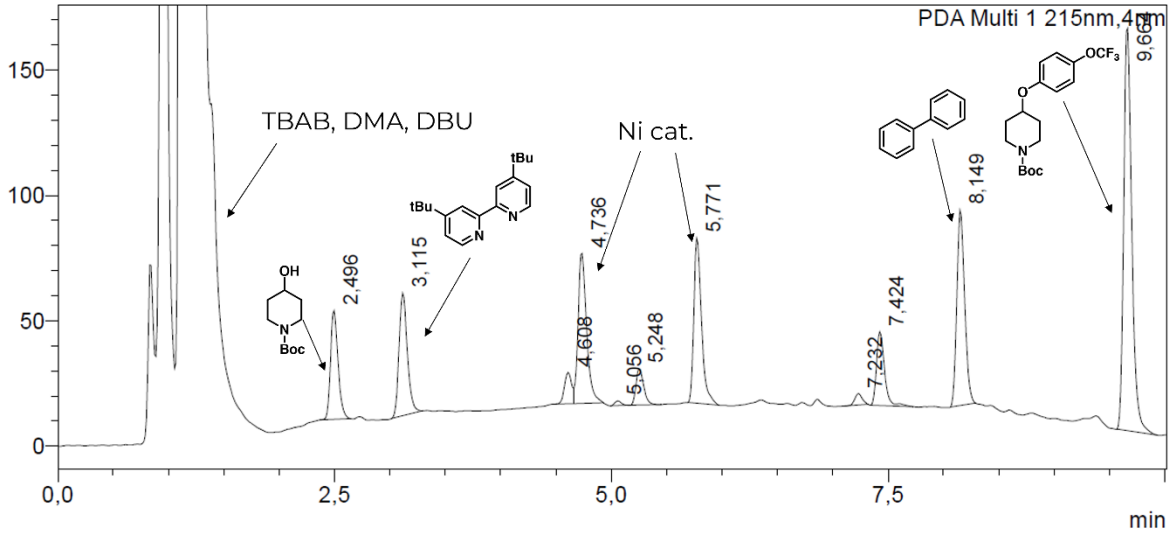


**Figure S5:** HPLC trace of a reaction mixture after 6F/mol.

Using GC-MS (after addition of $H_2O$, extraction with $Et_2O$ and drying over $Na_2SO_4$) some side products were identified:

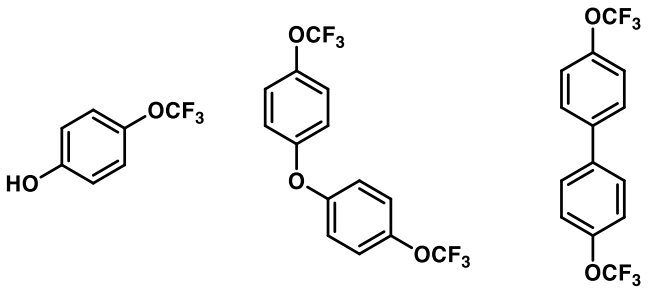

m/z = 178 m/z = 338 m/z = 322

## 3.3 Electrode Optimization

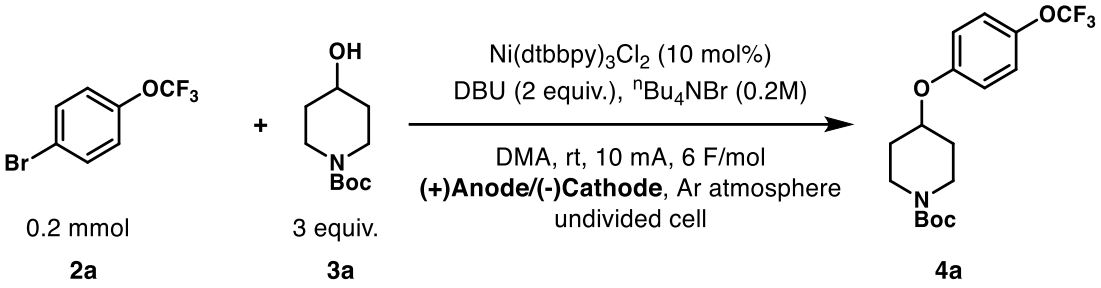


**Table S2:** Results of electrode optimization.

| Entry | Cathode | Anode | **2a** (%)[a] | **4a** (%)[a] |
|---|---|---|---|---|
| 1 | Ni Foam | RVC | <1 | 50 |
| 2 | Stainless Steel | Graphite | <1 | <1 |
| 3 | Nickel | RVC | <1 | <1 |
| 4 | Ni Foam | Graphite | 24 | 16 |
| 5 | Ni Foam | Glassy C | <1 | 24 |
| 6 | Ni Foam | C-Felt CeTech GF020 | 40 | 9 |
| 7 | Ni Foam | C-Felt AvCarb G280A | 24 | 27 |
| 8 | Ni Foam | C-Felt CeTech CF120 | 23 | 20 |
| 9 | Ni Foam | Impervious Graphite | 24 | 6 |

[a] Determined using calibrated HPLC analysis against biphenyl as standard.

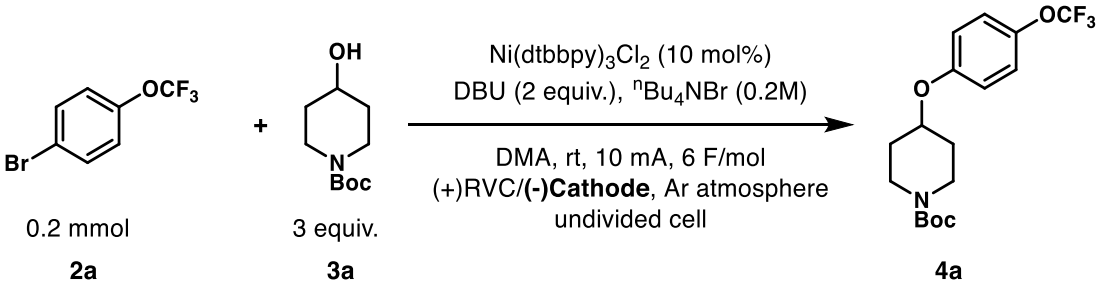


**Table S3:** Results of cathode optimization.

| Entry | Cathode | Anode | **2a** (%)[a] | **4a** (%)[a] |
|---|---|---|---|---|
| 1 | Ni Foam | RVC | <1 | 50 |
| 2 | RVC | RVC | <1 | 62 |
| 3 | Graphite | RVC | 2 | <1 |
| 4 | Stainless Steel | RVC | 6 | <1 |
| 5 | C-Felt CeTech GF020 | RVC | <1 | 43 |
| 6 | C-Felt AvCarb G280A | RVC | 1 | 32 |
| 7 | C-Felt CeTech CF120 | RVC | 44 | 23 |
| 8 | Sn | RVC | <1 | <1 |
| 9 | Zn | RVC | <1 | <1 |
| 10 | Leaded Bronze | RVC | 3 | <1 |
| 11 | Ti | RVC | 4 | <1 |
| 12 | Pb | RVC | 1 | <1 |
| 13 | BDD | RVC | 1 | <1 |

[a] Determined using calibrated HPLC analysis against biphenyl as standard.

## 3.4 Solvent Optimization

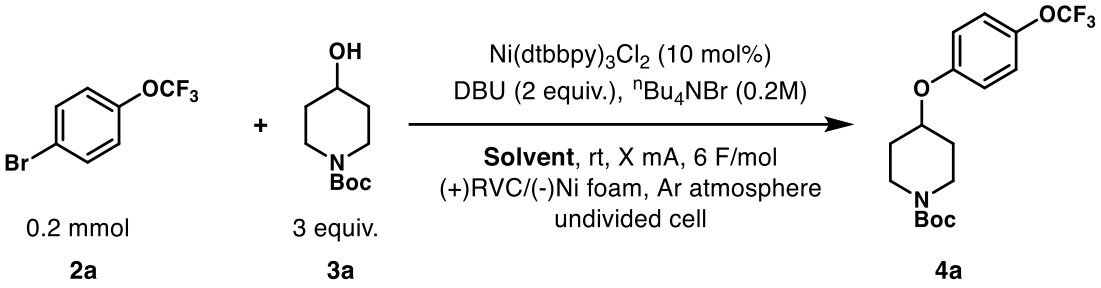


0.2 mmol **2a** | 3 equiv. **3a** | **4a**

**Table S4:** Results of the solvent optimization.

| Entry | Solvent | Current (mA) | **2a** (%)[a] | **4a** (%)[a] |
|---|---|---|---|---|
| 1 | DMA | 10 | <1 | 50 |
| 2 | Propylene Carbonate | 4 | <1 | <1 |
| 3 | MeCN | 10 | <1 | 15 |
| 4 | DMSO | 10 | <1 | 7 |
| 5 | DCM | 10 | 86 | <1 |

[a] Determined using calibrated HPLC analysis against biphenyl as standard.

## 3.5 Base Screening

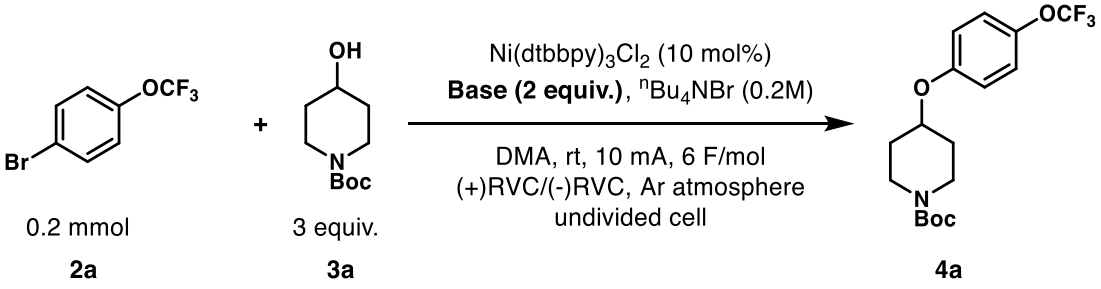


0.2 mmol **2a** | 3 equiv. **3a** | **4a**

**Table S5:** Results of the optimization of bases.

| Entry | Base | **2a** (%)[a] | **4a** (%)[a] |
|---|---|---|---|
| 1 | DBU | <1 | 62 |
| 2 | TMG | 82 | <1 |
| 3 | Pyridine | 90 | <1 |
| 4 | KOAc | 67 | <1 |
| 5 | $NEt_3$ | 10 | <1 |
| 6 | $CsCO_3$ | 86 | <1 |
| 7 | NaOMe | 10 | <1 |

[a] Determined using calibrated HPLC analysis against biphenyl as standard.

## 3.6 Supporting Electrolyte Screening

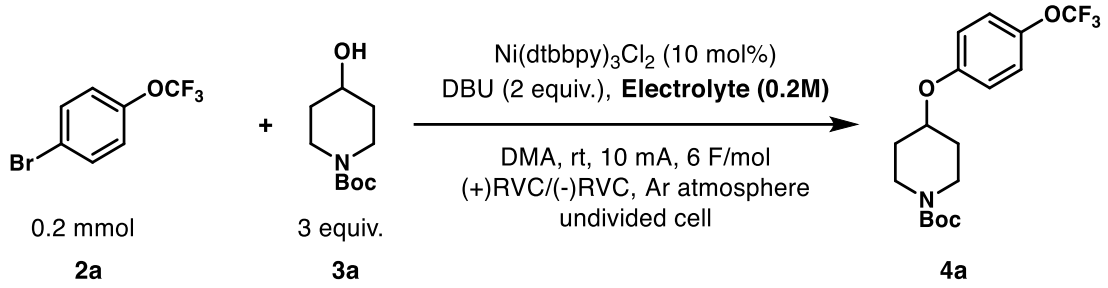


0.2 mmol **2a** | 3 equiv. **3a** | **4a**

**Table S6:** Results of the optimization of supporting electrolytes.

| Entry | Supporting Electrolyte (SE) | **2a** (%)[a] | **4a** (%)[a] |
|---|---|---|---|
| 1 | *n*-$Bu_4NBr$ (TBAB) | <1 | 62 |
| 2 | $Et_4NBF_4$ | 21 | 2 |
| 3 | *n*-$Bu_4NPF_6$ | 13 | 29 |
| 4 | $LiBF_4$ | 16 | 3 |
| 5 | *n*-$Bu_4NCl$ | 18 | 6 |
| 6 | LiBr | 56 | <1 |
| 7 | $Et_4NBr$ | 29 | 38 |
| 8 | $Me_4NBr$ | 61 | 1 |

[a] Determined using calibrated HPLC analysis against biphenyl as standard.

## 3.7 Optimization of Catalytic System in Batch

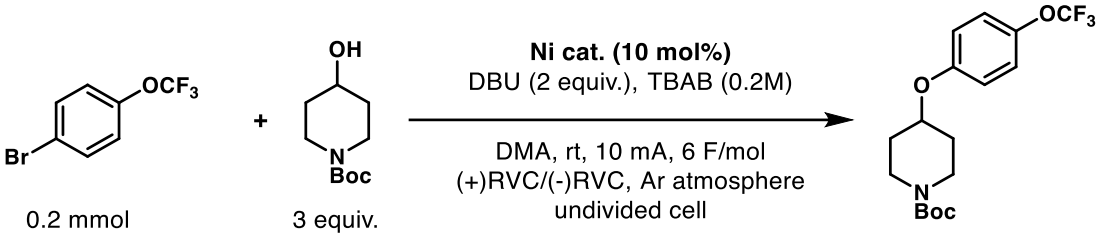


**Table S7:** Results of the optimization of the catalyst.

| Entry | Ni catalyst | **2a** (%)[a] | **4a** (%)[a] |
|---|---|---|---|
| 1 | $Ni(dtbbpy)_3Cl_2$ | <1 | 62 |
| 2 | $Ni(dtbbpy)_3Br_2$ | 25 | 35 |
| 3 | $Ni(bpy)_3Br_2$ | 19 | 41 |
| 4 | $NiCl_2$ | 73 | <1 |
| 5 | $NiCl_2$ ·glyme | 56 | <1 |

[a] Determined using calibrated HPLC analysis against biphenyl as standard.

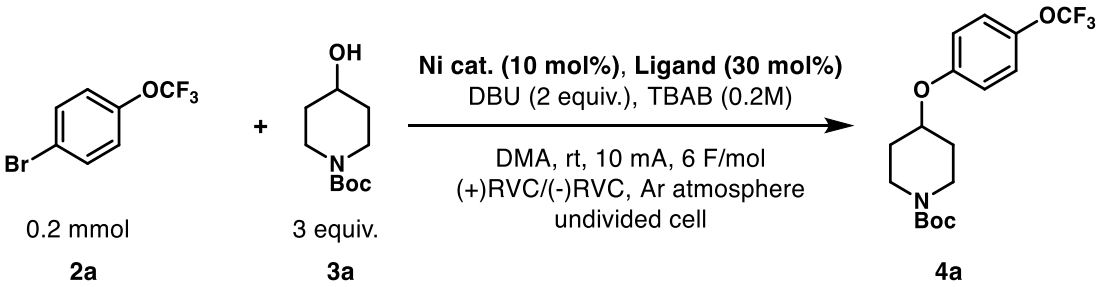


**Table S8:** Results of the optimization of nickel source and ligand.

| Entry | Ni catalyst | Ligand | **2a** (%)[a] | **4a** (%)[a] |
|---|---|---|---|---|
| 1 | $NiCl_2$ | - | 73 | <1 |
| 2 | $NiCl_2$ | dtbbpy | 61 | <1 |
| 3 | $NiCl_2$ | bpy | 73 | <1 |
| 4 | $NiCl_2$ | Neocuproin | 61 | <1 |
| 5 | $NiCl_2$ | Phenanthroline | 64 | <1 |
| 6 | $NiCl_2$·glyme | - | 56 | <1 |
| 7 | $NiCl_2$·glyme | dtbbpy | 29 | 38 |
| 8 | $NiCl_2$·glyme | bpy | 62 | 21 |
| 9 | $NiCl_2$·glyme | Neocuproin | 65 | <1 |
| 10 | $NiCl_2$·glyme | Phenanthroline | 52 | <1 |

[a] Determined using calibrated HPLC analysis against biphenyl as standard.

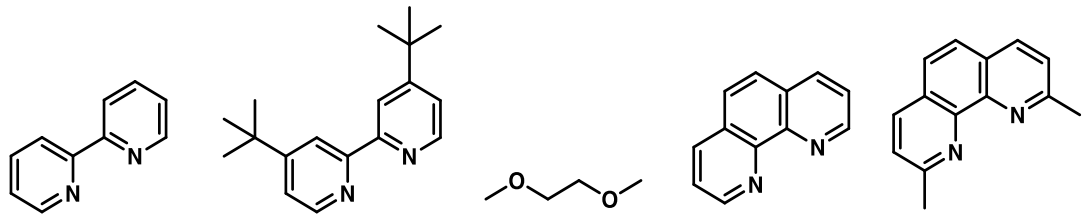

## 3.8 Optimization of Stoichiometry

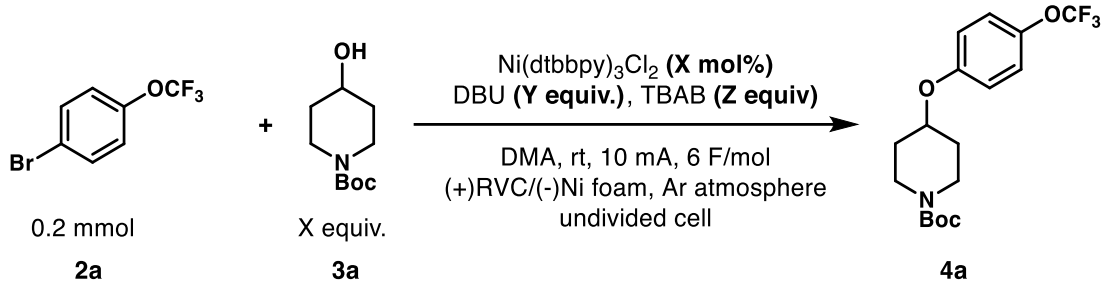


**Table S9:** Results of the optimization of equivalents in batch.

| Entry | Equiv. **3a** | Equiv. TBAB | Equiv.DBU | Catalyst Loading (%) | **2a** (%)[a] | **4a** (%)[a] |
|---|---|---|---|---|---|---|
| 1 | 3 | 3 | 2 | 10 | <1 | 50 |
| 2 | 3 | 3 | 1 | 10 | 27 | 16 |
| 3 | 3 | 3 | 3 | 10 | 19 | 33 |
| 4 | 2 | 3 | 2 | 10 | <1 | 30 |
| 5 | 3 | 2 | 2 | 10 | 13 | 39 |
| 6 | 3 | 3 | 2 | 5 | 13 | 16 |
| 7 | 3 | 3 | 2 | 15 | <1 | 61 |

[a] Determined using calibrated HPLC analysis against biphenyl as standard.

## 3.9 Moisture Sensitivity

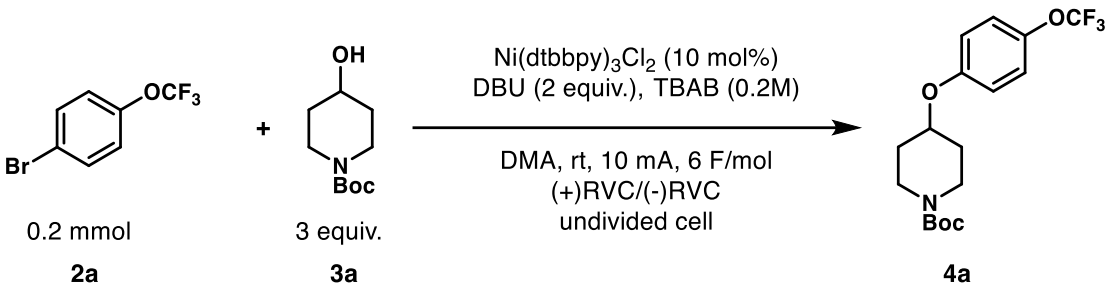


**Table S10:** Results of the air and moisture sensitivity reactions.

| Entry | Conditions | **2a** (%)[a] | **4a** (%)[a] |
|---|---|---|---|
| 1 | Ar balloon (standard) | <1 | 62 |
| 2 | Ar balloon (+ 5 equiv. $H_2O$) | 39 | 27 |
| 3 | Continuous Ar bubbling | <1 | 60 |
| 4 | Air | 11 | 48 |

[a] Determined using calibrated HPLC analysis against biphenyl as standard.

Different methods to make the reaction mixture inert were studied. Good results were achieved when attaching an argon balloon to the reaction mixture or when continuously bubbling argon through the mixture for the whole reaction time (~60% yield). Performing the reaction under air led to a slight drop in yield (48%) and deliberately adding 5 equivalents of water to the mixture, which was previously kept under inert atmosphere with argon, led to low conversion and lower yield (39% **2a** left, 27% **4a**). These results show that the reaction was sensitive to both water and air, with the effect of water being more pronounced than air.

## 3.10 Alternating Polarity Experiments

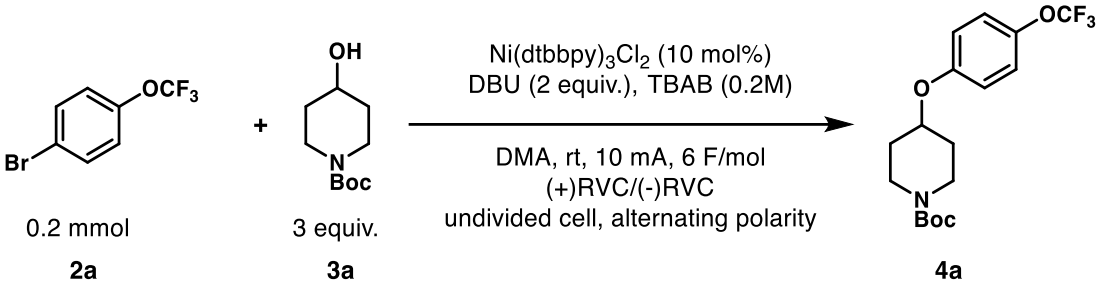


**Table S11:** Results of experiments with alternating polarity.

| Entry | Alternating polarity | **2a** (%)[a] | **4a** (%)[a] |
|---|---|---|---|
| 1 | - | <1 | 62 |
| 2 | 1/min | 21 | 5 |
| 3 | 1/(5 min) | 11 | 58 |

[a] Determined using calibrated HPLC analysis against biphenyl as standard.

Alternating polarity experiments (using IKA ElectraSyn 2.0) were performed. Alternating the polarity once per minute (entry 2) led to a decreased yield of only 5% of product **3**. When alternating the polarity was conducted less frequently (once every 5 minutes, entry 3) a similar performance to the standard optimized conditions without alternating polarity was observed (58% of **4a**).

## 3.11 Coulometric Karl-Fischer Titration

**Table S12**: Results of Karl-Fischer Titration.

| Entry | Analyzed Mixture | Concentration (mol/L) | Water content (ppm) |
|---|---|---|---|
| 1 | DMA | Neat | 98 ± 14 |
| 2 | Aryl Bromide **1** | 0.066 | 131 ± 31 |
| 3 | Boc-piperidine **2** | 0.2 | 142± 28 |
| 4 | DBU | 0.13 | 150 ± 3 |
| 5 | TBAB | 0.2 | 136 ± 7 |
| 6 | $Ni(dtbbpy)_3Cl_2$ | 0.0066 | 167 ± 13 |
| 7 | Reaction Mixture 1 | - | 246 ± 12 |
| 8 | Reaction Mixture 2 | - | 184 ± 5 |
| 9 | Reaction Mixture 3 | - | 77 ± 15 |

Karl-Fischer titration was performed using a coulometric instrument (Metrohm). Every mixture was analyzed in triplicates. Entry 1 is just pure dry DMA directly from the bottle, which was used for the reactions. Every other solution was prepared to correspond to the same concentration as under standard conditions dissolved in DMA. The analyzed simulated reaction mixtures contained all the components above in their corresponding concentrations. Reaction mixtures 1 and 2 correspond to mixtures that were prepared in identical ways like regular reaction mixtures on different days. Reaction mixture 3 was dried over 3 Å molecular sieves before being measured.

## 3.12 Photochemical Control Reaction

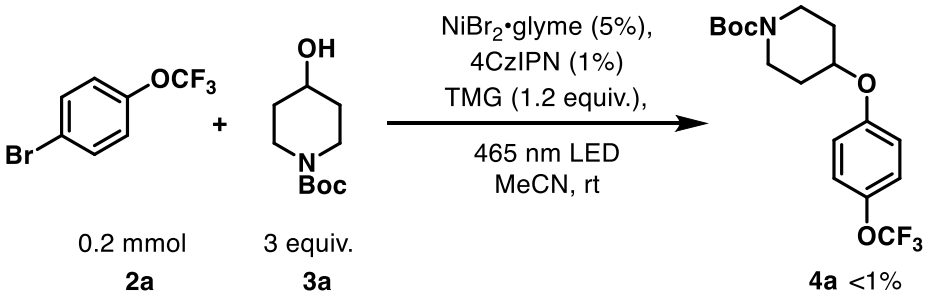


Applying literature conditions for photochemical ether bond formation.[2] No conversion to product was observed over 40 h of reaction time at room temperature.

# 4. Reproducibility Experiments

## 4.1 Reproducibility with reused Ni-Foam Electrodes

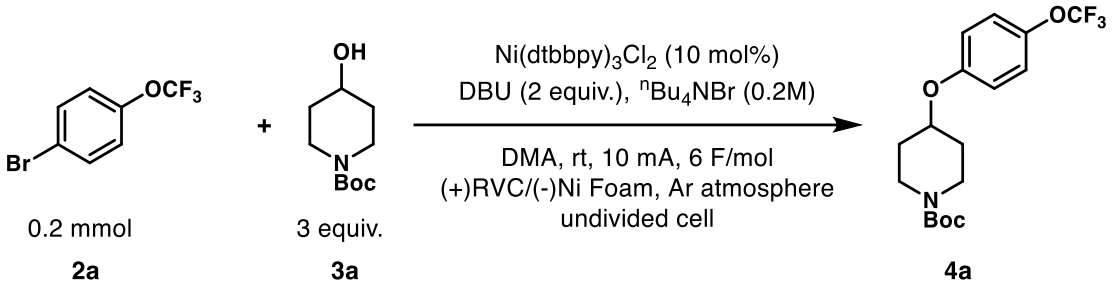


0.2 mmol **2a** | 3 equiv. **3a** | **4a**

**Table S13:** Results of Ni foam electrode reusability experiments.

| Entry | No of re-uses of Ni Foam | **2a** (%)[a] | **4a** (%)[a] |
|---|---|---|---|
| 1 | 0 | <1 | 51 |
| 2 | 1 | 11 | 4 |
| 3 | 2 | 6 | 62 |
| 4 | 3 | <1 | 54 |
| 5 | 4 | 59 | <1 |

[a] Determined using calibrated HPLC analysis against biphenyl as standard.

For this set of experiments RVC electrodes were cleaned following a standard procedure (ultrasonication in acetone and water followed by drying overnight). Ni foam electrodes were just washed with acetone and water. The set of experiments showed random fluctuations of the yield between <1 and 62% of **4a**, indicating that reproducibility seemed to be related mostly to the quality of RVC and not the Ni foam.

## 4.2 Reproducibility with RVC Electrodes

### Experimental Data

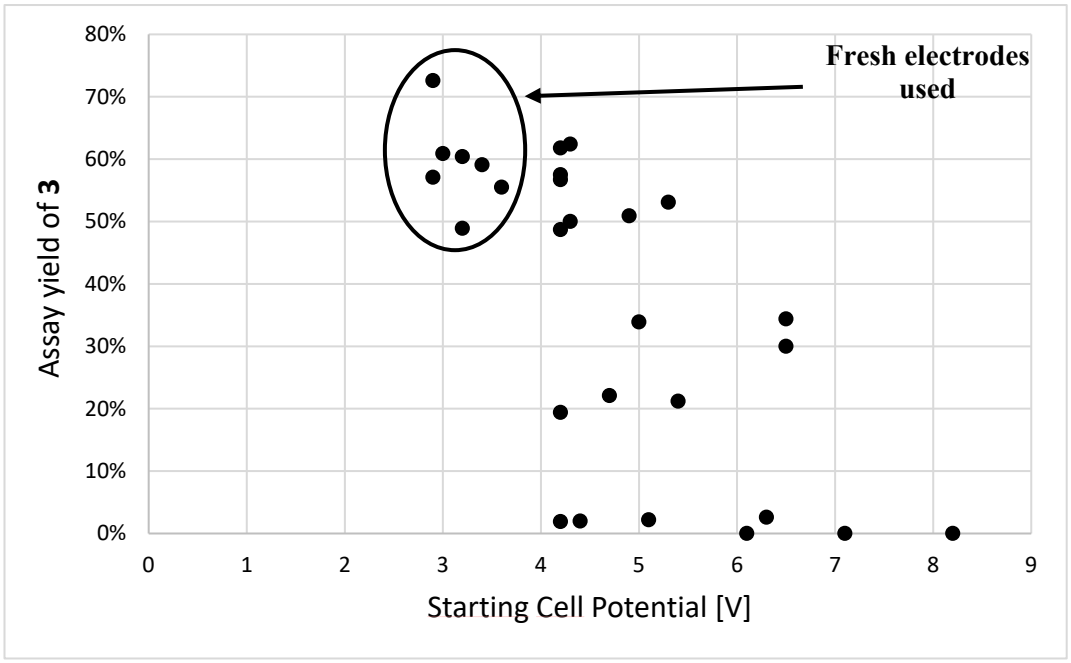


**Figure S6:** Reproducibility of experiments with reused RVC electrodes in relation to the measured starting cell potential.

Repeated experiments under standard optimized conditions using different RVC electrodes. When fresh RVC electrodes were employed the cell potential at the start of the reaction is around 3 V. With fresh electrodes a yield of **4a** around 59% ± 7% was reached. When re-using RVC electrodes* the starting cell potential varied greatly. At intermediate values of 3.5 – 5 V good results were not consistently achieved. When the starting cell potential is higher than 5.5 V a lowered yield was observed in all cases.

*RVC electrodes were cleaned between reactions by ultrasonication in water and acetone followed by drying at 100 °C overnight.

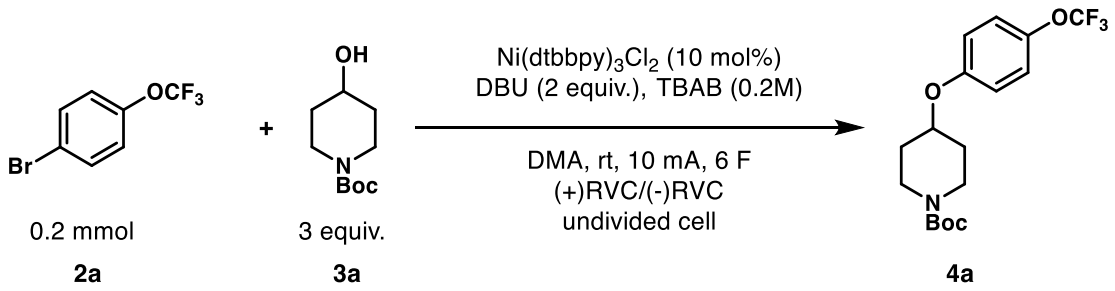


**Table S14:** Results of RVC electrode washing experiments.

| Entry | RVC wash | **2a** (%)[a] | **4a** (%)[a] |
|---|---|---|---|
| 1 | No wash | 53 | <1 |
| 2 | Acetone wash | <1 | 61 |
| 3 | Pentane wash | <1 | 61 |

[a] Determined using calibrated HPLC analysis against biphenyl as standard.

For some batches of RVC a drop in yield was observed even when using fresh RVC. **This could be solved by ultrasonication of the fresh electrodes in acetone or pentane followed by drying at 100 °C for 12 hours before use.**

## Analysis of RVC Surface using Scanning Electron Microscopy (SEM)

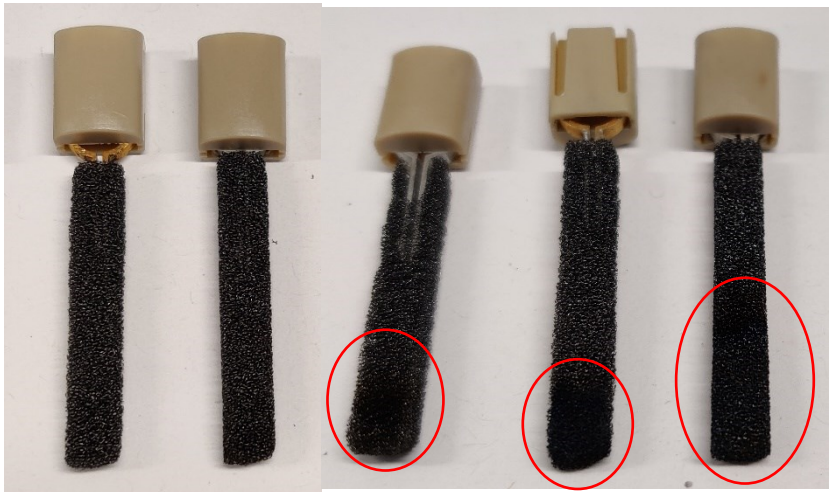

**Figure S7:** Left: Fresh RVC electrodes, right: RVC electrodes with visual contamination (circled in red).

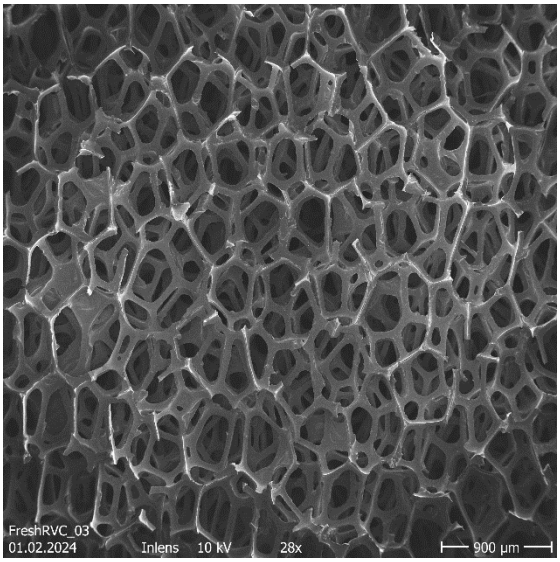


**Figure S8:** Structure of the RVC electrode surface.

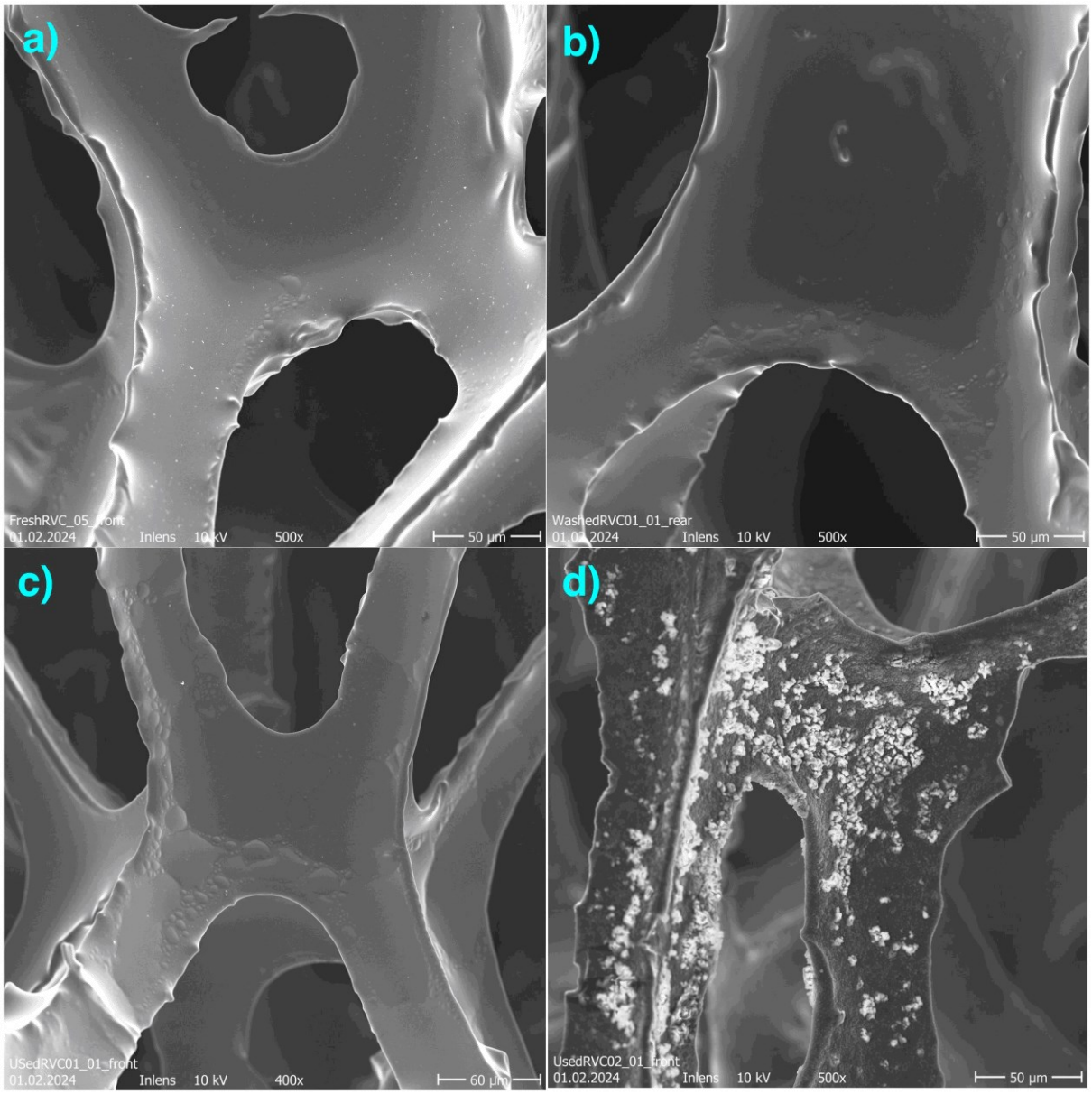


**Figure S9:** a) fresh RVC electrode as delivered, b) fresh RVC electrode after wash, c) used RVC electrode (no visual contamination), d) used RVC electrode with visual contamination (off coloring).

**Figure S9** a)-c) show clean electrode surface of working RVC electrodes. The unwashed electrode a) showed some small particles, which were not present on the washed electrodes. These small particles could likely be the cause of the reproducibility issues when using fresh electrodes (as described above). All electrode surfaces also showed some degree of pitting on the surface. This mechanical abrasion seemed to be more intense on the washed and used electrodes than on the fresh ones. Figure S9 d) showed deposition of small crystallites on the surface of a visually contaminated RVC electrode sample. These crystallites could be found only on the bottom part of the electrode where it was in contact with the reaction mixture during the electrochemical reaction. This showed that the solid was likely deposited from solution during the reaction. Analysis of the crystallites using an energy dispersive X-ray (EDX) detector indicated that they contain nickel and bromide. The source of the contamination was probably from the nickel catalyst (Ni) and the supporting electrolyte *n*-$Bu_4NBr$ (Br). Passivation of the electrode surface due to the deposition of this insoluble precipitate explained the decreased reaction performance of recycled electrodes.

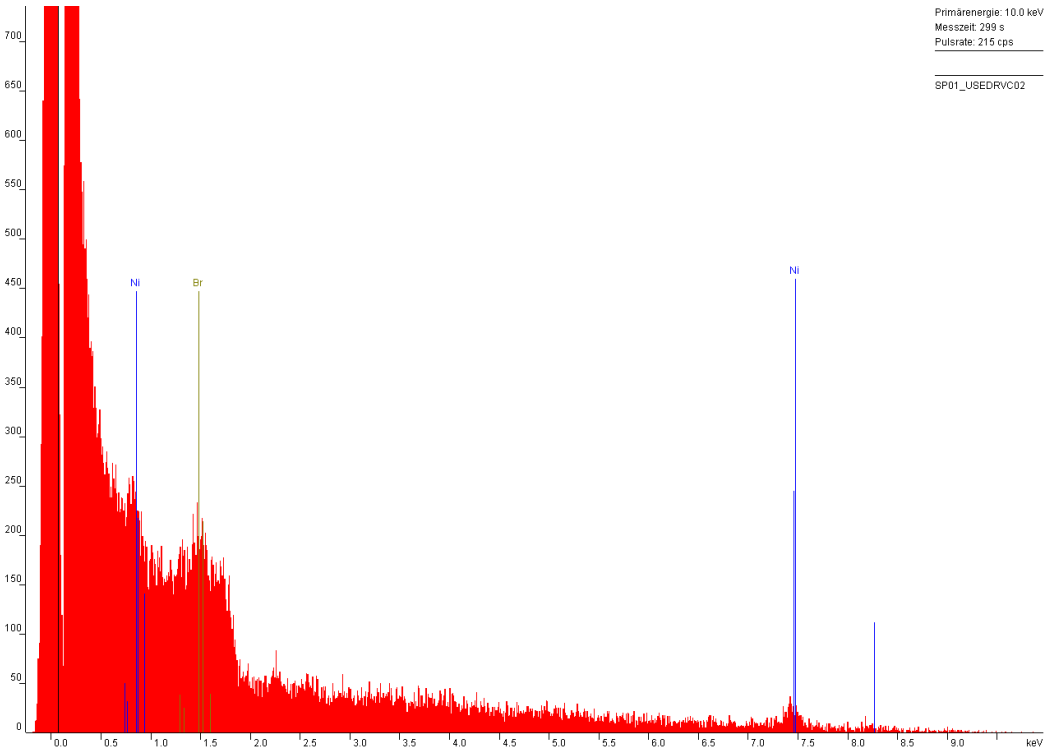


**Figure S10:** EDX measurement of crystallites on RVC electrode surface.

# 5. Other Batch Experiments

## 5.1 Catalyst Activation via DBU/TMG

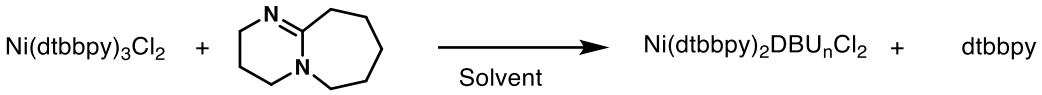


Experiment to elucidate the role of DBU in catalyst activation. $Ni(dtbbpy)_3Cl_2$ was dissolved in solvent. DBU was added portionwise and the reaction was analyzed using HPLC to measure the degree of dissociation of the ligand (dtbbpy) from the catalyst.

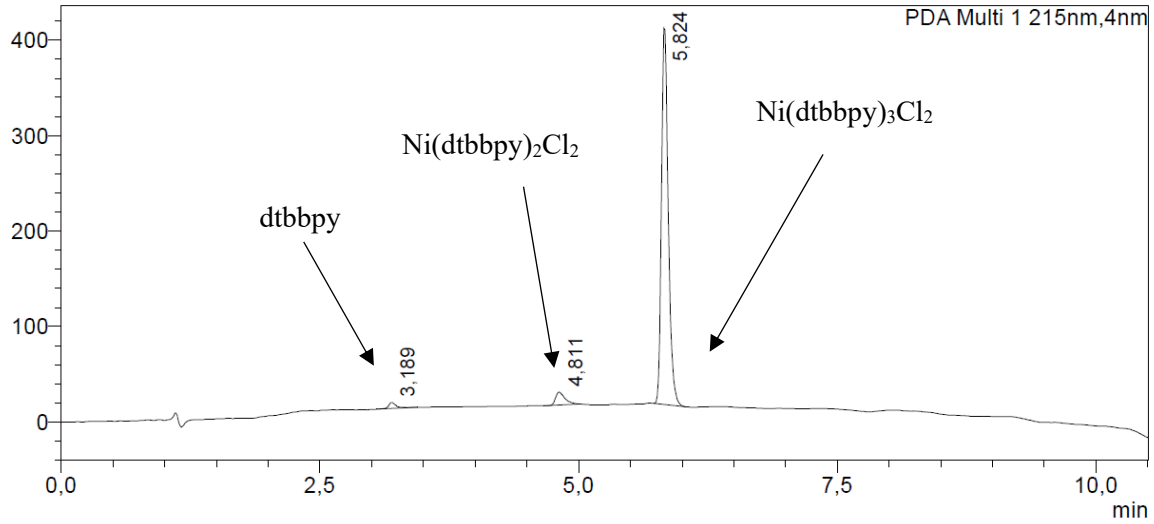


**Figure S11:** HPLC chromatogram of isolated $Ni(dtbbpy)_3Cl_2$ catalyst. In solution the catalyst was always in equilibrium with the form where one ligand was dissociated. On HPLC always three peaks were visible, corresponding to the $Ni(dtbbpy)_3Cl_2$ catalyst, the dtbbpy ligand and one peak most likely corresponding to the activated catalyst, where one dtbbpy equivalent was dissociated.

**Table S15:** Results of catalyst activation experiments with DBU as base.

| Entry | Solvent | DBU (equiv.) | Area % Ni Cat | Area % Ligand | Area % Cat - Ligand |
|---|---|---|---|---|---|
| 1 | MeOH | 0 | 94 | 2 | 4 |
| 2 | MeOH | 1 | 81 | 6 | 13 |
| 3 | MeOH | 2 | 71 | 11 | 18 |
| 4 | MeOH | 4 | 74 | 10 | 17 |
| 5 | DMA | 0 | 89 | 3 | 7 |
| 6 | DMA | 4 | 25 | 26 | 49 |
| 7 | DMA | 8 | 23 | 32 | 45 |
| 8 | DMA | 16 | 21 | 39 | 41 |

When adding DBU as base to a solution of the catalyst more dissociation of ligand was observed. After about 2 equivalents of base this trend seemed to reach a plateau, leading to no further dissociation. In general, a higher degree of dissociation was observed when using DMA when compared to methanol as solvent.

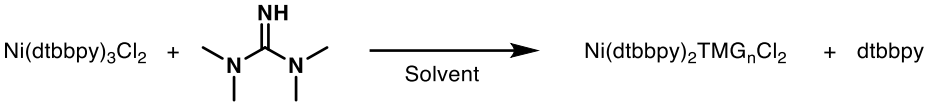


**Table S16:** Results of catalyst activation experiments with TMG as base.

| Entry | Solvent | TMG (equiv.) | Area % Ni Cat | Area % Ligand | Area % Cat - Ligand |
|---|---|---|---|---|---|
| 1 | MeOH | 0 | 92 | 2 | 6 |
| 2 | MeOH | 1 | 88 | 4 | 8 |
| 3 | MeOH | 2 | 83 | 7 | 11 |
| 4 | MeOH | 4 | 81 | 8 | 11 |
| 5 | DMA | 0 | 89 | 3 | 8 |
| 6 | DMA | 4 | 68 | 12 | 20 |
| 7 | DMA | 8 | 56 | 18 | 26 |
| 8 | DMA | 16 | 53 | 19 | 28 |

When performing the same experiment with tetramethylguanidine (TMG) as a base instead of DBU a similar trend was observed. In general, a lower level of dissociation was observed when using TMG instead of DBU. This might explain why using DBU as a base was essential to a successful reaction.

## 5.2 Slow Addition of Aryl Bromide

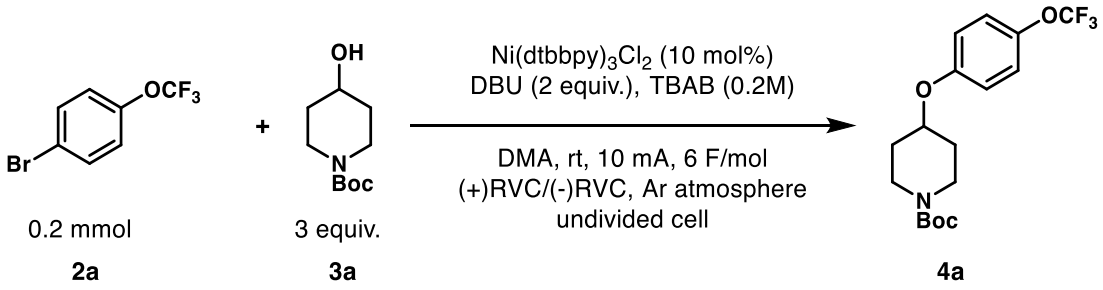


The reaction solution was prepared following the general procedure for batch reactions, but without adding aryl bromide **2a**. Aryl bromide **2a** was dissolved in 500 µL of DMA and slowly added over the course of the reaction using a single shot syringe pump (Harvard). This experiment was performed to increase the excess of hydroxy piperidine **3a** at any given timepoint to increase the selectivity for product **3**. Two attempts were performed adding aryl bromide **4a** over different periods of time.

When feeding **2a** over 3h (almost the whole reaction time - 3h 13 min for 6 F/mol) full conversion of **2a** was observed, while only 18% of product **4a** were formed. When adding **2a** quickly over 5 min 53% of **4a** were formed. No increment in selectivity could be achieved by this method.

# 6. Flow Optimization

## 6.1 Single Pass Flow Experiments

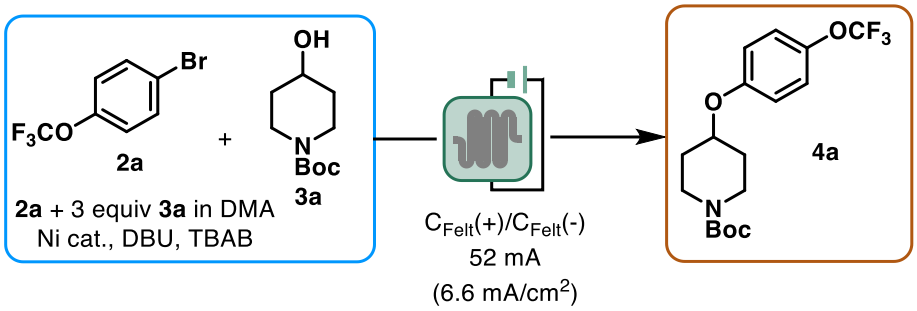


All single pass experiments were performed using a syringe pump (Syrris Asia). For fluidic inlet/outlet port $A_1$ and $A_2$ were used on the cathode side.

**Table S17:** Results of single pass flow experiments.

| Entry | Charge (F/mol) | Flow Rate (µL/min) | **2a** (%)[a] | **4a** (%)[a] |
|---|---|---|---|---|
| 1 | 2 | 241 | 35 | <1 |
| 2 | 4 | 121 | 16 | <1 |
| 3 | 6 | 81 | 4 | <1 |
| 4[b] | 6 | 81 | 9 | <1 |

[a] Determined by calibrated HPLC analysis against Biphenyl as standard. [b] Reversed polarity (inlet and outlet at the anode side).

Conversion of **1** increased with higher amount of added charge. Product **3** was not obtained under all conditions. The low flow rates required for single pass flow did not seem to be sufficient to ensure efficient mass transfer inside the reactor. Considering that the carbon felt electrodes are porous, a higher level of turbulence was required to ensure sufficient contact times with both anode and cathode.


**Figure S12:** Different electrode separator materials for use in the parallel plate flow reactor.

Different types of separator materials between the two electrodes were tested (**Figure S12**). The PTFE mesh showed good electrical conductivity without short circuit, when minimum 4 layers were used. Furthermore, a moderate resistance to liquid flow was observed. This hindered the flow through the mesh, but did not cause any pressure build up, when the liquid was forced through the membrane. The PTFE membrane showed good electrical isolation, but also high resistance to liquid flow, which caused pressure build-up and breaking of the membrane in some cases. The glass microfiber membrane was not mechanically stable, resulting in a short circuit.

**Table S18:** Results of further single pass flow experiments with PTFE membrane as electrode separator.

| Entry | Charge (F/mol) | Flow Rate (µL/min) | **2a** (%)[a] | **4a** (%)[a] |
|---|---|---|---|---|
| 1 | 2 | 241 | 46 | <1 |
| 2 | 4 | 121 | 23 | <1 |
| 3 | 6 | 81 | <1 | <1 |

[a] Determined by calibrated HPLC analysis against Biphenyl as standard.

When PTFE membrane as electrode separator was used instead of PTFE mesh a similar trend was observed, leading to a progressing conversion of **2a** when higher amount of charge passed. However, product **4a** was not observed.

## 6.2 Recirculation Flow Experiments

### Reactor configuration

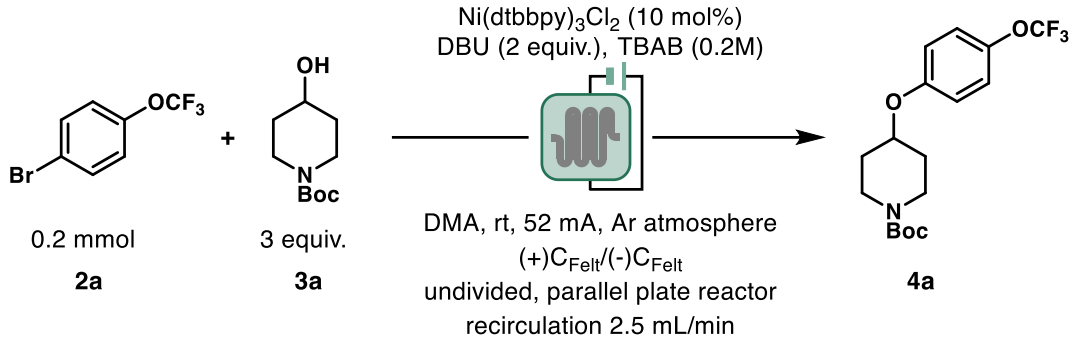


**Table S19:** Optimization of configuration of fluidic connections in flow in recirculation mode.

| Entry | Charge (F/mol) | Current (mA) | Fluidic connections (In → Out) | **2a** (%)[a] | **4a** (%)[a] |
|---|---|---|---|---|---|
| 1 | 2 | 52 | $A_1$ → $A_2$ | 26 | 3 |
| 2 | 4 | 52 | $A_1$ → $A_2$ | <1 | 3 |
| 3 | 6 | 52 | $A_1$ → $A_2$ | <1 | 2 |
| 4 | 2 | 52 | $A_1$,$A_3$ → $A_2$,$A_4$ | 17 | 2 |
| 5 | 4 | 52 | $A_1$,$A_3$ → $A_2$,$A_4$ | <1 | 2 |
| 6 | 2 | 52 | $A_1$ → $A_4$ | 26 | 10 |
| 7 | 4 | 52 | $A_1$ → $A_4$ | 3 | 11 |
| 8 | 2 | 26 | $A_1$ → $A_4$ | 22 | 13 |
| 9 | 2 | 10 | $A_1$ → $A_4$ | 45 | 10 |
| 10 | 4 | 10 | $A_1$ → $A_4$ | 32 | 12 |

[a] Determined by calibrated HPLC analysis against Biphenyl as standard.

Different configurations of the fluidic connections were tried. Going in and out of the reactor on the same electrode side ($A_1$→ $A_2$) led to low yield of **4a** (2-3 %). Going in and out of the reactor on both sides simultaneously led to low yield as well (2%).
When going through the reactor diagonally ($A_1$→$A_4$) a higher yield of 10-11% **4a** was achieved, probably due to more efficient mass transfer. Variation of the applied current to lower amount leads to minor improvements in yield (13% and 12% at 26 mA and 10 mA respectively).

### Different Electrode materials in flow

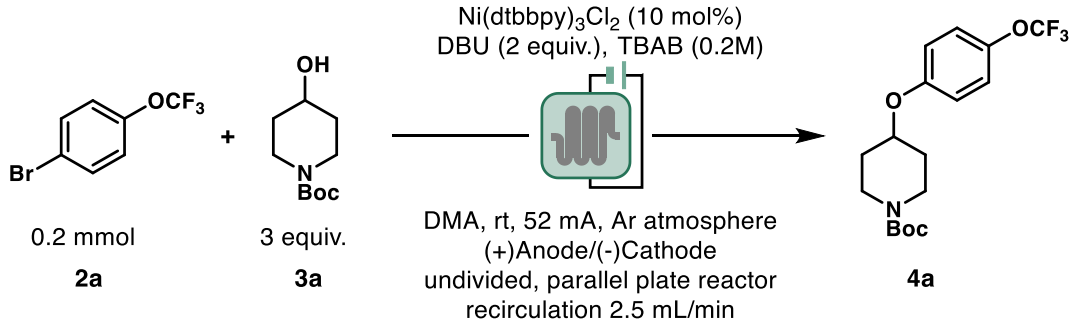


**Table S20:** Results of recirculation flow experiments with different electrode materials

| Entry | Charge (F/mol) | Electrode Material | **2a** (%)[a] | **4a** (%)[a] |
|---|---|---|---|---|
| 1 | 4 | Carbon Felt CeTech GFC020 | 3 | 11 |
| 2 | 4 | Carbon Felt AvCarb GF120 | <1 | 2 |
| 3 | 4 | Graphite | 82 | trace |

[a] Determined by calibrated HPLC analysis against Biphenyl as standard.

When different types of carbon felt electrode was tested (AvCarb GF120), lower yield of just 2% **4a** was achieved, and high conversion of **2a** was observed. When graphite electrodes were tested, a modified setup was used. Instead of the PTFE mesh separators a 0.3 mm thick polymer spacer with a reaction channel was used. The use of graphite as both anode and cathode led to low conversion of **1** and almost no formation of **4a**.

## Optimization of Flow Rates

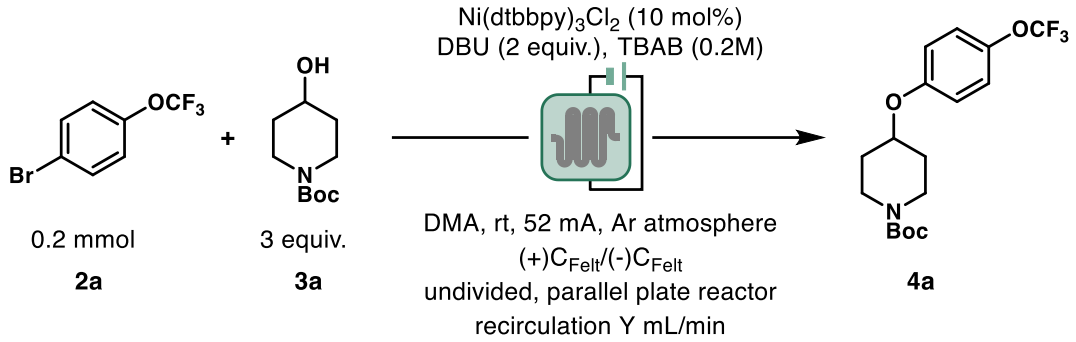


**Table S21:** Optimization of flow parameters in recirculation flow mode.

| Entry | Charge (F/mol) | Current (mA) | Flow rate (mL/min) | **2a** (%)[a] | **4a** (%)[a] |
|---|---|---|---|---|---|
| 1a | 2 | 52 | 2.5 | 26 | 10 |
| 1b | 4 | 52 | 2.5 | 3 | 11 |
| 2a | 2 | 52 | 10 | 42 | 21 |
| 2b | 4 | 52 | 10 | 14 | 25 |
| 3a | 2 | 26 | 10 | 48 | 18 |
| 3b | 4 | 26 | 10 | 41 | 22 |
| 4a[b] | 2 | 52 | 10 | 39 | 29 |
| 4b[b] | 4 | 52 | 10 | <1 | 46 |
| 5a[b] | 2 | 52 | 20 | 37 | 40 |
| 5b[b] | 4 | 52 | 20 | <1 | 59 |
| 6a[b] | 2 | 52 | 40 | 34 | 40 |
| **6b**[b] | **4** | **52** | **40** | **<1** | **61** |
| 7a[b] | 2 | 104 | 40 | 55 | 14 |
| 7b[b] | 4 | 104 | 40 | 43 | 15 |
| **8**[b,c] | **4** | **52** | **40** | **<1** | **66** |

[a] Determined by calibrated HPLC analysis against Biphenyl as standard. [b] Continuous Ar bubbling through the reaction mixture. [c] Reaction with 0.1 M concentration of **2a**.

Increase of the recirculation flow rate led to a drastic increase in yield from 11% **4a** at 2.5 mL/min to 25% at 10 mL/min (entries 1 and 2). Decrease of current to 26 mA leads to slightly lower yield (22%, **Table S21, Entry 3**). Interestingly low conversion towards product was observed after 2F. This indicated catalyst deactivation after some time. The problem of catalyst deactivation could be resolved by keeping the reaction mixture inert during the experiment by bubbling argon through the reaction.* Using this improved methodology full conversion of **2a** and 46% of **4a** was achieved (entry 4). Finally, by increasing the flow rate to 20 mL/min the yield was increased to 59% (entry 5). Further increase of flow rate to 40 mL/min did not lead to a lot of increase in yield 61% of **4a** (entry 6). Doubling the current to 104 mA led to a steep decrease of yield to 15% (entry 7).
The conditions from entry 6 were chosen as optimal conditions. Several repeats of the reaction at these conditions showed the reaction to be reproducible.

* A modified procedure where argon was bubbled through the reaction during the pre-stirring for 30 min and then a balloon with Ar was attached for the rest of the reaction was attempted. Under these conditions a lowered conversion of just 53% and an assay of 25% **3** was achieved.

## Recycle of Carbon Felt Electrodes

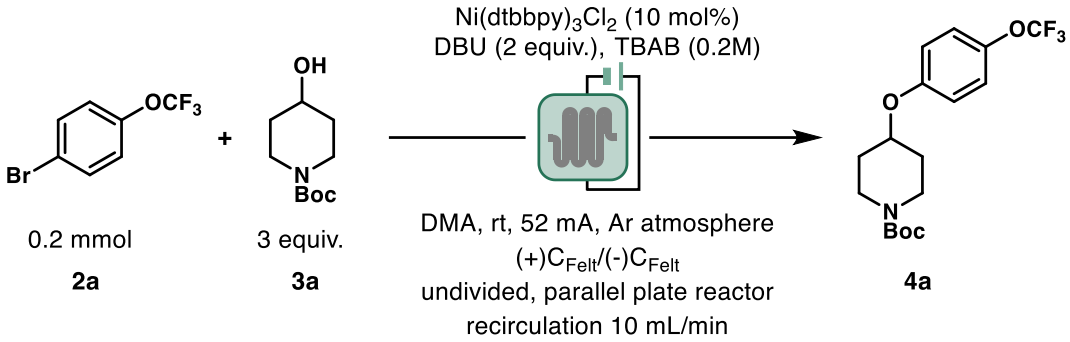


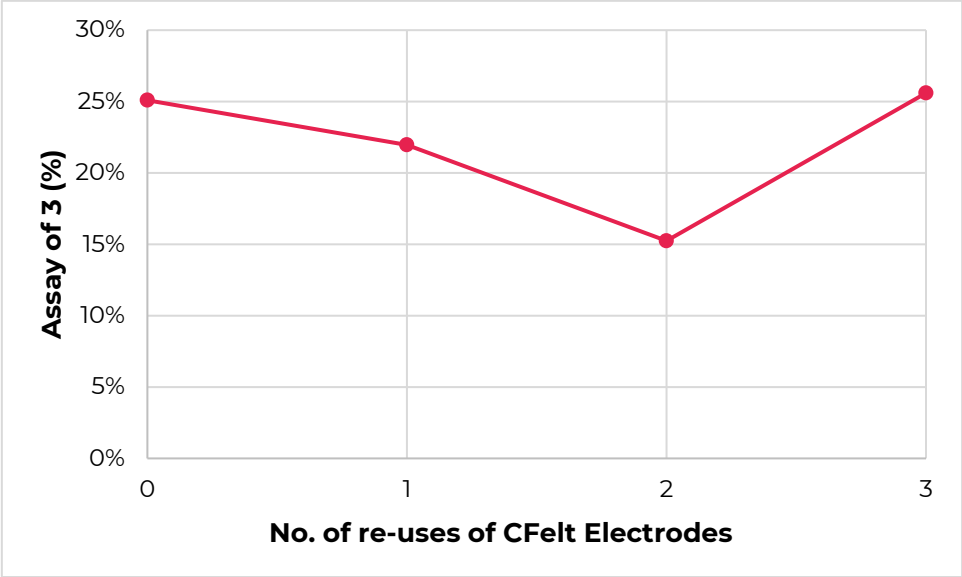


**Figure S13:** Assay yield of **4a** vs number of re-uses of carbon felt electrodes without disassembly of the reactor.

The standard procedure between flow reactions contemplates to disassemble and clean the reactor and use fresh carbon felt electrodes for each reaction.
For this experiment the reactor was not disassembled, but instead flushed extensively with DMA and isopropanol. As shown in **Figure S13** the assay yield of **4a** decreased with each use, when the reactor was not disassembled. Reactivity can be restored using the same electrodes when the reactor was disassembled and the electrodes ultrasonicated in $H_2O$ and acetone.

**Final Setup**

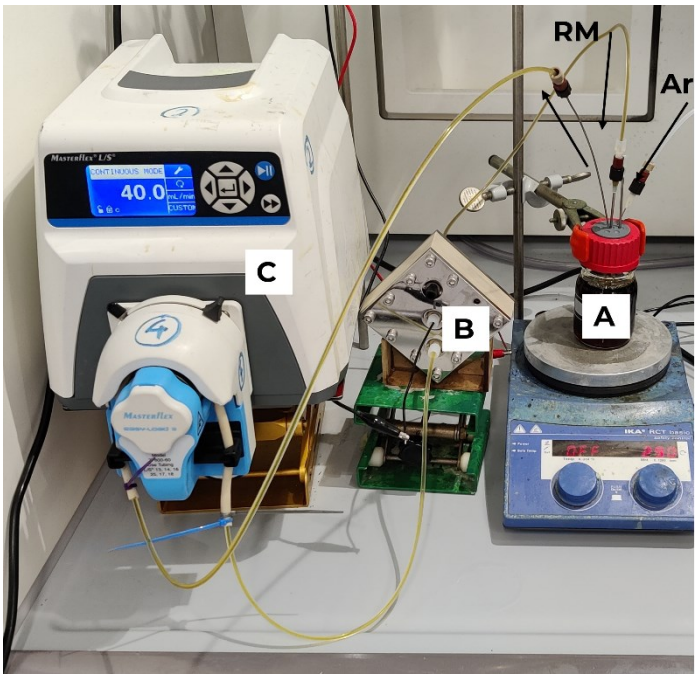


**Figure S14:** Final flow setup: A: Reservoir of reaction mixture. B: Parallel plate reactor C: Masterflex L/S peristaltic pump.

Reaction mixtures were prepared in a vessel closed with a septum (A). Argon was continuously bubbled into the solution using an Ar line attached to a needle. A second needle was used for pressure release, to avoid build-up of pressure in the system. The reaction mixture was then pumped out of the vessel using a needle attached to PFA tubing (1/16” i.d.), with a proper adapter. For pumping of liquids, a peristaltic pump (Masterflex L/S, easy load II pump head) was employed. Via another piece of PFA tubing (1/16” i.d.) the reaction was fed into the parallel plate electrochemical flow reactor. After passing through the reactor the mixture returned into the glass vessel using PFA tubing (1/16” i.d.).

## 6.3 Design of Experiments (DoE) for Flow Experiments

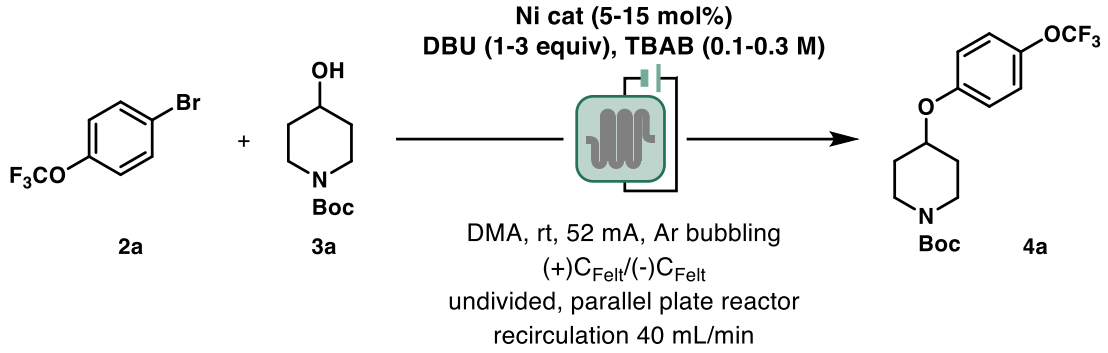


For further optimization and exploration of chemical space in flow a design of experiments (DoE) approach was selected. A four-parameter, two-level reduced central composite face design (CCF) was implemented, corresponding to 23 experiments including 3 center point repeats to measure reproducibility (See table). DBU equivalents were varied between 1 and 3, equivalents of substrate **3a** between 1.5 and 4.5, catalyst loading between 5 and 15% and equivalents of TBAB between 1.5 and 4.5. The responses of the optimization experiments, shown in **Table S22**, were fitted to polynomial models by using a statistical experimental design software package (Modde v13). A model was successfully fitted for the HPLC assay yield of product **4a** using multiple linear regression (MLR). The model was generated by including all main and interaction terms and then non-significant terms were removed. A good fit was achieved with $R^2 = 0.93$. The increase of all four factors was shown to have a positive effect on the yield of **4a**. The most pronounced effects were observed for the increase of equivalents of **3a** and catalyst loading. The effects of DBU and TBAB equivalents were less pronounced. Taking into account economic factors and the limited solubility of the nickel catalyst the center point conditions were considered to be the optimal conditions also after performing this optimization.

**Table S22:** Results of the DoE. Exp 21-23 are the center point repeats.

| Exp No. | Run Order | DBU equiv. | **3a** equiv. | Cat. Loading (%) | TBAB equiv. | Assay **4a** (%) |
|---|---|---|---|---|---|---|
| 1 | 16 | 1 | 1.5 | 5 | 1.5 | 29 |
| 2 | 20 | 3 | 1.5 | 5 | 1.5 | 23 |
| 3 | 9 | 1 | 4.5 | 5 | 1.5 | 45 |
| 4 | 4 | 3 | 1.5 | 15 | 1.5 | 46 |
| 5 | 19 | 1 | 4.5 | 15 | 1.5 | 48 |
| 6 | 23 | 3 | 4.5 | 15 | 1.5 | 60 |
| 7 | 2 | 1 | 1.5 | 5 | 4.5 | 41 |
| 8 | 17 | 1 | 4.5 | 5 | 4.5 | 43 |
| 9 | 1 | 3 | 4.5 | 5 | 4.5 | 19 |
| 10 | 10 | 1 | 1.5 | 15 | 4.5 | 25 |
| 11 | 14 | 3 | 1.5 | 15 | 4.5 | 50 |
| 12 | 13 | 3 | 4.5 | 15 | 4.5 | 59 |
| 13 | 11 | 1 | 3 | 10 | 3 | 43 |
| 14 | 5 | 3 | 3 | 10 | 3 | 55 |
| 15 | 15 | 2 | 1.5 | 10 | 3 | 48 |
| 16 | 22 | 2 | 4.5 | 10 | 3 | 57 |
| 17 | 7 | 2 | 3 | 5 | 3 | 52 |
| 18 | 21 | 2 | 3 | 15 | 3 | 67 |
| 19 | 3 | 2 | 3 | 10 | 1.5 | 41 |
| 20 | 8 | 2 | 3 | 10 | 4.5 | 59 |
| 21 | 18 | 2 | 3 | 10 | 3 | 60 |
| 22 | 12 | 2 | 3 | 10 | 3 | 54 |
| 23 | 6 | 2 | 3 | 10 | 3 | 54 |

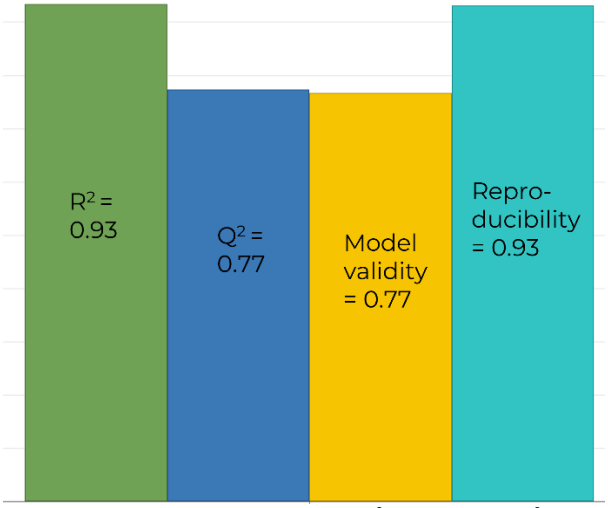


**Figure S15:** Summary of the fit for the performed DoE. A high $R^2 > 0.9$ and $Q^2 > 0.5$ showed a good model with high significance. The model validity of 0.77 indicated a valid model without any outliers. The reproducibility was also >0.9, which demonstrates that the reactions are reproducible.

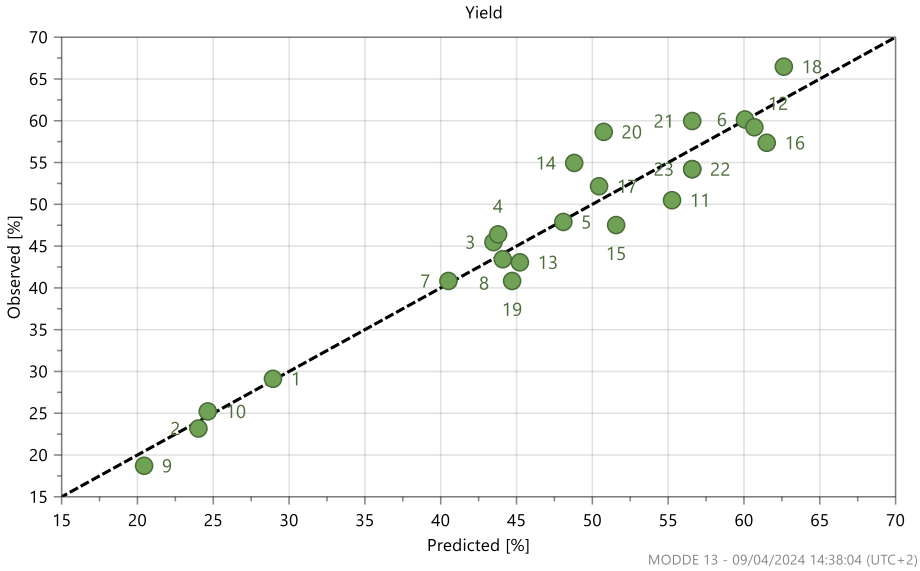


**Figure S16:** Observed vs Predicted values: Measured assay yields are plotted vs values predicted by the model. No statistical outliers and a good fit could be obtained.

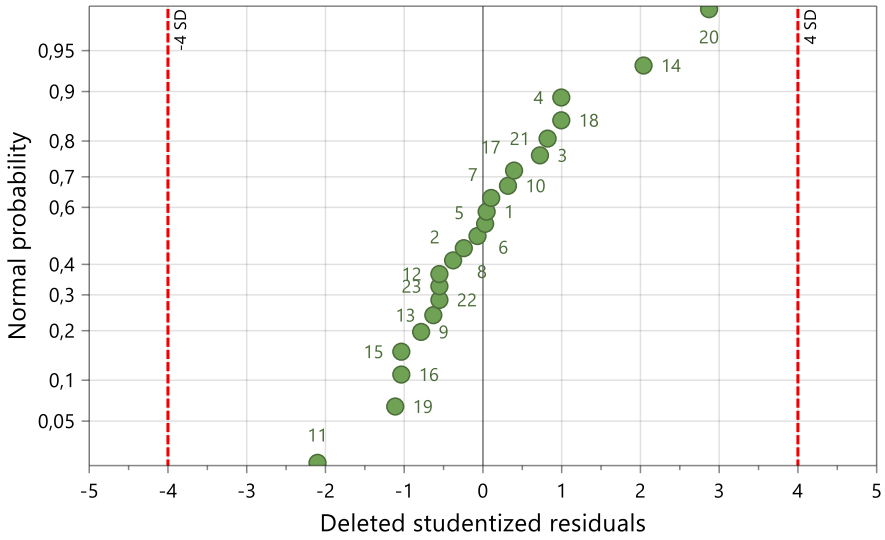


**Figure S17:** Residuals plot for the results of the DoE

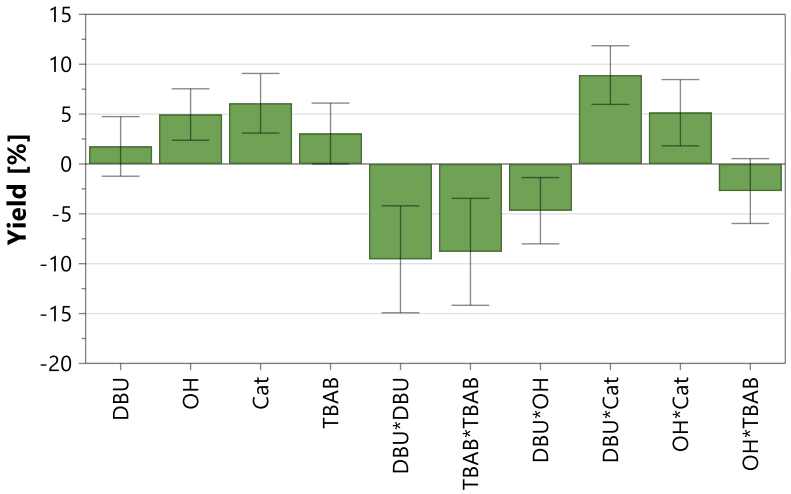


**Figure S18:** Coeffeicients plot showed the positive influence on yield of DBU equiv., equiv. of **2** (OH), TBAB equiv. and catalyst loading. Additionally there were several relevant interaction and square terms, showing the non-linearity of the influences of the different factors.

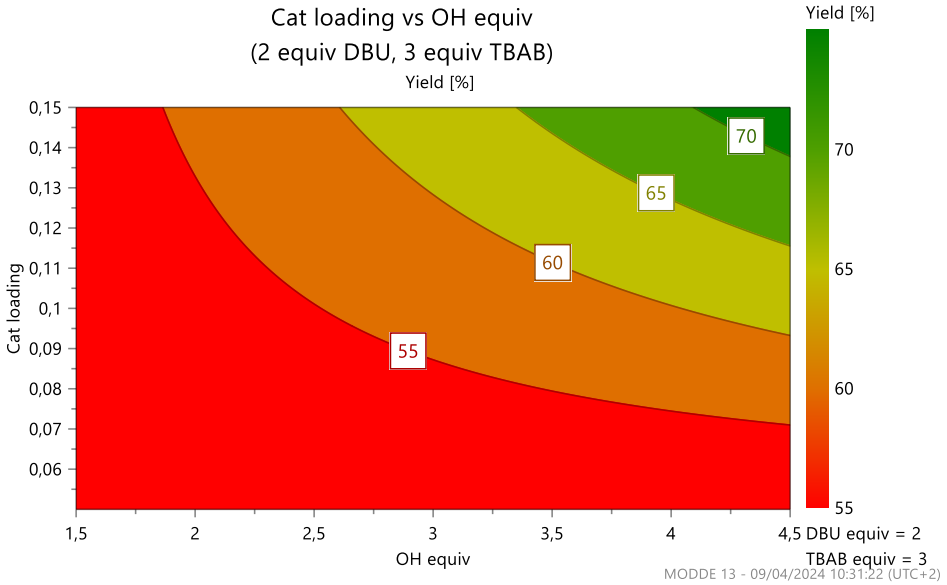


**Figure S19:** Contour plot showing Catalyst loading vs OH equiv. at 2 equiv. DBU and 3 equiv. TBAB.

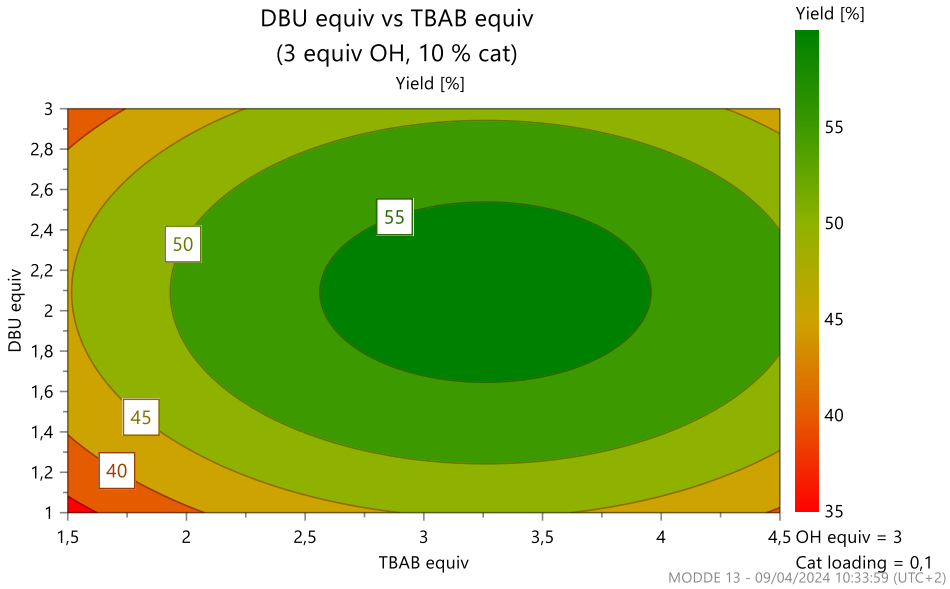


**Figure S20:** Contour plot showing DBU equiv. vs TBAB equiv. at 3 equiv. OH and 10% catalyst.

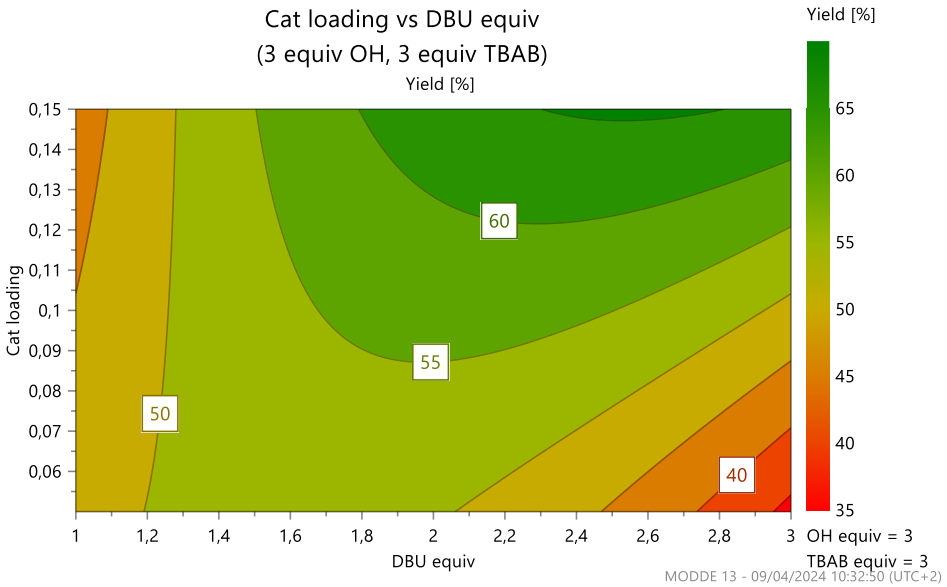


**Figure S21:** Contour plot showing DBU equiv. vs Cat loading at 3 equiv. OH and 3 equiv. TBAB.

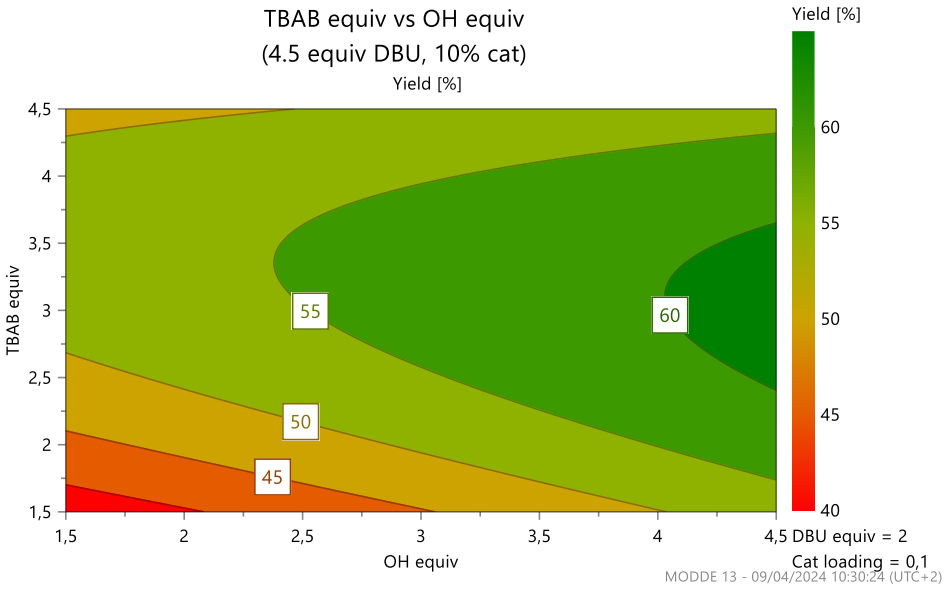


**Figure S22:** Contour plot showing OH equiv. vs TBAB equiv. at 2 equiv. DBU and 10% catalyst.

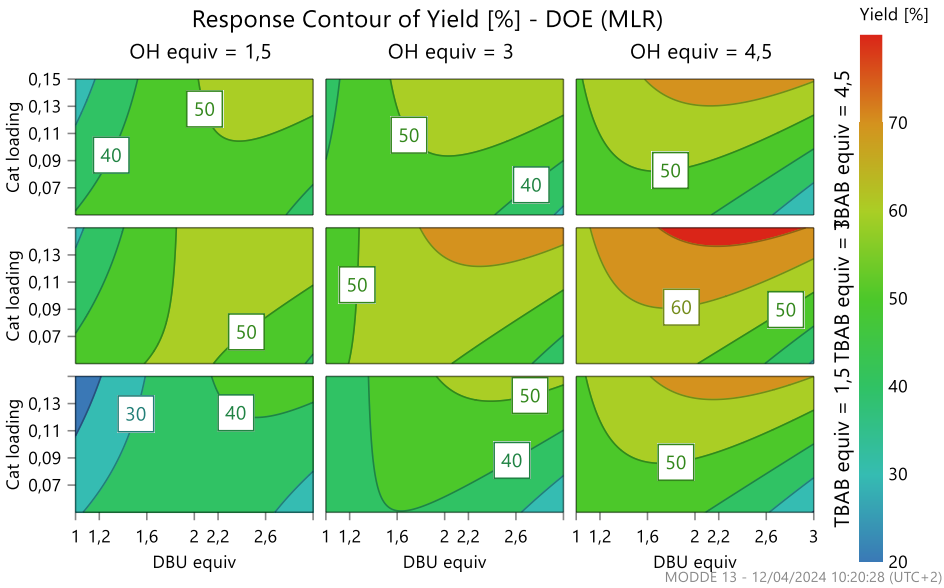


**Figure S23:** Contour plots showing all different parameters.

## 6.4 Kinetic Experiments

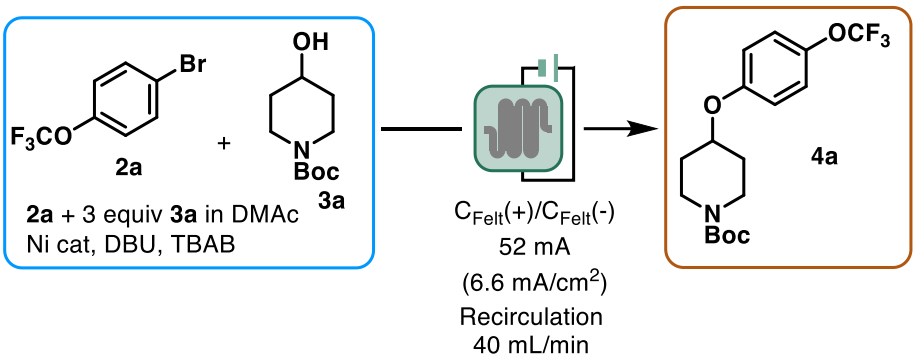


The reaction was performed under standard optimized conditions (0.066 M concentration of **2a**). Samples were taken after each 0.5 F/mol. A linear generation of product **4a** with a concurrent decrease in substrate **2a** was observed. The experiment was stopped after 6 F/mol, which resulted in 64% assay yield of **4a**.

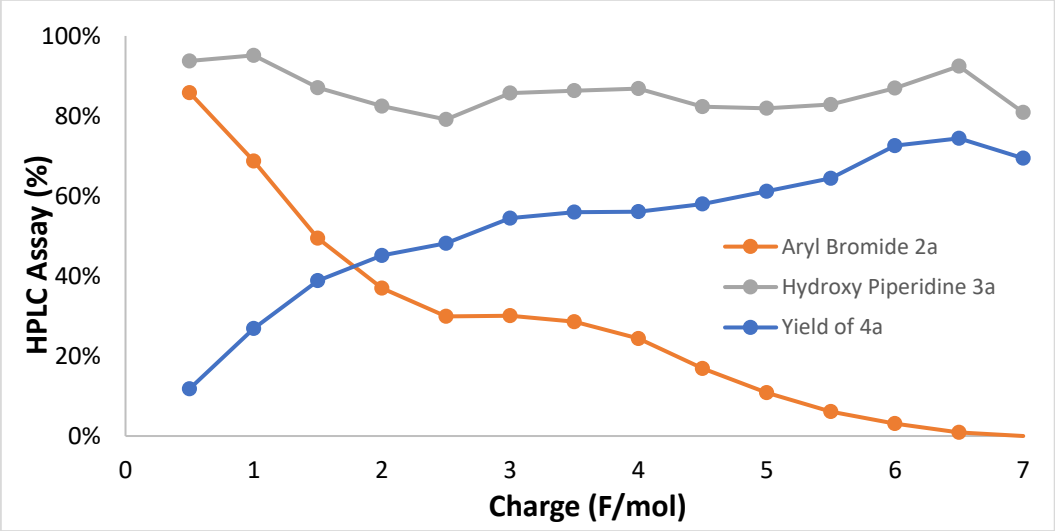


**Figure S24:** Kinetics of the flow reaction at 0.066 M concentration of **2a**.

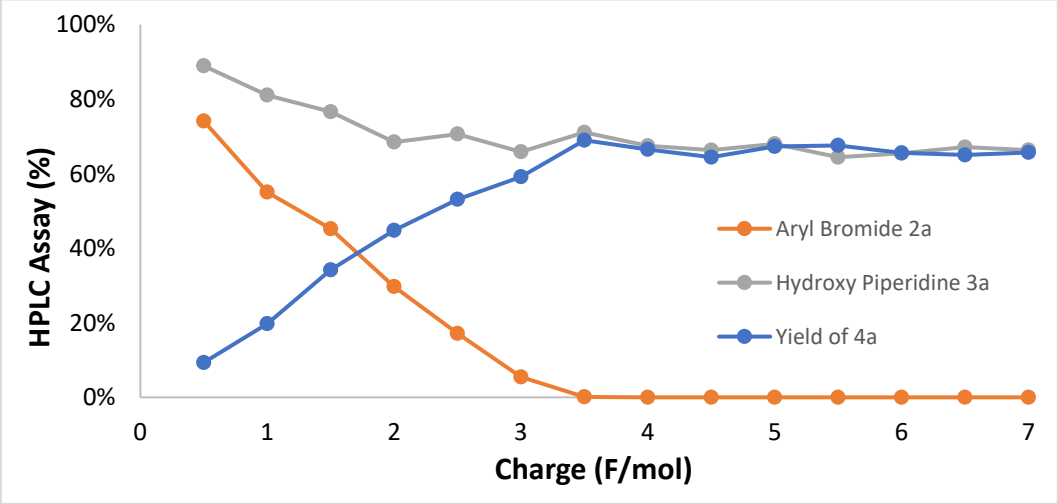


**Figure S25:** Kinetics of the flow reaction at 0.1 M concentration of **2a**.

Just like at lower concentration a linear increase of **4a** and a concurrent decrease of substrates **2a** and **3a** was observed. Full conversion of **2a** was observed after 3.5 F/mol. An assay yield of ~65% **4a** was achieved. Around 66% of **4a** were left at the end of the reaction corresponding to 1 equivalent being consumed. The obtained assays for all substrates and products were constant when more current was passed. No degradation of **4a** was observed when leaving the reaction on for longer.

# 7. Substrate Scope

## 7.1 Alcohol Scope

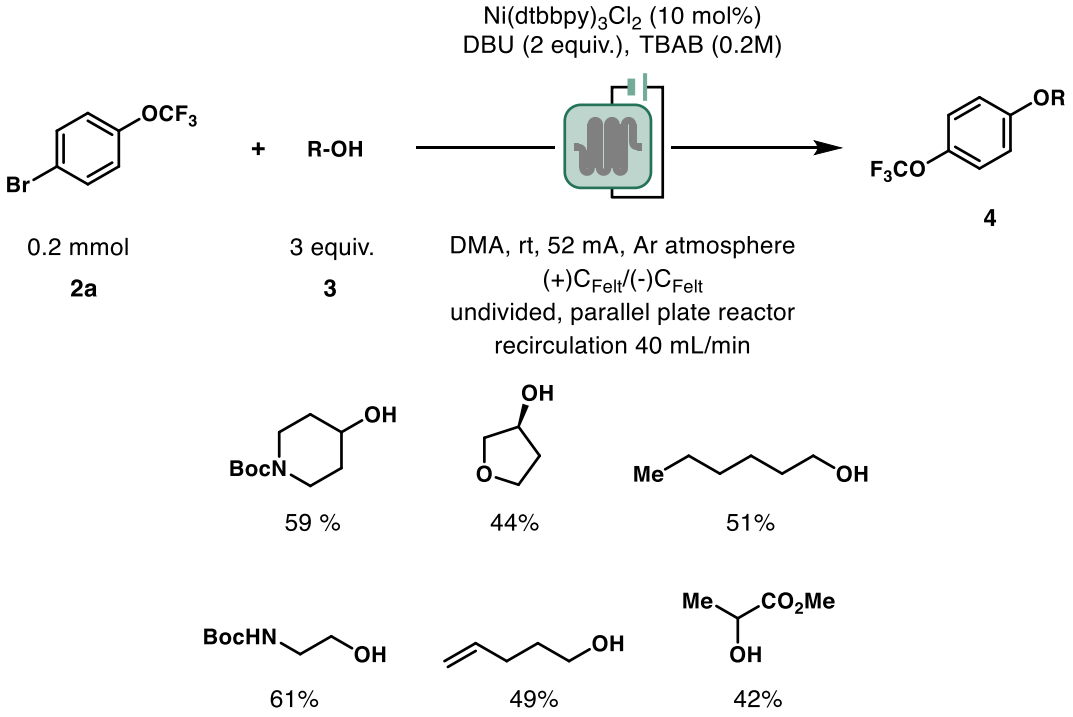


## 7.2 Aryl Bromide Scope

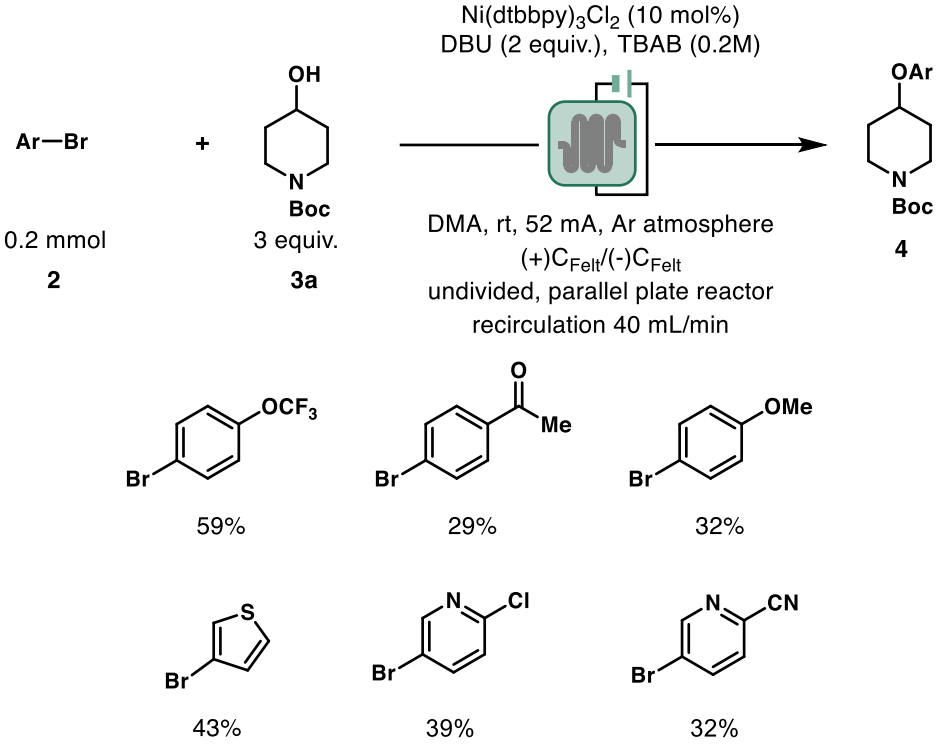


**Note:** Both electron poor and electron-rich bromo (hetero)arenes showed decrease performance when compared to the model substrate (balanced electronics). Bromo acetophenone led to a high amount of phenol as the side product: oxidative addition is fast with electron poor cycles, but the reductive elimination with the alcohol was not so efficient leading to side reaction in this part of the catalytic cycle. Electron rich cycles like bromo anisole on the other hand led to very slow oxidative addition → slow conversion (bromo anisole was reacted for 15 F/mol to reach almost full conversion).

## 7.3 Scope Limitations

Aryl Bromides:

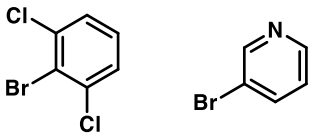

dehalogenation



trace

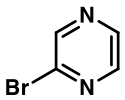

0%

trace

Alcohols:

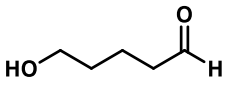

0%

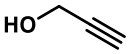

0%

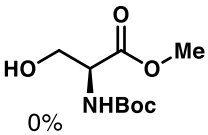

0%

# 8. Characterization Data

**Compound 1**

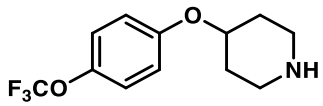


Following the Scale-up Flow Procedure with 1-bromo-4-(trifluoromethoxy)benzene (1.49 mL, 10 mmol, 1.0 equiv.) and *N*-boc-4-hydroxypiperidine (6.04 g, 30 mmol, 3.0 equiv.) in DMA (100 mL) for 3.5 F/mol afforded 1.754 mg (63%, 95% purity) of the title compound as off-white amorphous solid after purification using extractions (no column chromatography needed).

**Physical state:** off-white amorphous solid.

**$^{1}$H NMR** (300 MHz, $CDCl_3$) δ 7.18 – 7.05 (m, 2H), 6.95 – 6.82 (m, 2H), 4.32 (tt, *J* = 8.3, 3.9 Hz, 1H), 3.20 – 3.07 (m, 2H), 2.73 – 2.71 (m, 2H), 2.13 – 1.92 (m, 2H), 1.74 – 1.58 (m, 2H).

**$^{13}$C NMR** (75 MHz, $CDCl_3$) δ 156.1, 142.8 (d, *J* = 2.2 Hz), 122.6, 120.7 (d, *J* = 256.0 Hz), 117.0, 74.2, 44.1, 32.5.

**$^{19}$F NMR** (282 MHz, $CDCl_3$) δ -58.4.

**HRMS (ESI-TOF):** calculated for $C_{12}H_{15}F_3NO_2$ $[M+H]^+$: 262.1049 found 262.1056.

## Compound 4a[3]

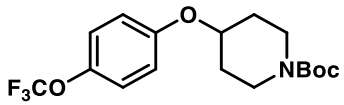


Following the General Flow Procedure with 1-bromo-4-(trifluoromethoxy)benzene (298 µL, 2 mmol, 1.0 equiv.) and *N*-boc-4-hydroxypiperidine (1.21 g, 6 mmol, 3.0 equiv.) in DMA (20 mL) for 4 F/mol afforded 424 mg (59%) of the title compound as a colorless oil after purification by column chromatography (normal phase, gradient elution, ethyl acetate/petrol ether from 0% to 25%).

**Physical state:** colorless oil.

**$^{1}$H NMR** (300 MHz, $CDCl_3$) δ 7.19 – 7.05 (m, 2H), 6.95 – 6.78 (m, 2H), 4.43 (tt, *J* = 7.1, 3.5 Hz, 1H), 3.76 – 3.62 (m, 2H), 3.41 – 3.26 (m, 2H), 1.99 – 1.83 (m, 2H), 1.82 – 1.62 (m, 2H), 1.47 (s, 9H).

**$^{13}$C NMR** (75 MHz, $CDCl_3$) δ 155.8, 155.0, 143.0 (d, *J* = 1.9 Hz), 122.7, 120.7 (d, *J* = 256.2 Hz), 117.0, 79.8, 72.9, 40.7, 30.5, 28.6.

**$^{19}$F NMR** (282 MHz, $CDCl_3$) δ -58.4.

**HRMS (ESI-TOF):** calculated for $C_{17}H_{22}F_3NO_4$ $[M\text{-boc}+2H]^+$: 262.1049 found: 262.1049.

## Compound 4b

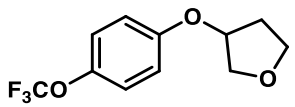

Following the General Flow Procedure with 1-bromo-4-(trifluoromethoxy)benzene (198.4 µL, 1.33 mmol, 1.0 equiv.) and tetrahydrofuran-3-ol (320 µL, 4 mmol, 3.0 equiv.) in DMA (20 mL) for 6 F/mol afforded 145 mg (44%) of the title compound as a pale yellow oil after purification by column chromatography (normal phase, gradient elution, ethyl acetate/petrol ether from 5% to 25%).

**Physical state:** pale yellow oil.

**$^{1}$H NMR** (300 MHz, $CDCl_3$) δ 7.20 – 7.06 (m, 2H), 6.91 – 6.76 (m, 2H), 4.89 (ddt, *J* = 6.1, 4.3, 2.3 Hz, 1H), 4.06 – 3.82 (m, 4H), 2.37 – 2.04 (m, 2H).

**$^{13}$C NMR** (75 MHz, $CDCl_3$) δ 156.0, 143.0 (d, *J* = 2.0 Hz), 122.7, 120.7 (d, *J* = 256.2 Hz), 116.2, 77.9, 73.1, 67.3, 33.0.

**$^{19}$F NMR** (282 MHz, $CDCl_3$) δ -58.4.

## Compound 4c[4]

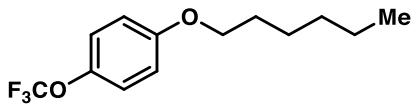


Following the General Flow Procedure with 1-bromo-4-(trifluoromethoxy)benzene (198.4 µL, 1.33 mmol, 1.0 equiv.) and *n*-hexanol (499 µL, 4 mmol, 3.0 equiv.) in DMAc (20 mL) for 6 F/mol afforded 178 mg (61%) of the title compound as a colorless oil after purification by column chromatography (normal phase, gradient elution, ethyl acetate/petrol ether from 0% to 15%).

**Physical state:** colorless oil.

**$^{1}$H NMR** (300 MHz, $CDCl_3$) δ 7.19 – 7.07 (m, 2H), 6.93 – 6.81 (m, 2H), 3.94 (t, *J* = 6.5 Hz, 2H), 1.85 – 1.70 (m, 2H), 1.54 – 1.40 (m, 2H), 1.40 – 1.25 (m, 4H), 0.99 – 0.85 (m, 3H).

**$^{13}$C NMR** (75 MHz, $CDCl_3$) δ 157.8, 142.7 (d, *J* = 2.1 Hz), 122.5, 120.7 (d, *J* = 255.9 Hz), 115.3, 68.6, 31.7, 29.3, 25.8, 22.8, 14.2.

**$^{19}$F NMR** (282 MHz, $CDCl_3$) δ -58.4.

## Compound 4d

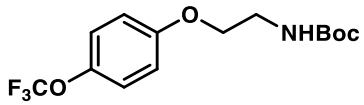


Following the General Flow Procedure with 1-bromo-4-(trifluoromethoxy)benzene (298 µL, 2 mmol, 1.0 equiv.) and *N*-boc-ethanolamine (967.2 mg, 6 mmol, 3.0 equiv.) in DMA (20 mL) for 6 F/mol afforded 393 mg (61%) of the title compound as a yellow oil after purification by column chromatography (normal phase, gradient elution, ethyl acetate/petrol ether from 0% to 25%).

**Physical state:** yellow oil.

**$^{1}$H NMR** (300 MHz, $CDCl_3$) δ 7.19 – 7.09 (m, 2H), 6.92 – 6.83 (m, 2H), 4.98 (bs, 1H), 4.00 (t, *J* = 5.1 Hz, 2H), 3.53 (q, *J* = 5.4 Hz, 2H), 1.45 (s, 9H).

**$^{13}$C NMR** (75 MHz, $CDCl_3$) δ 157.2, 156.0z, 143.1 (d, *J* = 2.0 Hz), 122.6, 120.7 (d, *J* = 256.0 Hz), 115.3, 79.8, 67.7, 40.2, 28.5.

**$^{19}$F NMR** (282 MHz, $CDCl_3$) δ -58.4.

**HRMS (ESI-TOF):** calculated for $C_9H_{11}F_3NO_2$ $[M+HCOOH-H]^+$: 366.1170 found: 366.1200.

## Compound 4e

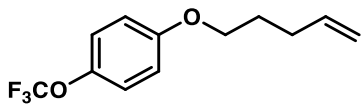

Following the General Flow Procedure with 1-bromo-4-(trifluoromethoxy)benzene (198.4 µL, 1.33 mmol, 1.0 equiv.) and pent-4-en-1-ol (412 µL, 4 mmol, 3.0 equiv.) in DMAc (20 mL) for 6 F/mol afforded 162 mg (49%) of the title compound as a yellow oil after purification by column chromatography (normal phase, gradient elution, ethyl acetate/petrol ether from 0% to 15%).

**Physical state:** yellow oil.

**$^{1}$H NMR** (300 MHz, $CDCl_3$) δ 7.19 – 7.07 (m, 2H), 6.94 – 6.82 (m, 2H), 5.85 (ddt, *J* = 16.9, 10.2, 6.6 Hz, 1H), 5.14 – 4.96 (m, 2H), 3.95 (t, *J* = 6.4 Hz, 2H), 2.31 – 2.17 (m, 2H), 1.89 (dq, *J* = 8.2, 6.6 Hz, 2H).

**$^{13}$C NMR** (75 MHz, $CDCl_3$) δ 157.7, 142.7 (d, *J* = 2.0 Hz), 137.8, 122.5, 120.7 (d, *J* = 256.0 Hz), 115.5, 115.3, 67.7, 30.2, 28.5.

**$^{19}$F NMR** (282 MHz, $CDCl_3$) δ -58.4.

**HRMS (ESI-TOF):** calculated for $C_{12}H_{14}F_3O_2$ $[M+H]^+$: 247.0941 found: 247.0929.

## Compound 4f

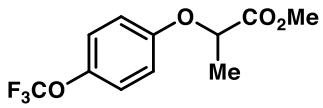


Following the General Flow Procedure with 1-bromo-4-(trifluoromethoxy)benzene (298 µL, 2 mmol, 1.0 equiv.) and methyl lactate (573 µL, 6 mmol, 3.0 equiv.) in DMA (20 mL) for 8 F/mol afforded 220 mg (42%) of the title compound as a pale yellow oil after purification by column chromatography (normal phase, gradient elution, ethyl acetate/petrol ether from 5% to 20%).

**Physical state:** pale yellow oil.

**$^{1}$H NMR** (300 MHz, $CDCl_3$) δ 7.19 – 7.06 (m, 2H), 6.91 – 6.80 (m, 2H), 4.73 (q, *J* = 6.8 Hz, 1H), 3.76 (s, 3H), 1.62 (d, *J* = 6.8 Hz, 3H).

**$^{13}$C NMR** (75 MHz, $CDCl_3$) δ 172.4, 156.1, 143.5 (d, *J* = 2.0 Hz), 122.6, 120.7 (d, *J* = 256.2 Hz), 116.1, 73.1, 52.3, 18.7.

**$^{19}$F NMR** (282 MHz, $CDCl_3$) δ -58.4.

**HRMS (ESI-TOF):** calculated for $C_{11}H_{12}F_3O_4$ $[M+H]^+$: 265.0682 found: 265.0692.

## Compound 4g[5]

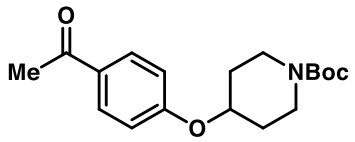


Following the General Flow Procedure with 4'-bromoacetophenone (265 mg, 1.33 mmol, 1.0 equiv.) and *N*-boc-4-hydroxypiperidine (805 mg, 4 mmol, 3.0 equiv.) in DMAc (20 mL) for 6 F/mol afforded 122 mg (29%) of the title compound as a white amorphous solid after purification by column chromatography (normal phase, gradient elution, ethyl acetate/petrol ether from 0% to 25%). During the extractive part of the workup the organic phase was washed an extra 3x with NaOH (1M aq., 100 mL) to separate the phenol side product.

**Physical state:** white amorphous solid.

**$^{1}$H NMR** (300 MHz, $CDCl_3$) δ 8.00 – 7.85 (m, 2H), 6.97 – 6.87 (m, 2H), 4.57 (tt, *J* = 7.2, 3.6 Hz, 1H), 3.68 (ddd, *J* = 13.5, 7.6, 3.8 Hz, 2H), 3.36 (ddd, *J* = 13.6, 7.6, 3.9 Hz, 2H), 2.54 (s, 3H), 2.04 – 1.86 (m, 2H), 1.84 – 1.64 (m, 2H), 1.46 (s, 9H).

**$^{13}$C NMR** (75 MHz, $CDCl_3$) δ 196.8, 161.4, 154.9, 130.8, 130.5, 115.3, 79.8, 72.3, 40.4, 30.5, 28.5, 26.5.

## Compound 4h

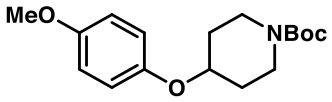


Following the General Flow Procedure with 4-bromoanisole (167 µL mg, 1.33 mmol, 1.0 equiv.) and *N*-boc-4-hydroxypiperidine (805 mg, 4 mmol, 3.0 equiv.) in DMA (20 mL) for 16 F/mol afforded 130 mg (32%) of the title compound as yellow oil after purification by column chromatography (normal phase, gradient elution, ethyl acetate/petrol ether from 0% to 25%).

**Physical state:** Yellow oil.

**$^{1}$H NMR** (300 MHz, $CDCl_3$) δ 6.91 – 6.73 (m, 4H), 4.31 (tt, *J* = 7.2, 3.6 Hz, 1H), 3.75 (s, 3H), 3.74 – 3.64 (m, 2H), 3.28 (ddd, *J* = 13.5, 7.9, 3.8 Hz, 2H), 1.95 – 1.80 (m, 2H), 1.79 – 1.59(m, 2H) 1.46 (s, 9H).

**$^{13}$C NMR** (75 MHz, $CDCl_3$) δ 155.0 154.3, 151.2, 118.0, 116.1, 114.8, 79.7, 73.5, 55.8, 41.0, 28.5.

**HRMS (ESI-TOF):** calculated for $C_{12}H_{18}NO_2$ [M-Boc+2H]+: 208.1338 found: 208.1339

## Compound 4i

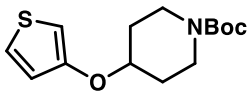


Following the General Flow Procedure with 3-bromo-thiophene (124.6 µL, 1.33 mmol, 1.0 equiv.) and *N*-boc-4-hydroxypiperidine (805 mg, 4 mmol, 3.0 equiv.) in DMAc (20 mL) for 6 F/mol afforded 162 mg (43%) of the title compound as a white amorphous solid after purification by column chromatography (normal phase, gradient elution, ethyl acetate/petrol ether from 5% to 20%).

**Physical state:** white amorphous solid.

**$^{1}$H NMR** (300 MHz, $CDCl_3$) δ 7.16 (dd, *J* = 5.2, 3.1 Hz, 1H), 6.74 (dd, *J* = 5.2, 1.5 Hz, 1H), 6.27 (dd, *J* = 3.2, 1.6 Hz, 1H), 4.30 (tt, *J* = 7.2, 3.6 Hz, 1H), 3.68 (ddd, *J* = 13.4, 7.5, 3.8 Hz, 2H), 3.31 (ddd, *J* = 13.5, 7.7, 3.9 Hz, 2H), 2.00 – 1.85 (m, 2H), 1.83 – 1.66 (m, 2H), 1.46 (s, 9H).

**$^{13}$C NMR** (75 MHz, $CDCl_3$) δ 155.9, 154.9, 124.8, 120.3, 99.4, 79.7, 74.7, 40.8, 28.6.

**HRMS (ESI-TOF):** calculated for $C_9H_{13}NOS$ $[M\text{-}Boc+2H]^+$: 184.0796 found: 184.0807

## Compound 4j

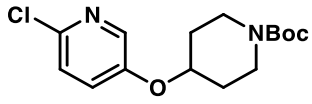


Following the General Flow Procedure with 5-bromo-2-chloropyridine (256 mg, 1.33 mmol, 1.0 equiv.) and *N*-boc-4-hydroxypiperidine (805 mg, 4 mmol, 3.0 equiv.) in DMAc (20 mL) for 6 F/mol afforded 164 mg (39%) of the title compound as an off-white amorphous solid after purification by column chromatography (normal phase, gradient elution, ethyl acetate/petrol ether from 0% to 25%, silica was neutralized with petrol ether + 1% triethylamine before starting the chromatography).

**Physical state:** off-white amorphous solid.

**$^{1}$H NMR** (300 MHz, $CDCl_3$) δ 8.03 (dd, *J* = 2.7, 1.0 Hz, 1H), 7.26 – 7.12 (m, 2H), 4.45 (tt, *J* = 7.2, 3.6 Hz, 1H), 3.67 (ddd, *J* = 13.5, 7.5, 3.9 Hz, 2H), 3.32 (ddd, *J* = 13.6, 7.7, 3.8 Hz, 2H), 1.98 – 1.83 (m, 2H), 1.80 – 1.63 (m, 2H), 1.44 (s, 9H).

**$^{13}$C NMR** (75 MHz, $CDCl_3$) δ 154.8, 152.8, 142.8, 138.3, 126.4, 124.6, 79.9, 73.5, 40.5, 30.3, 28.5.

**HRMS (ESI-TOF):** calculated for $C_{11}H_{14}ClN_2O_3$ $[M+HCOOH-H]^-$: 357.1223 found: 357.1252

## Compound 4k

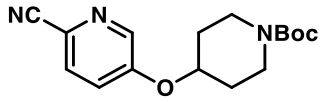


Following the General Flow Procedure with 5-bromo-picolinonitrile (243.4 mg, 1.33 mmol, 1.0 equiv.) and *N*-boc-4-hydroxypiperidine (805 mg, 4 mmol, 3.0 equiv.) in DMAc (20 mL) for 6 F/mol afforded 130 mg (32%) of the title compound as an off-white amorphous solid after purification by column chromatography (normal phase, gradient elution, ethyl acetate/petrol ether from 10% to 40%, silica was neutralized with petrol ether + 1% triethylamine before starting the chromatography).

**Physical state:** white amorphous solid.

**$^{1}$H NMR** (300 MHz, $CDCl_3$) δ 8.35 (dd, *J* = 2.9, 0.7 Hz, 1H), 7.63 (dd, *J* = 8.6, 0.6 Hz, 1H), 7.28 – 7.19 (m, 1H), 4.60 (tt, *J* = 7.2, 3.6 Hz, 1H), 3.69 (ddd, *J* = 13.7, 7.6, 3.9 Hz, 2H), 3.36 (ddd, *J* = 13.6, 7.7, 3.9 Hz, 2H), 2.06 – 1.88 (m, 2H), 1.85 – 1.68 (m, 2H), 1.46 (s, 9H).

**$^{13}$C NMR** (75 MHz, $CDCl_3$) δ 155.9, 154.8, 141.2, 129.7, 125.4, 121.4, 117.6, 80.1, 73.5, 40.5, 30.2, 28.5.

**HRMS (ESI-TOF):** calculated for $C_{12}H_{14}N_3O_3$ $[M+HCOOH-H]^-$: 348.1565 found: 348.1585

# 9. References


1. Zhang, H.-J.; Chen, L.; Oderinde, M. S.; Edwards, J. T.; Kawamata, Y.; Baran, P. S. *Angew. Chem. Int. Ed.* **2021**, *60*, 20700-20705. DOI: 10.1002/anie.202107820
2. Ghosh, I.; Shlapakov, N.; Karl, T. A.; Düker, J.; Nikitin, M.; Burykina, J. V.; Ananikov, V. P.; König, B. *Nature* **2023**, *619*, 87-93. DOI: 10.1038/s41586-023-06087-4
3. Chen, Z.; Jiang, Y.; Zhang, L.; Guo, Y.; Ma, D. *J. Am. Chem. Soc.* **2019**, *141*, 3541-3549. DOI: 10.1021/jacs.8b12142
4. Yoshizawa, A.; Segawa, S.; Ogasawara, F. *Chem. Mater.*, **2005**, *17*, 6442-6446. DOI: 10.1021/cm051441q
5. Shen, X.; Neumann, C. N.; Kleinlein, C.; Goldberg, N. W.; Ritter, T. *Angew. Chem. Int. Ed.* **2015**, *54*, 5662-5665. DOI: 10.1002/anie.201500902

# 10. NMR Spectra

Compound **1** $^{1}$H NMR (300 MHz, $CDCl_3$)

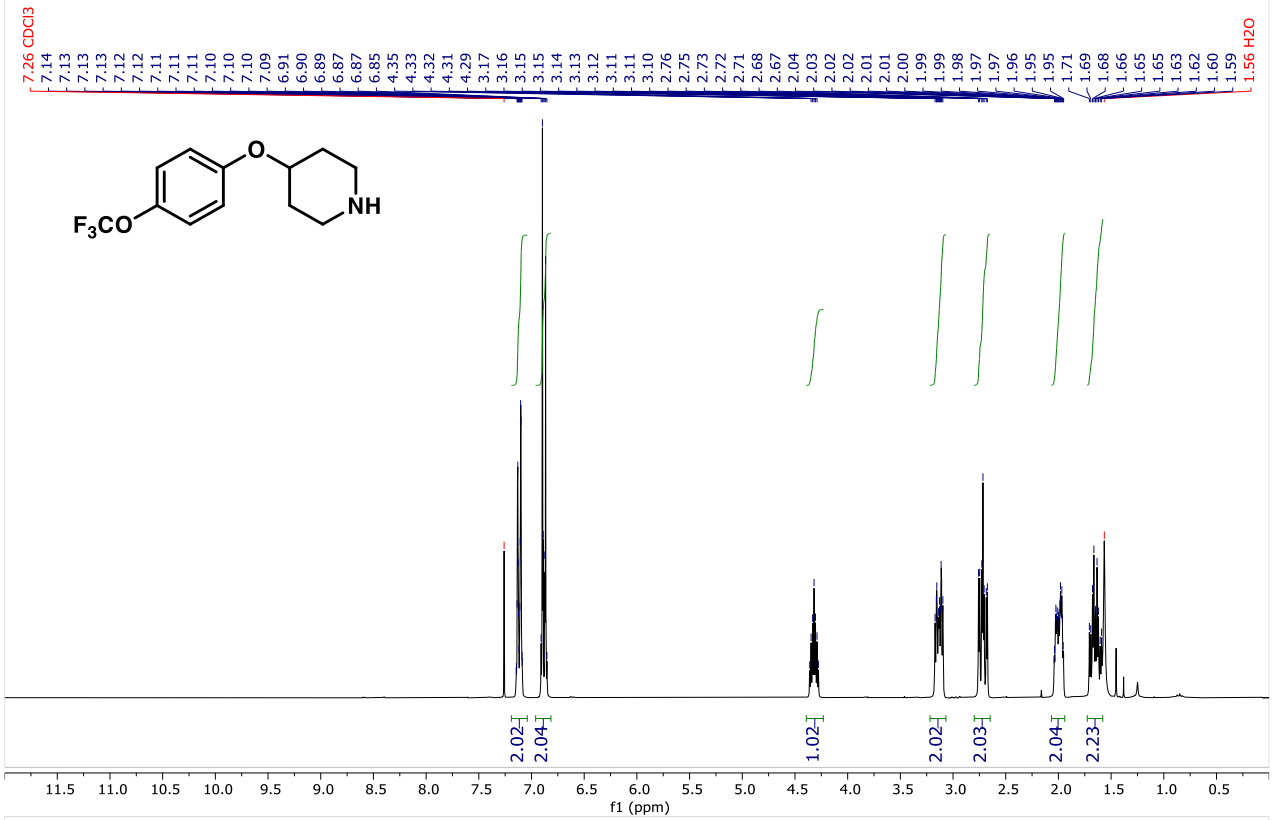


Compound **1** $^{13}$C NMR (75 MHz, $CDCl_3$)

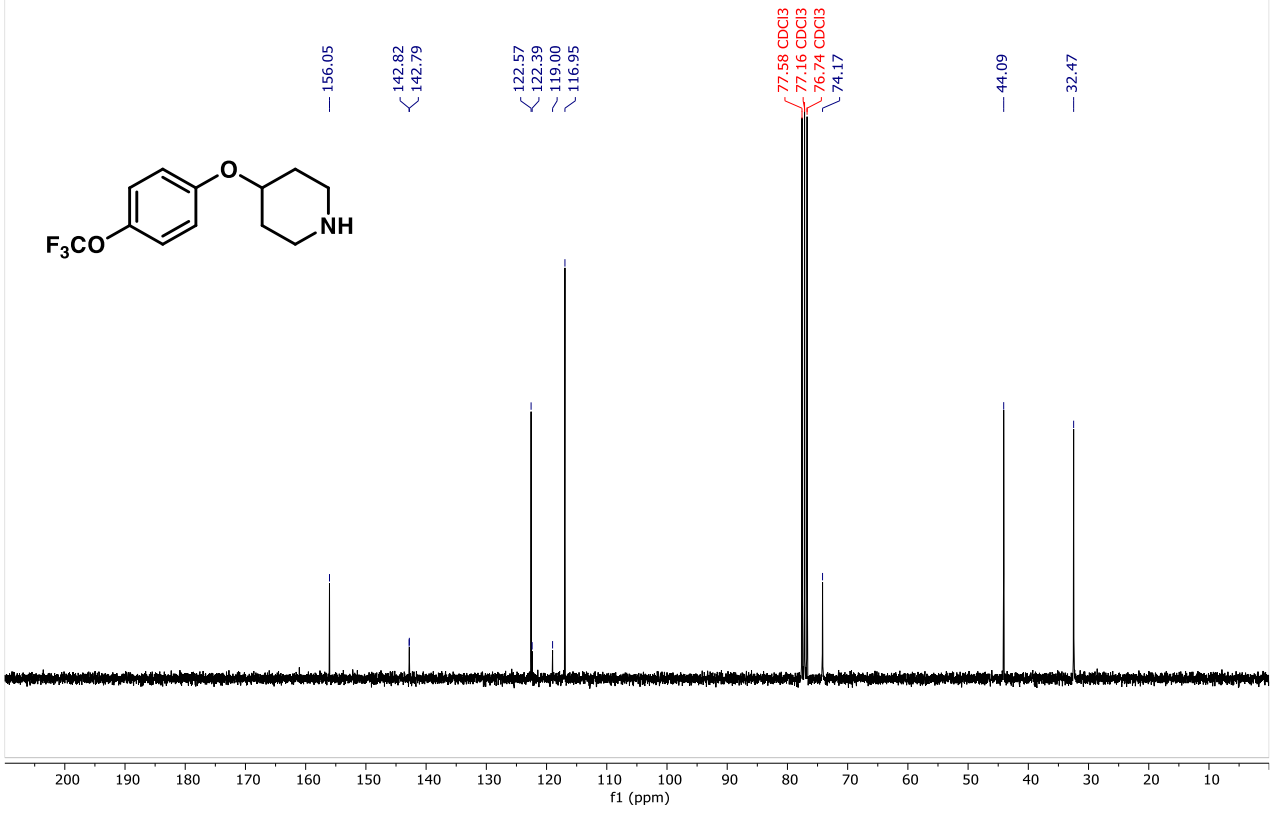

Compound **1** $^{19}F$ NMR (282 MHz, $CDCl_3$)

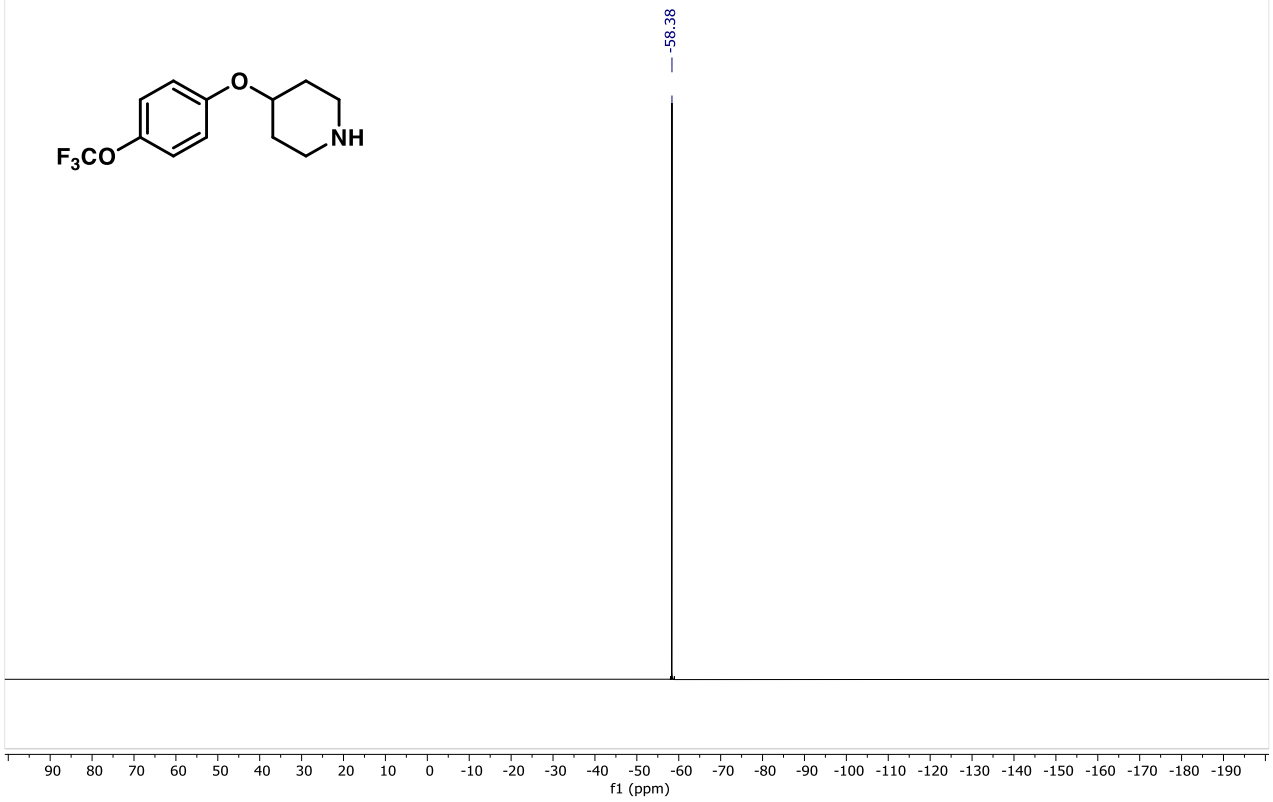

Compound **4a** $^{1}$H NMR (300 MHz, $CDCl_3$)

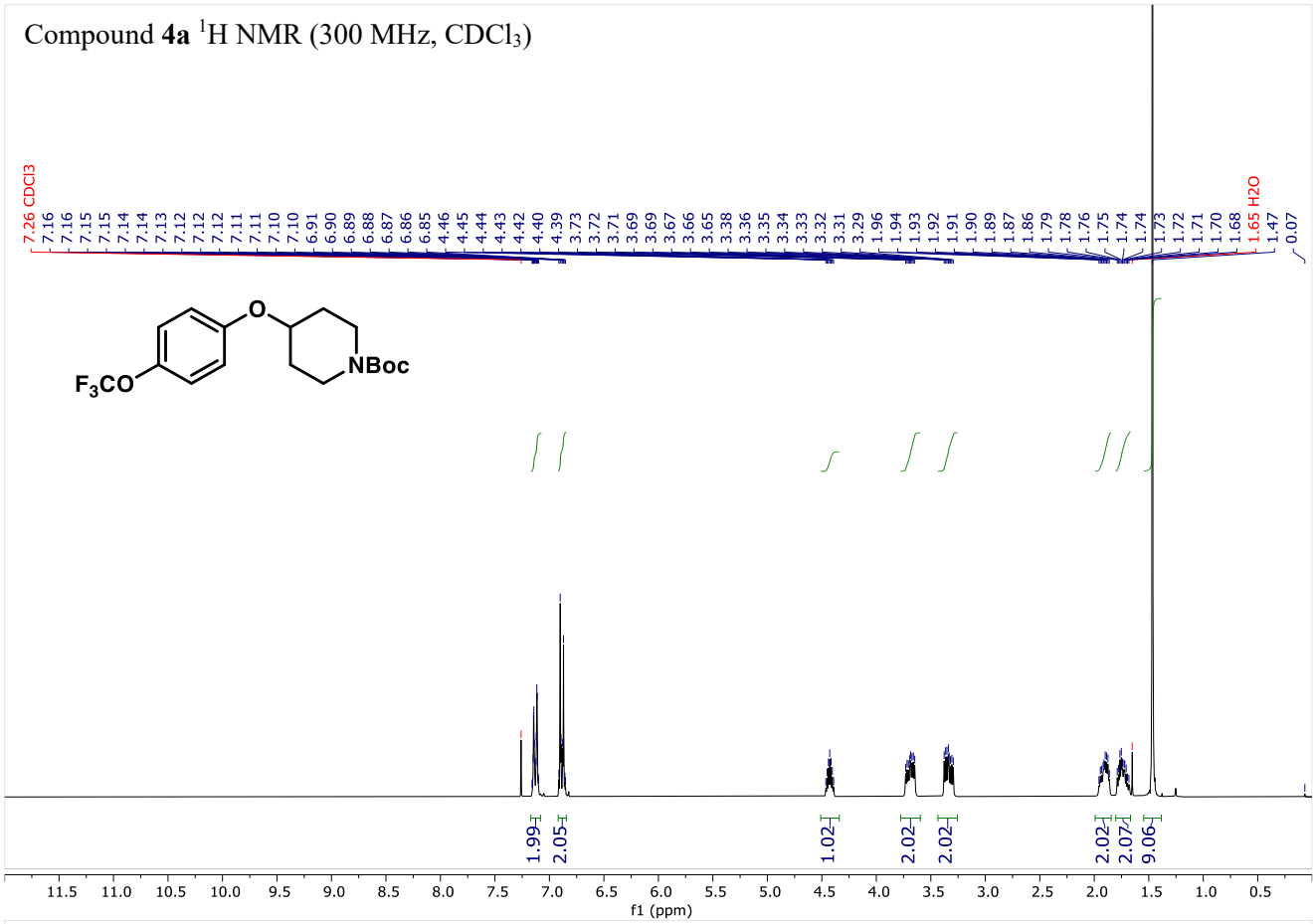


Compound **4a** $^{13}$C NMR (75 MHz, $CDCl_3$)

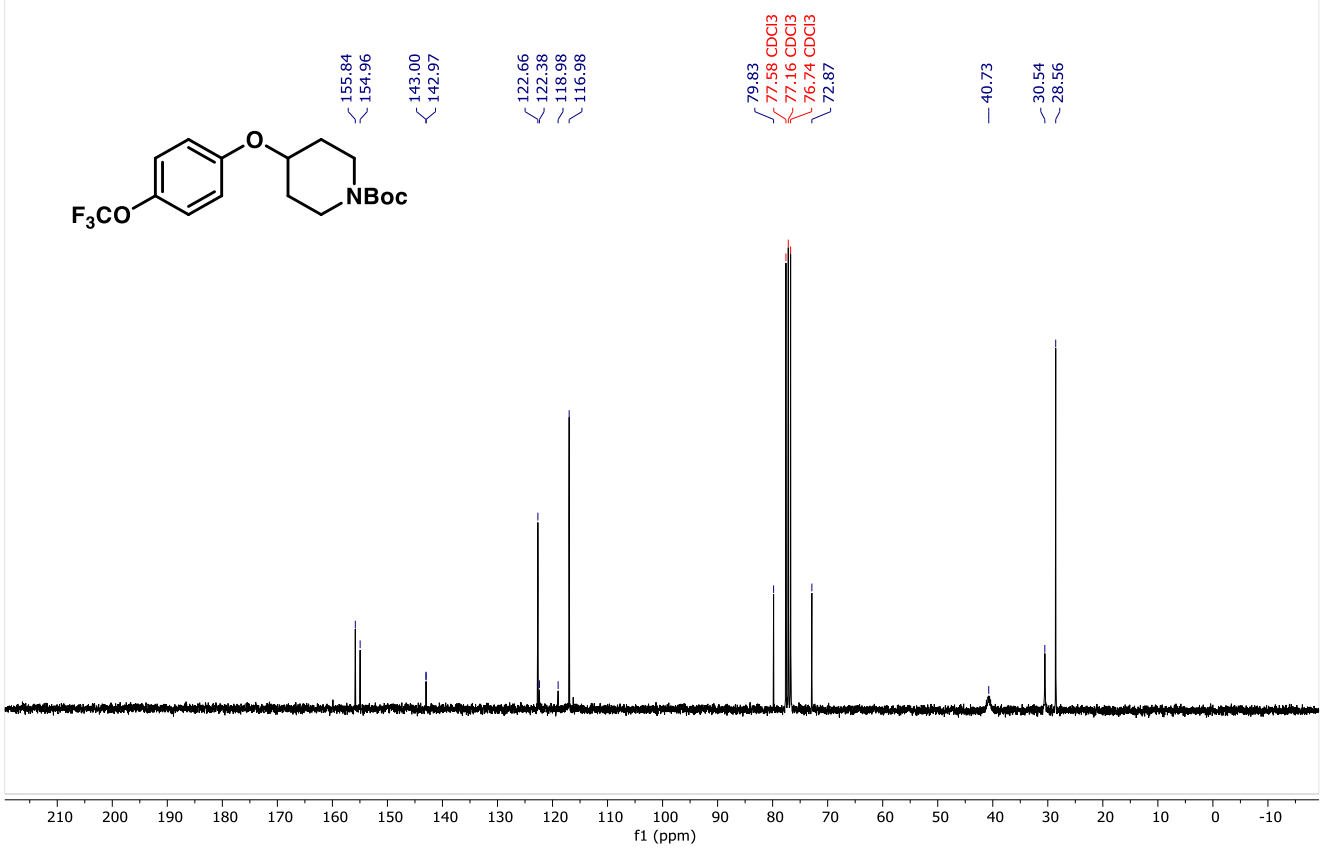

Compound **4a** $^{19}F$ NMR (282 MHz, $CDCl_3$)

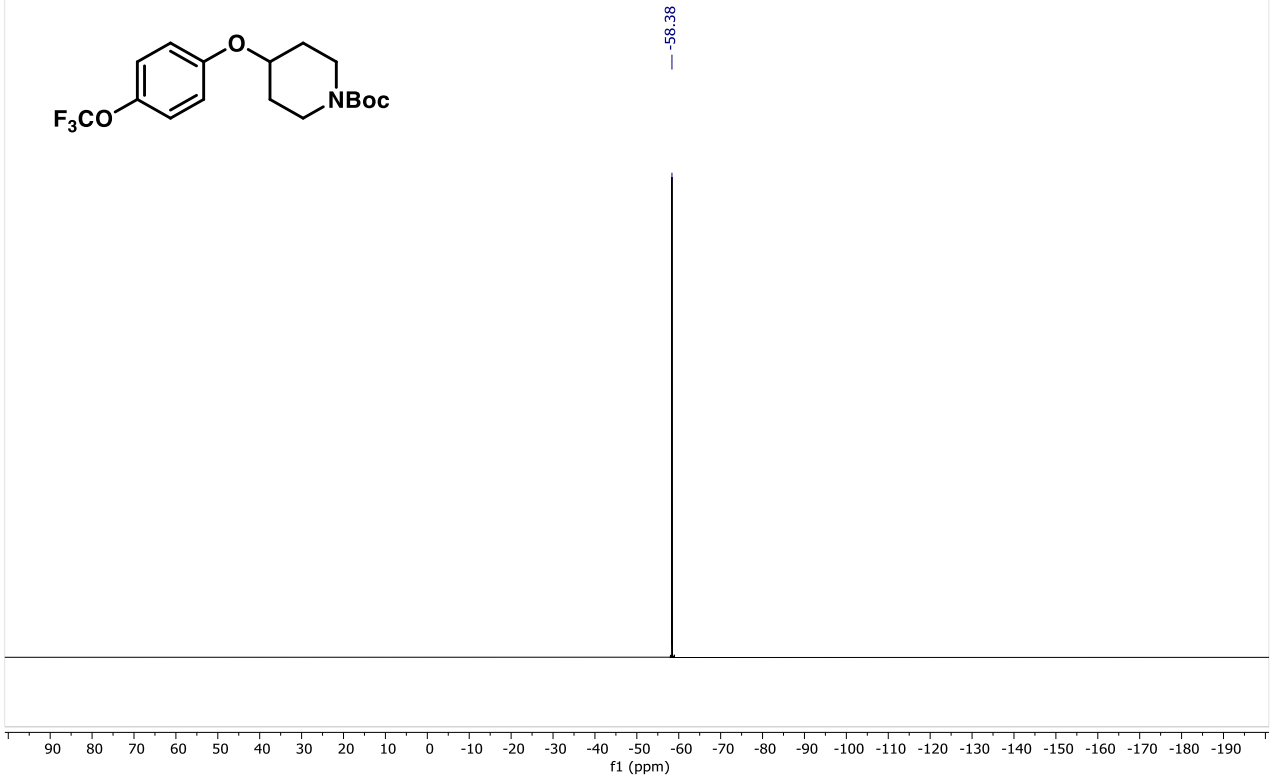

Compound **4b** $^{1}H$ NMR (300 MHz, $CDCl_3$)

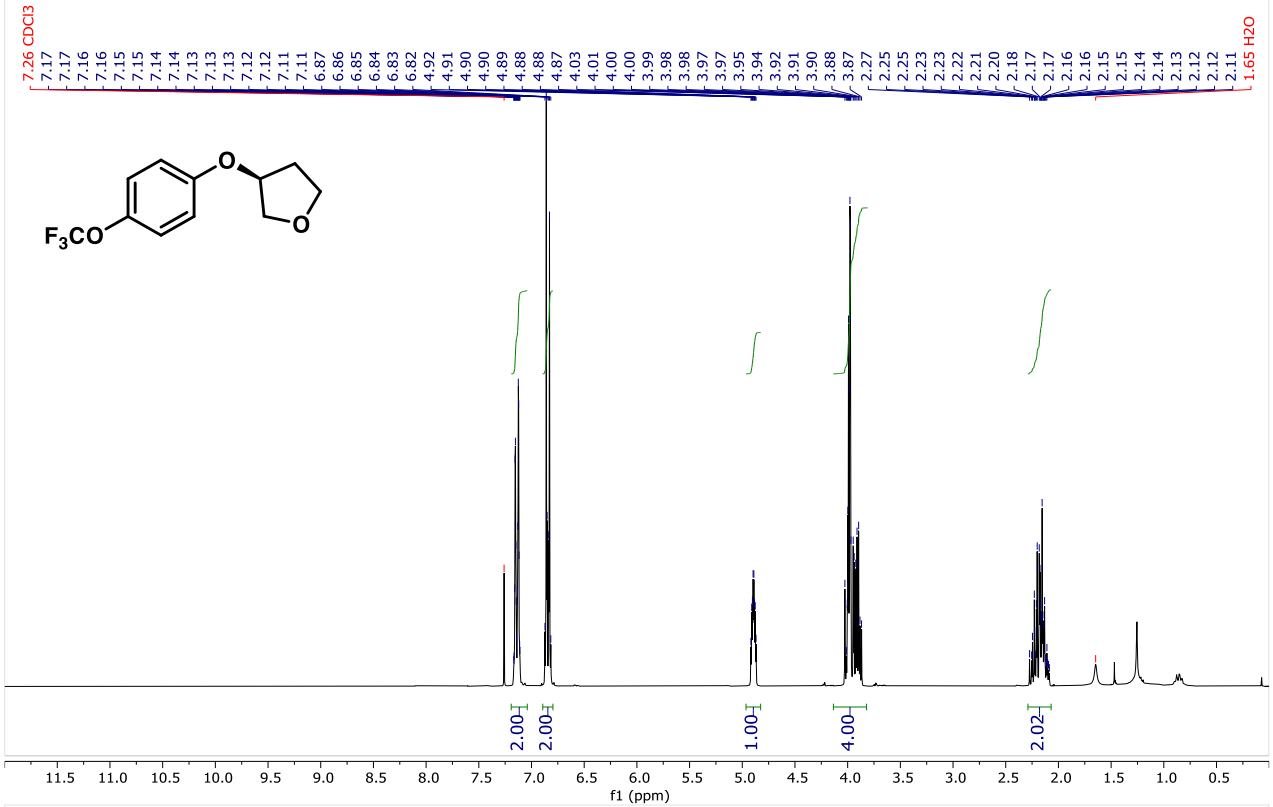


Compound **4b** $^{13}C$ NMR (75 MHz, $CDCl_3$)

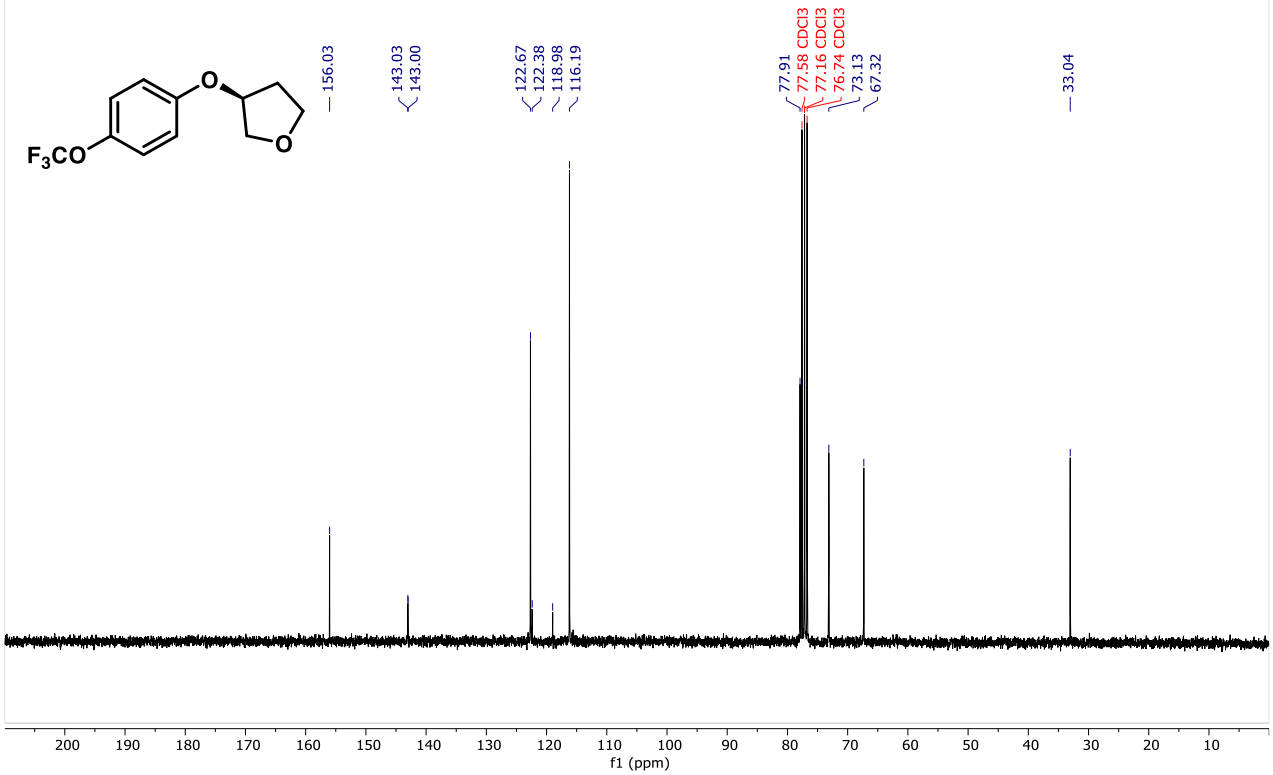

Compound **4b** $^{19}F$ NMR (282 MHz, $CDCl_3$)

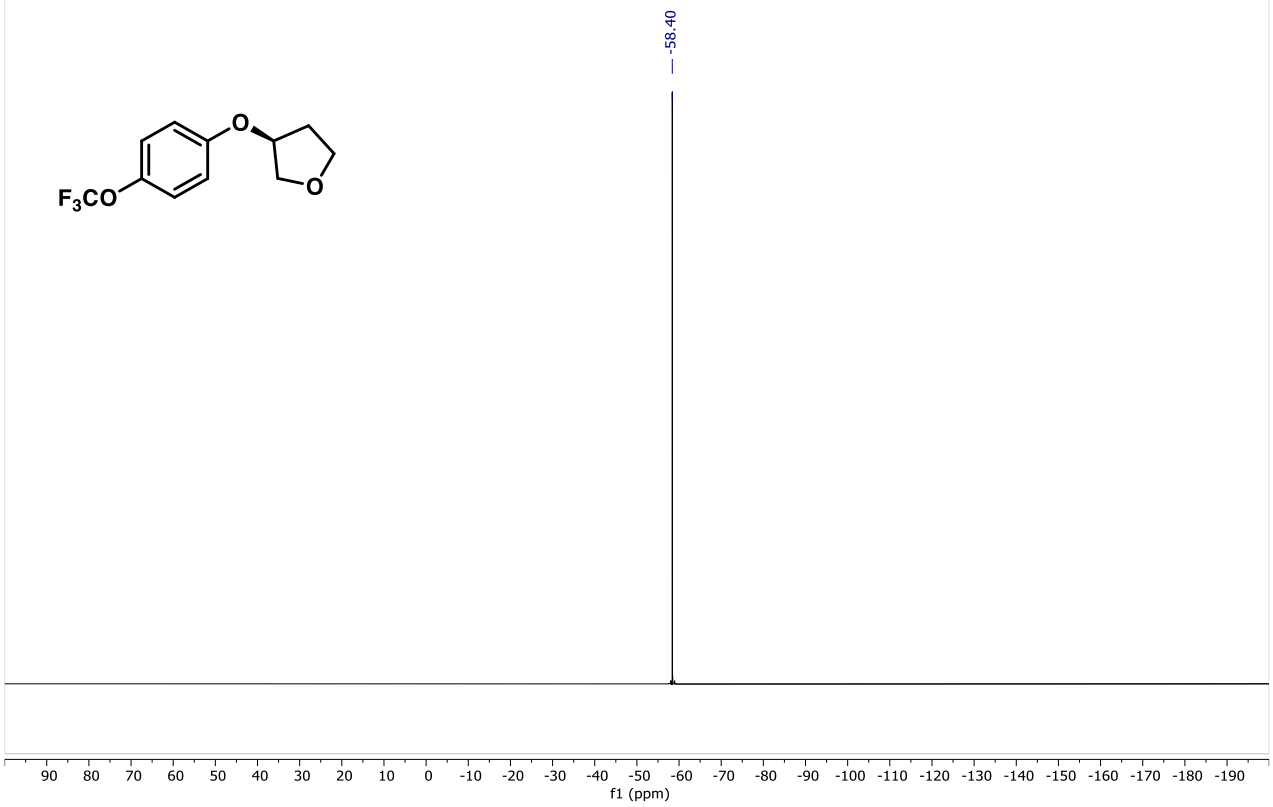

Compound **4c** $^{1}$H NMR (300 MHz, $CDCl_3$)

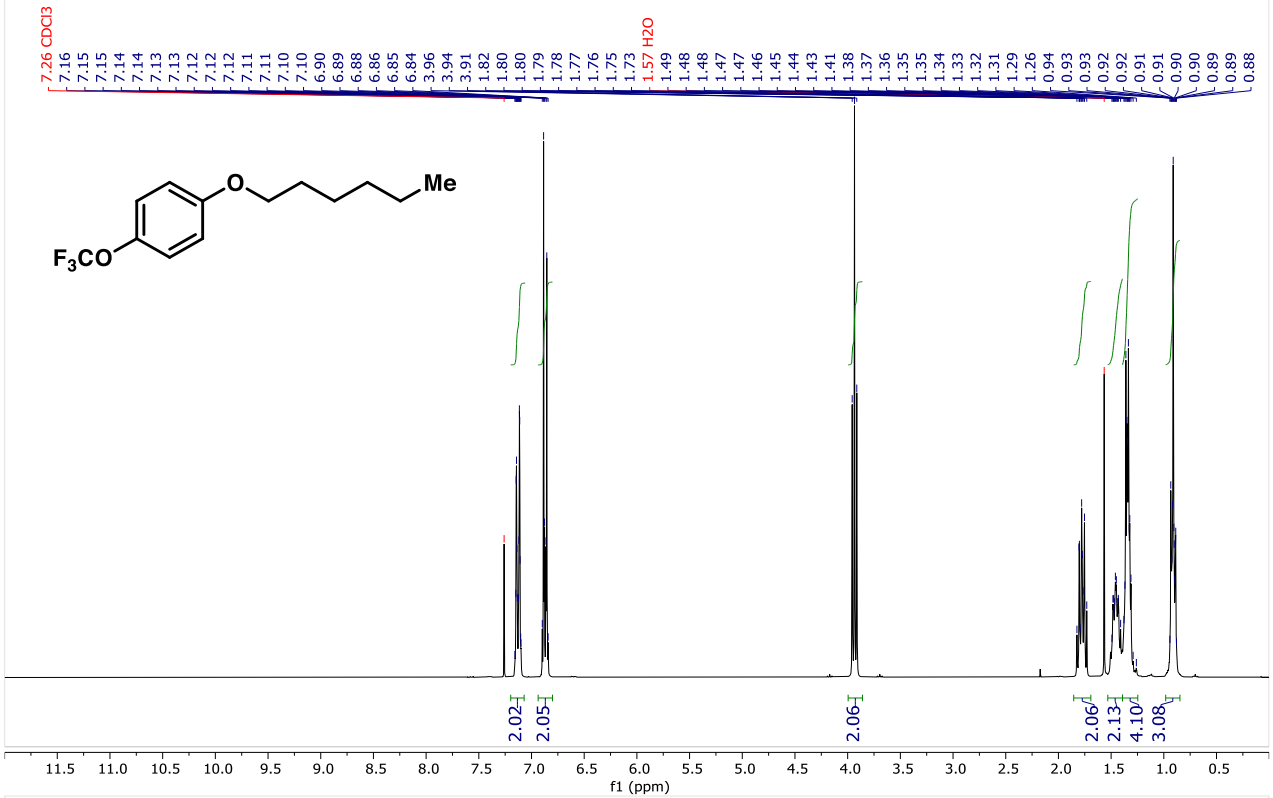


Compound **4c** $^{13}$C NMR (75 MHz, $CDCl_3$)

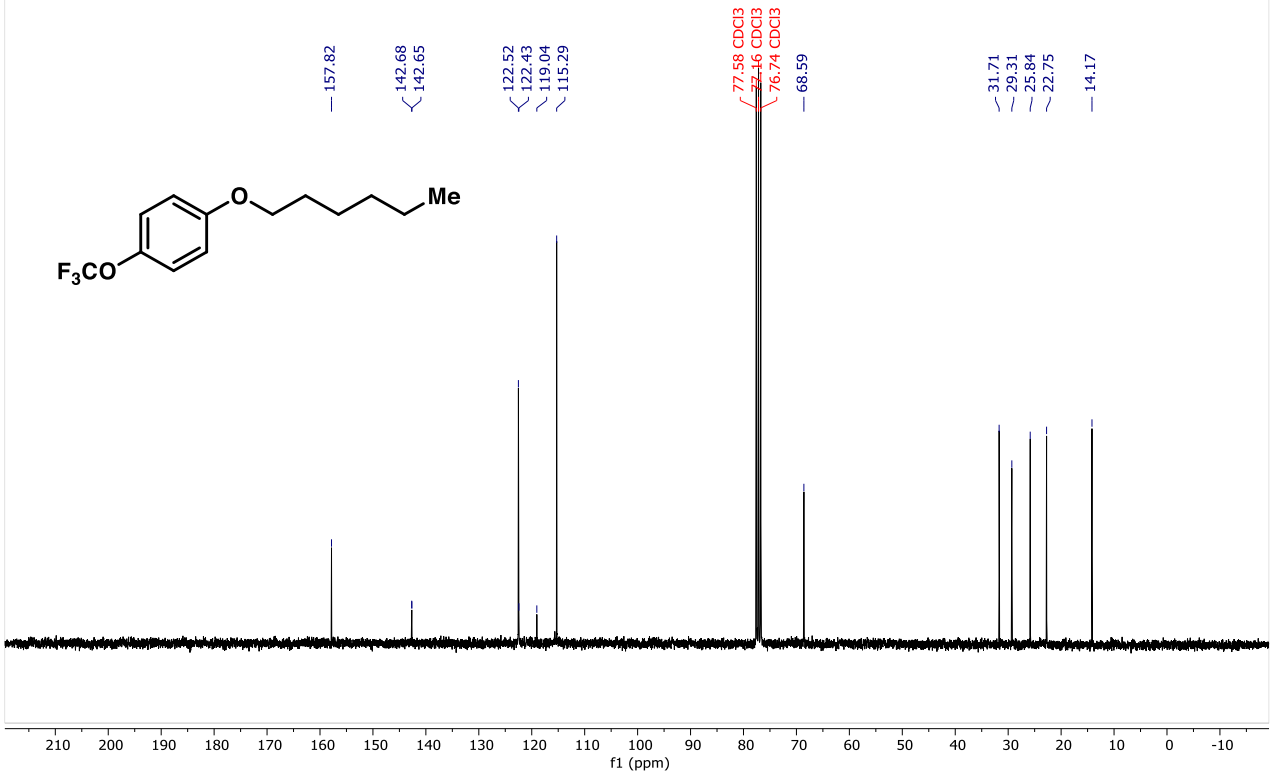

Compound **4c** $^{19}F$ NMR (282 MHz, $CDCl_3$)

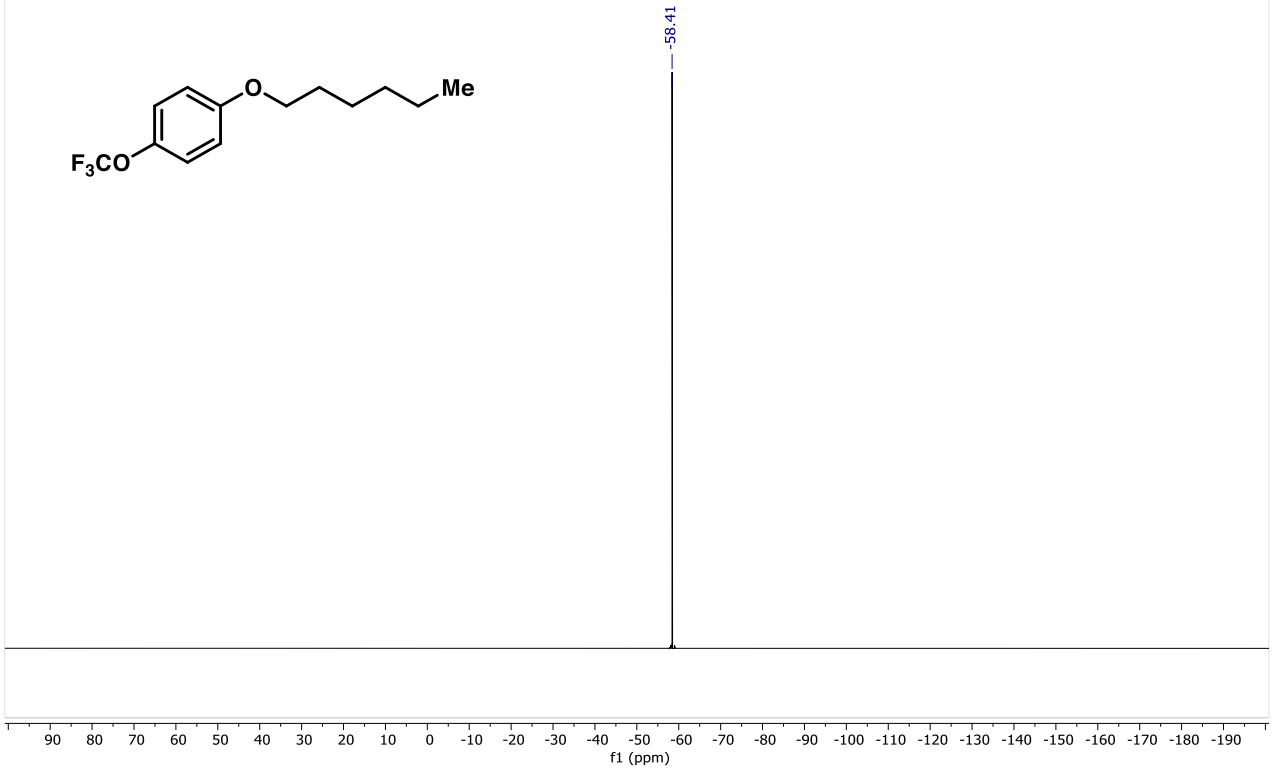

Compound **4d** $^{1}$H NMR (300 MHz, $CDCl_3$)

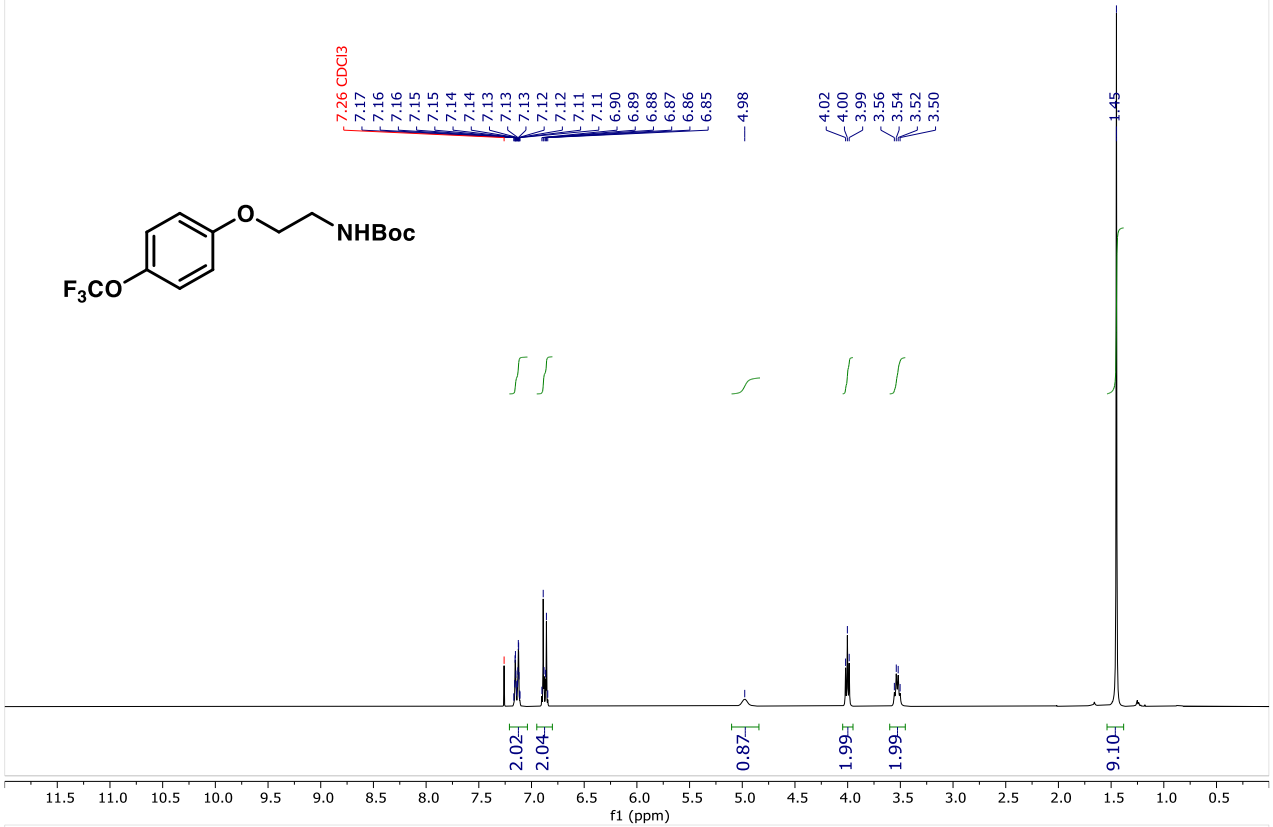


Compound **4d** $^{13}$C NMR (75 MHz, $CDCl_3$)

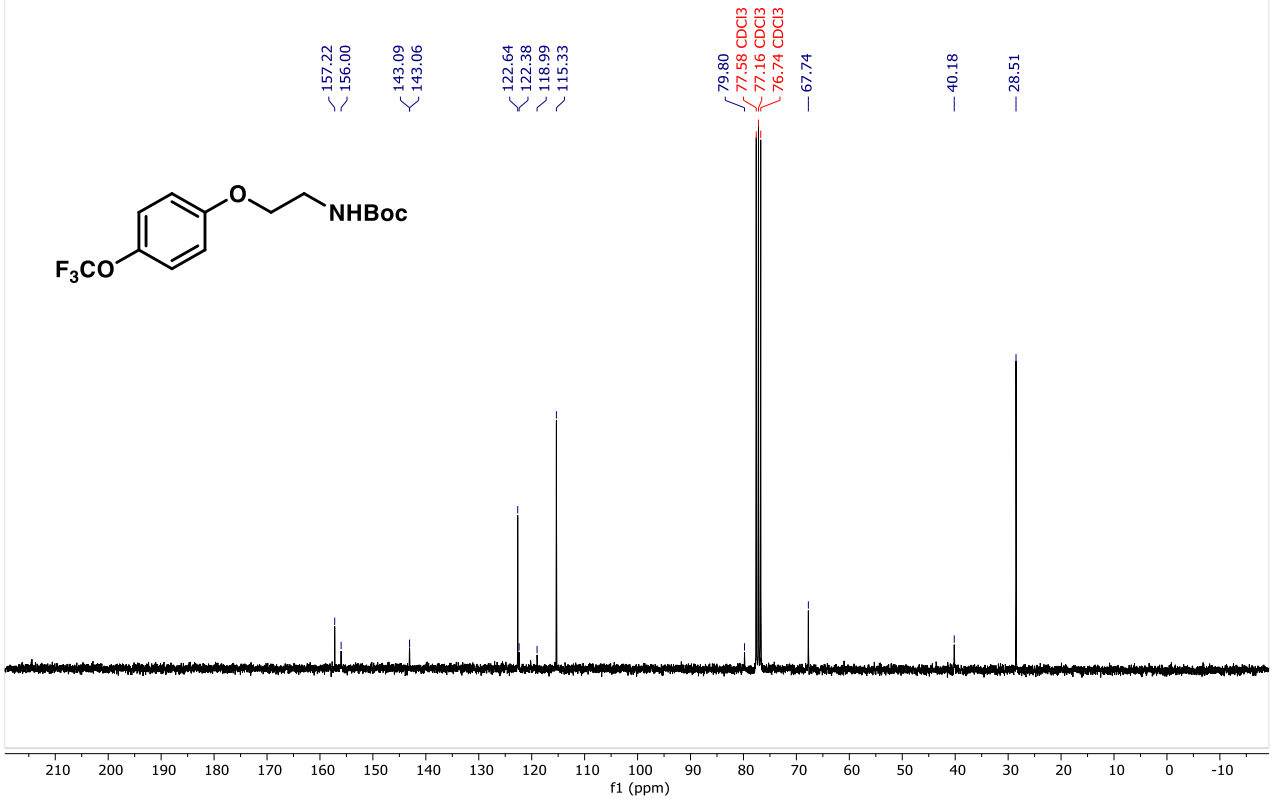

Compound **4d** $^{19}F$ NMR (282 MHz, $CDCl_3$)

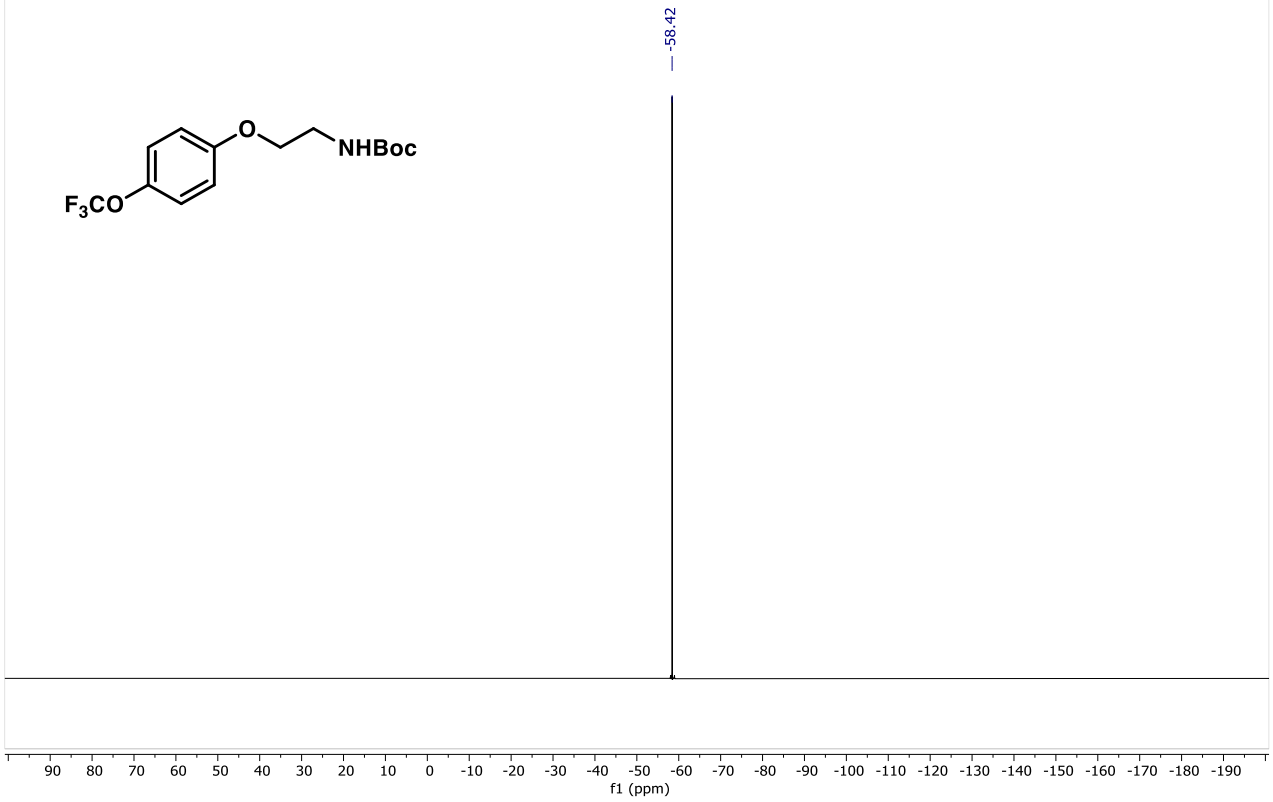

Compound **4e** $^{1}H$ NMR (300 MHz, $CDCl_3$)

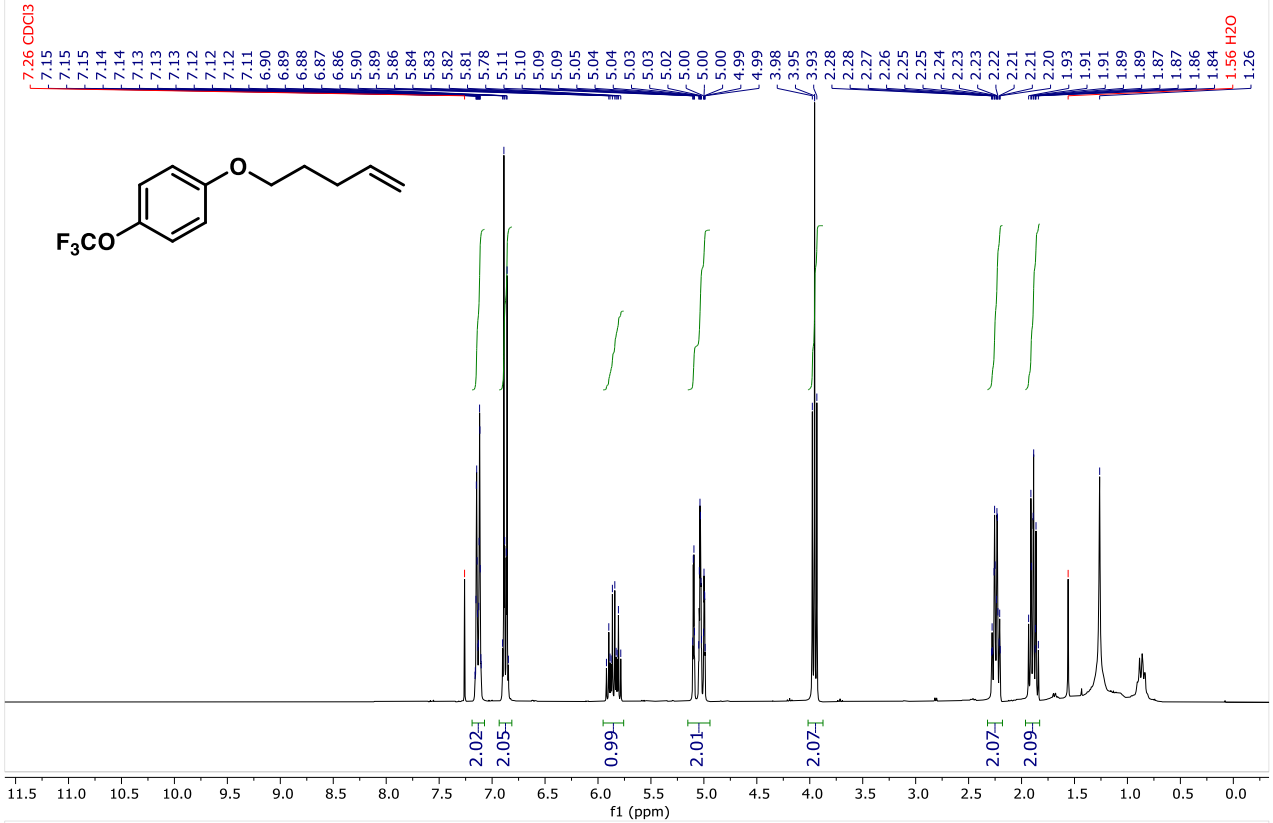


Compound **4e** $^{13}C$ NMR (75 MHz, $CDCl_3$)

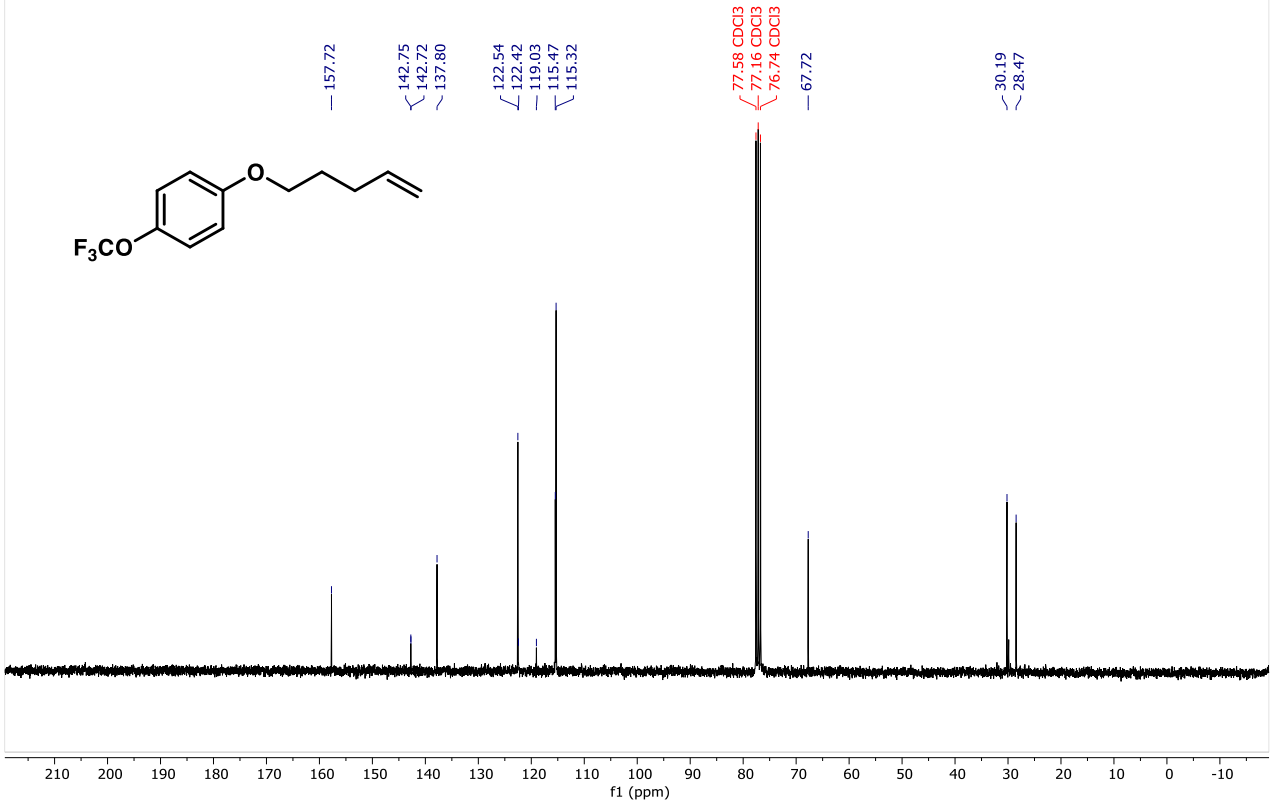

Compound **4e** $^{19}F$ NMR (282 MHz, $CDCl_3$)

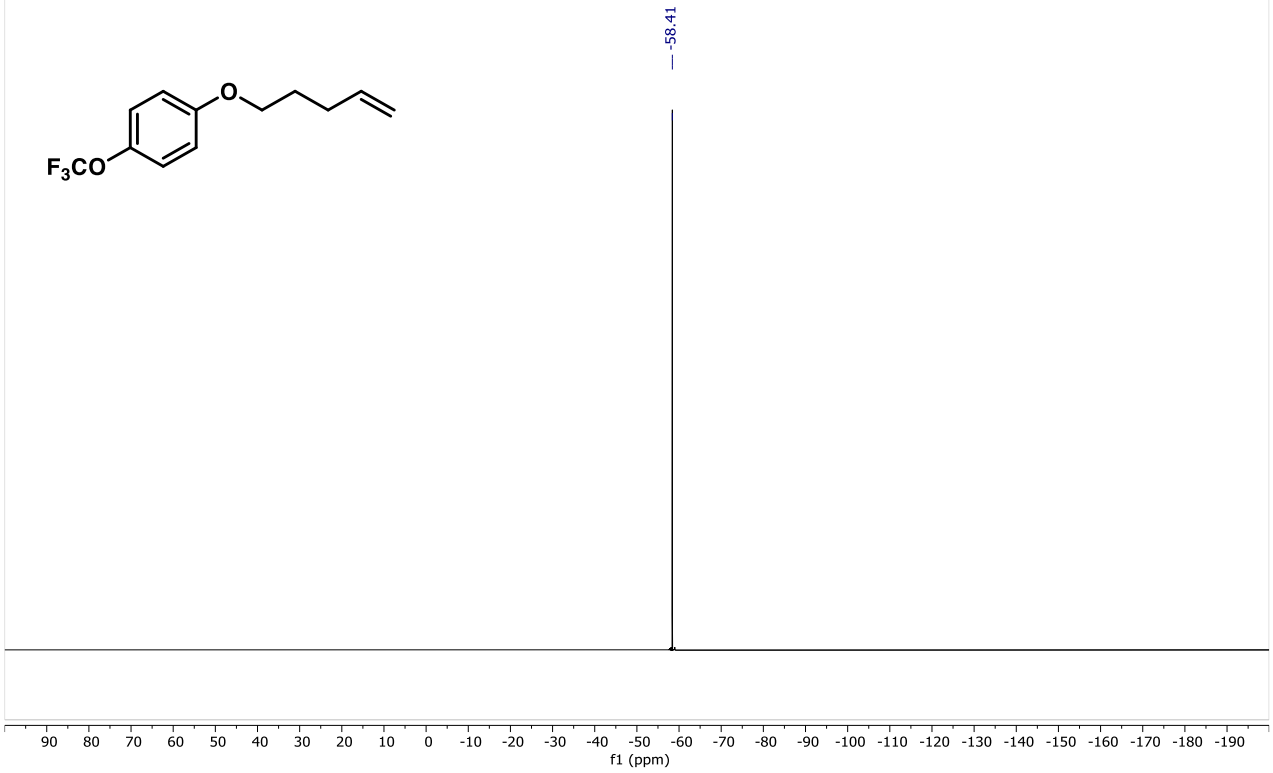

Compound **4f** $^{1}$H NMR (300 MHz, $CDCl_3$)

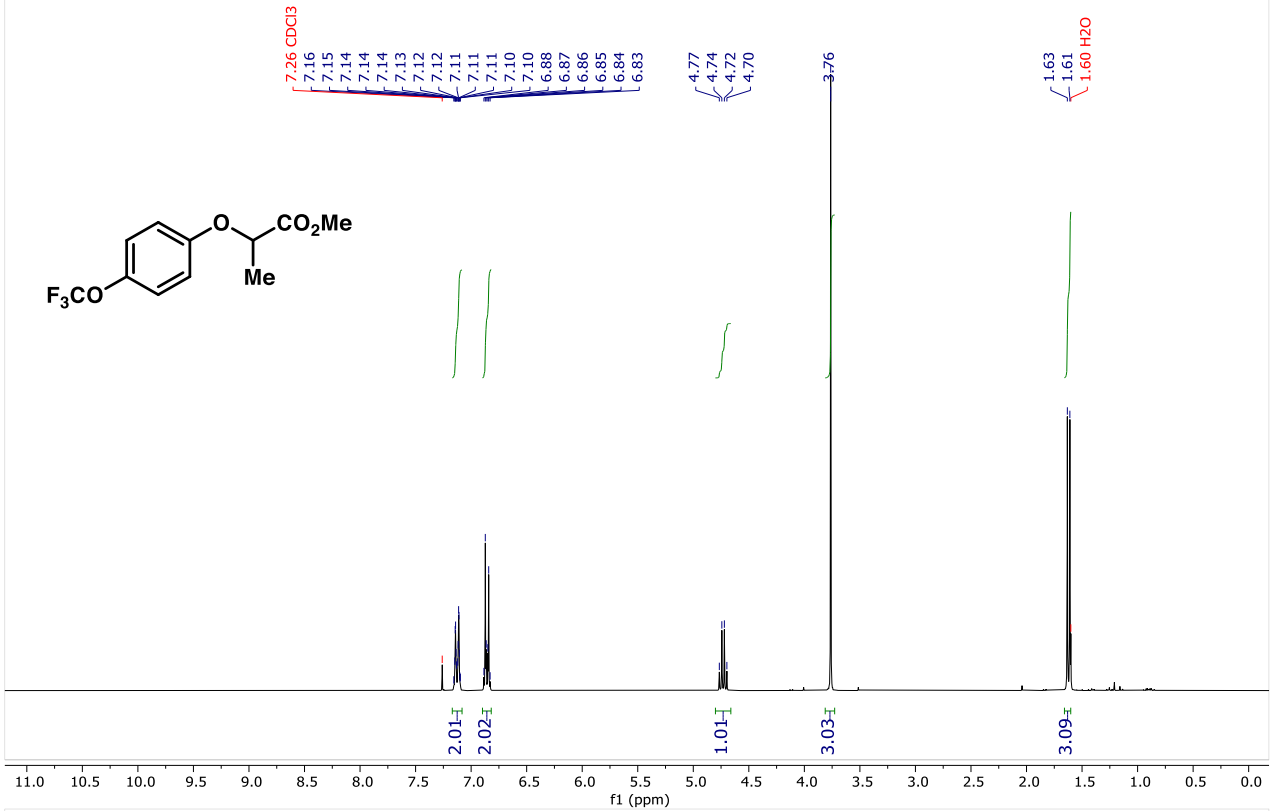


Compound **4f** $^{13}$C NMR (75 MHz, $CDCl_3$)

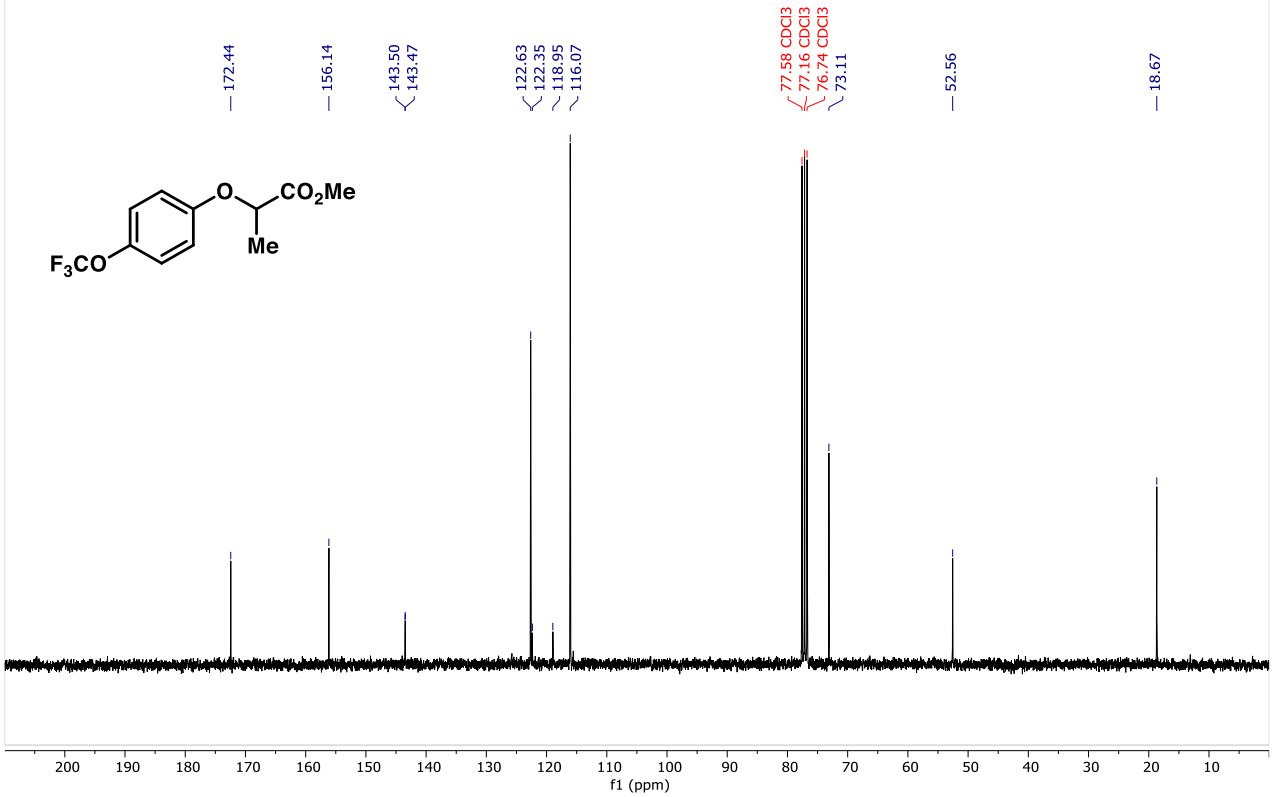

Compound **4f** $^{19}F$ NMR (282 MHz, $CDCl_3$)

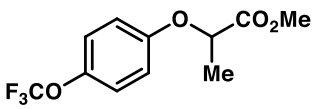

Compound **4g** $^{1}$H NMR (300 MHz, $CDCl_3$)

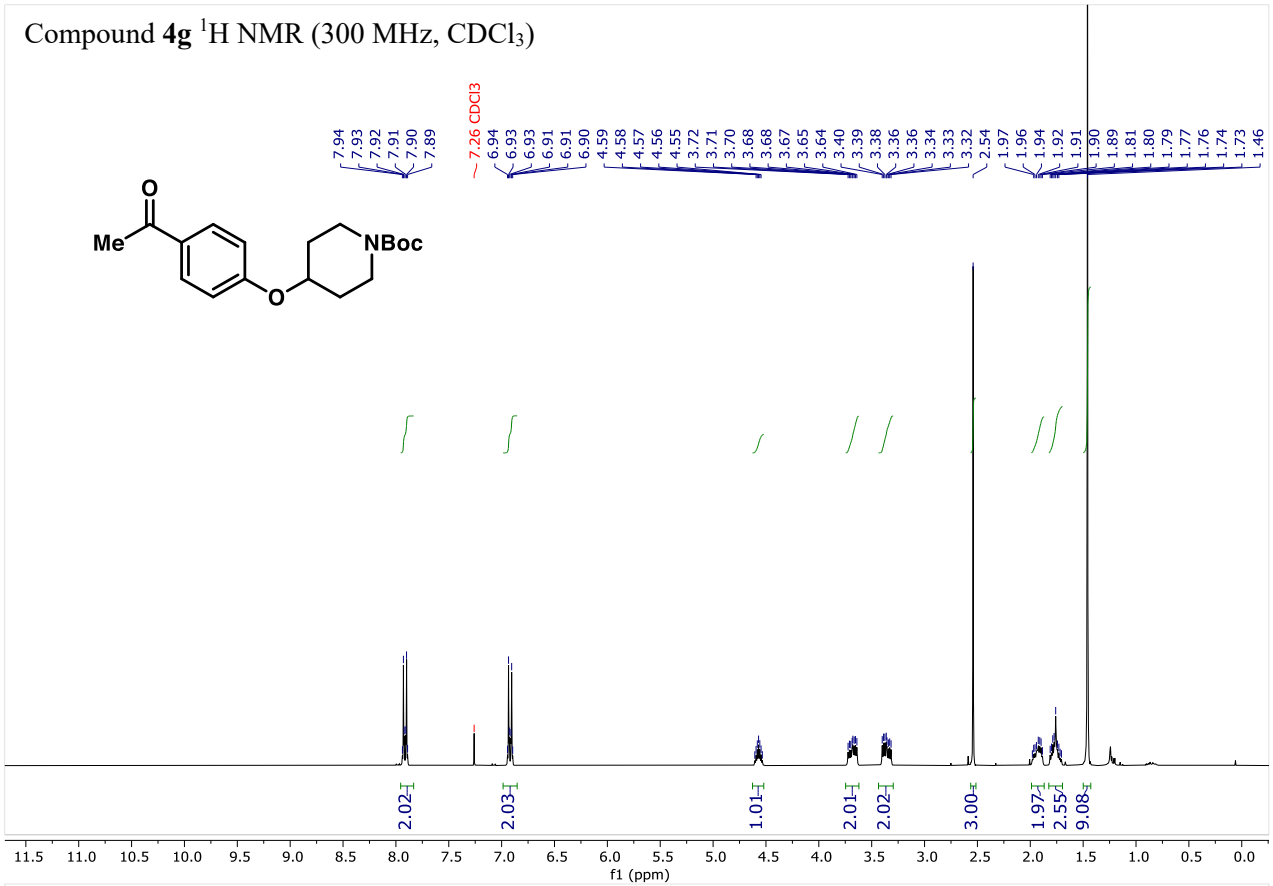


Compound **4g** $^{13}$C NMR (75 MHz, $CDCl_3$)

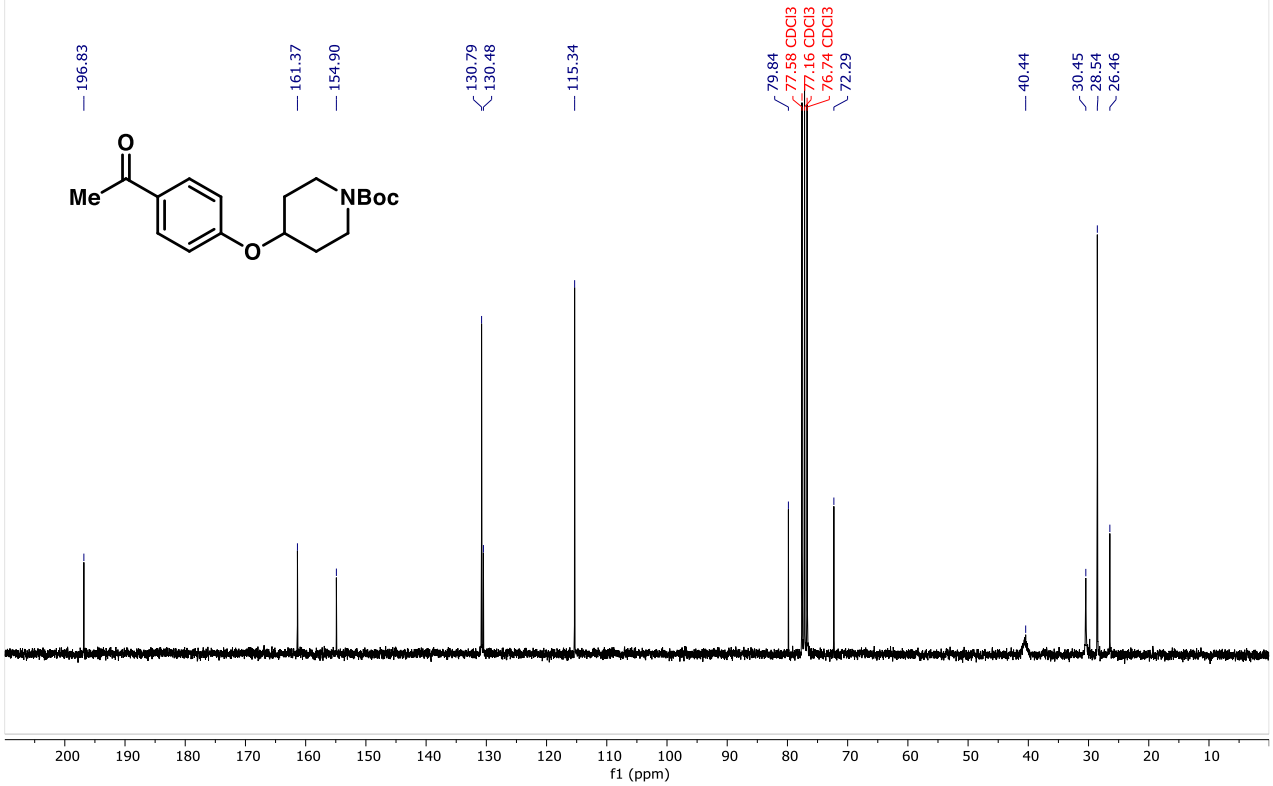

Compound **4h** $^{1}H$ NMR (300 MHz, $CDCl_3$)

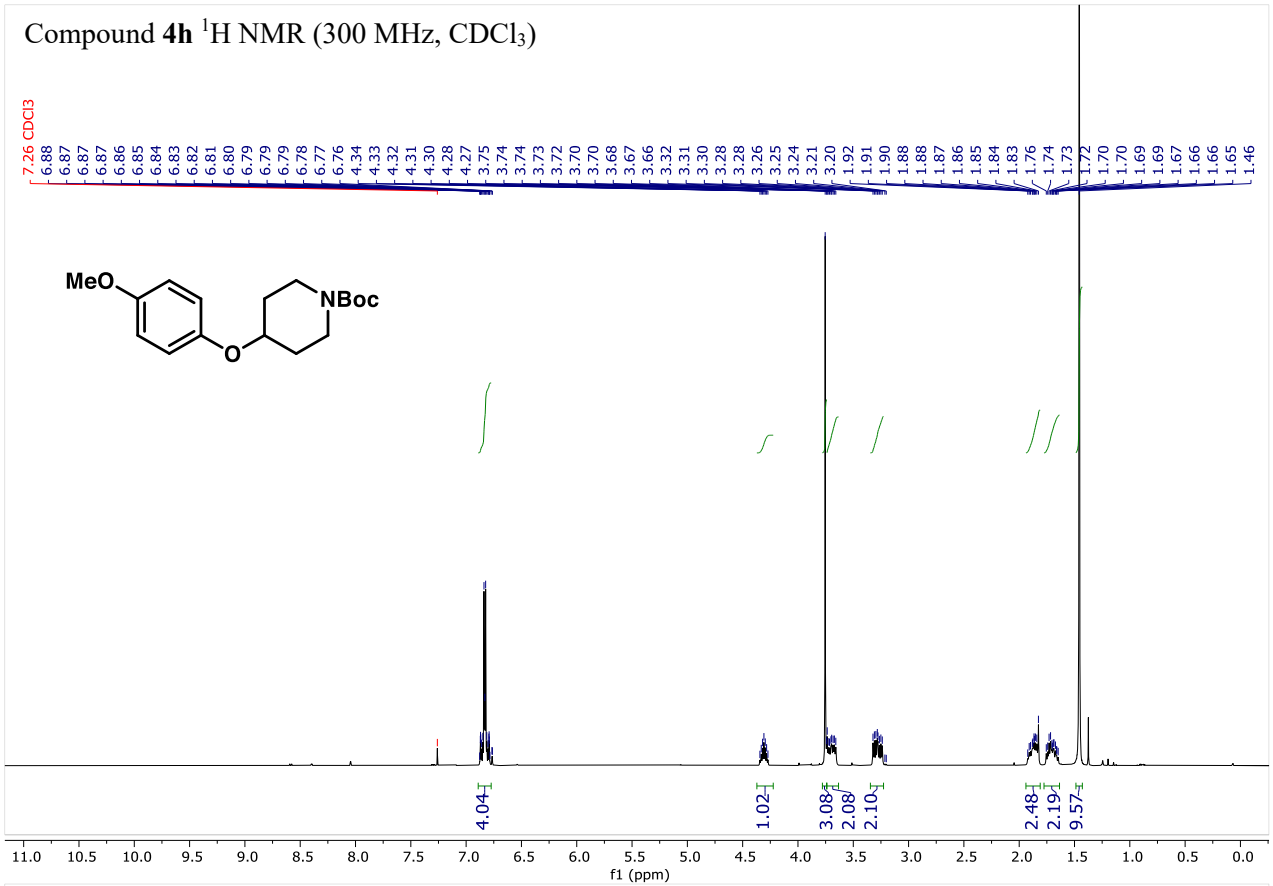


Compound **4h** $^{13}C$ NMR (75 MHz, $CDCl_3$)

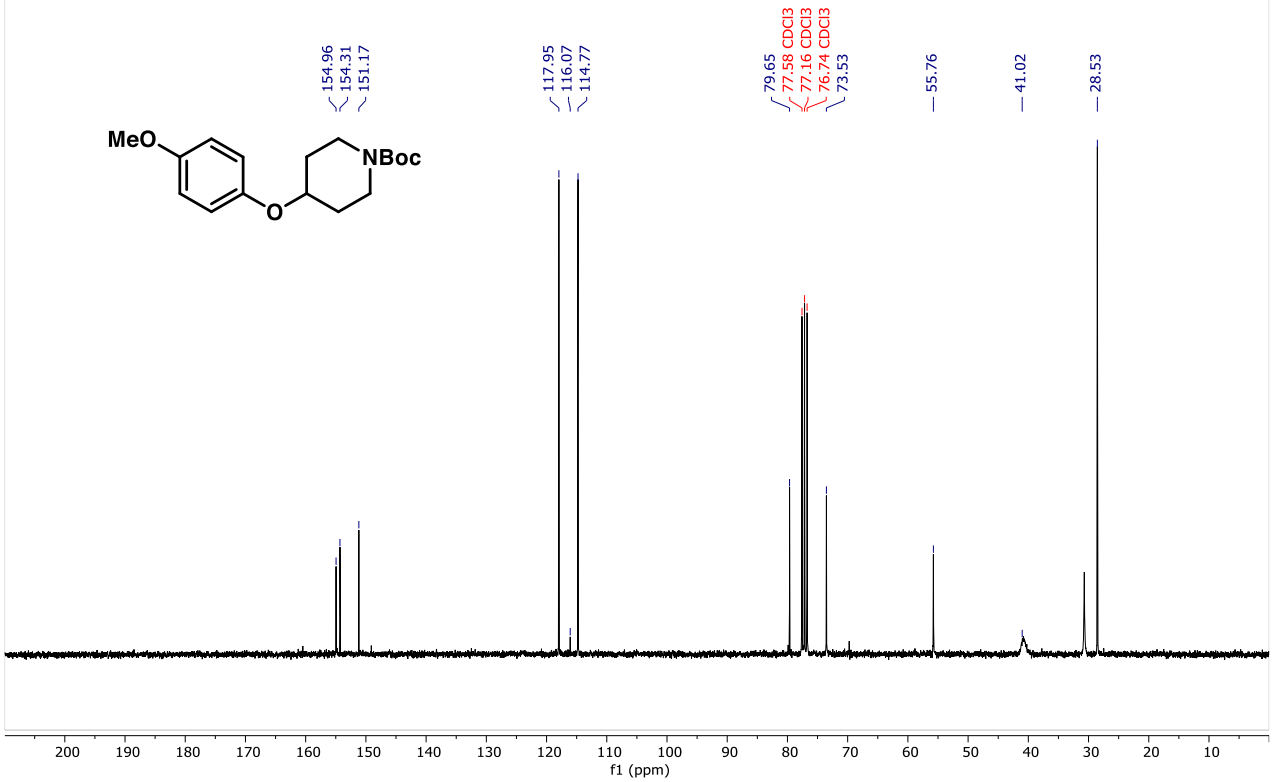

Compound **4i** $^{1}$H NMR (300 MHz, $CDCl_3$)

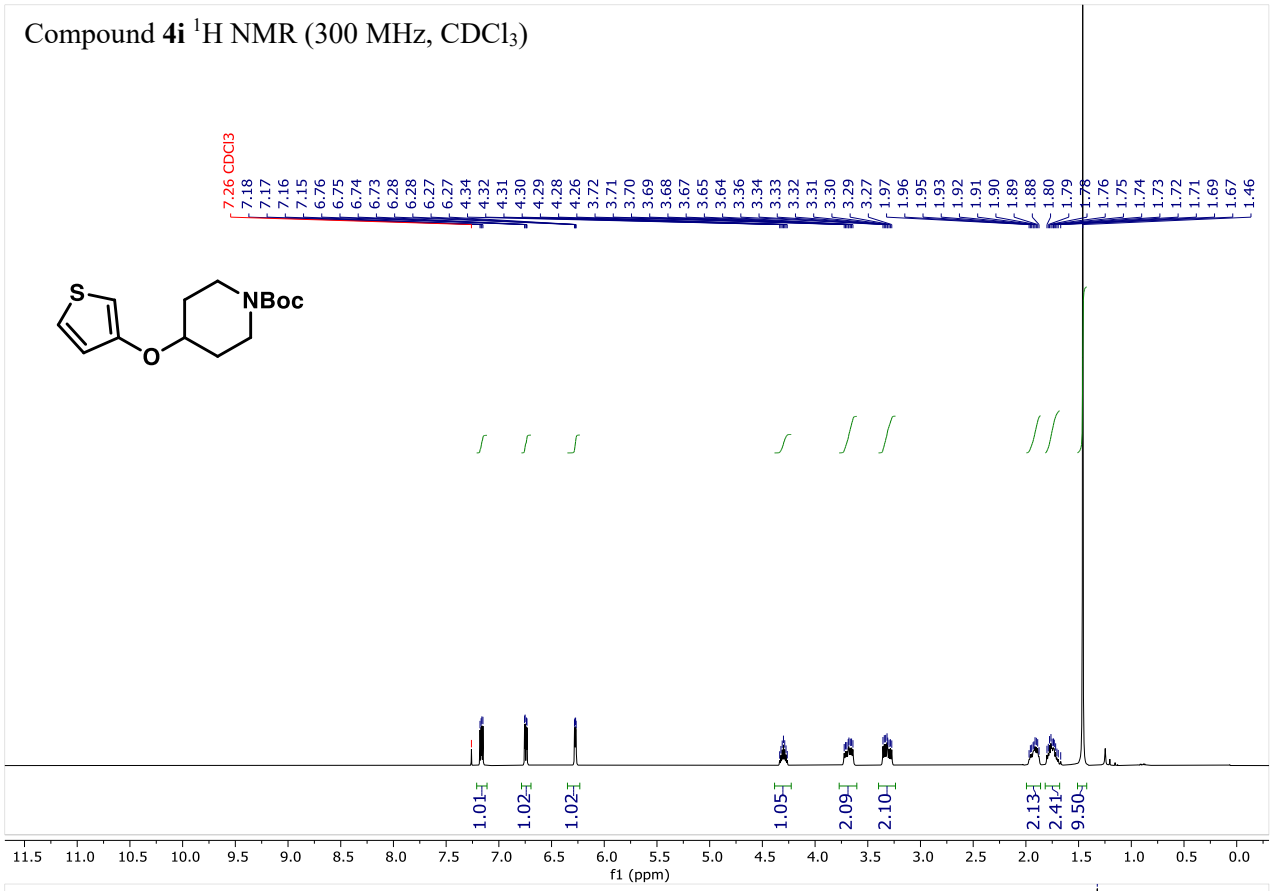


Compound **4i** $^{13}$C NMR (75 MHz, $CDCl_3$)

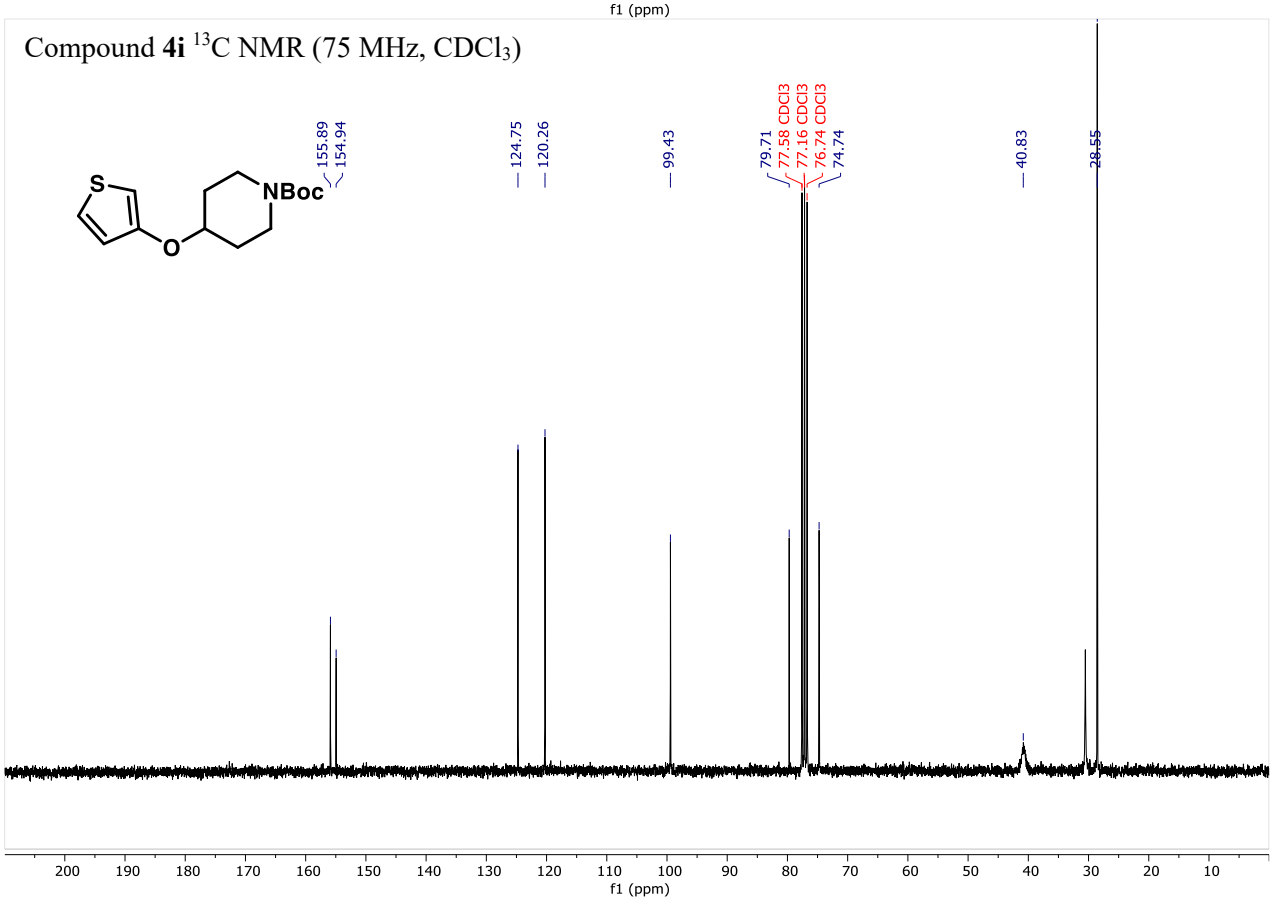

Compound **4j** $^{1}H$ NMR (300 MHz, $CDCl_3$)

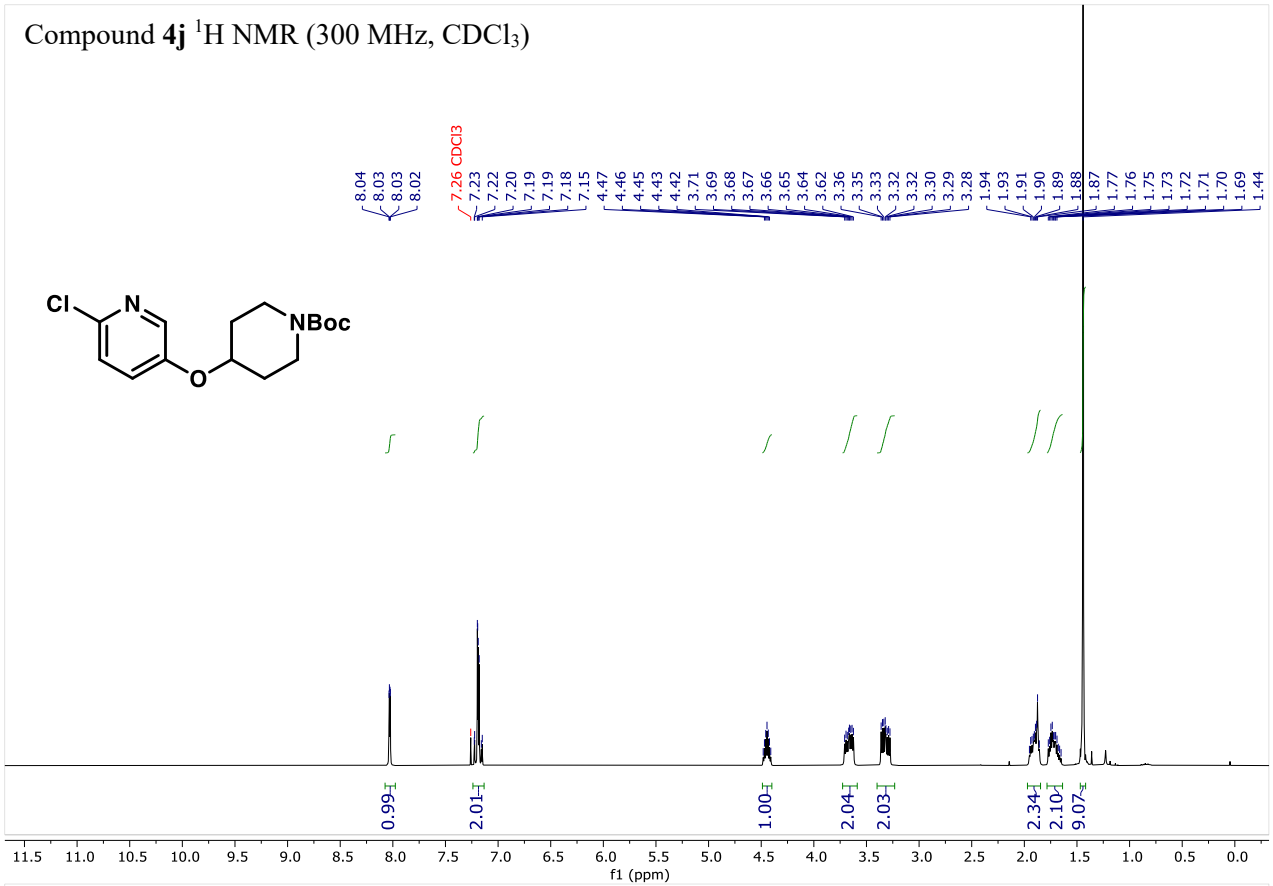


Compound **4j** $^{13}C$ NMR (75 MHz, $CDCl_3$)

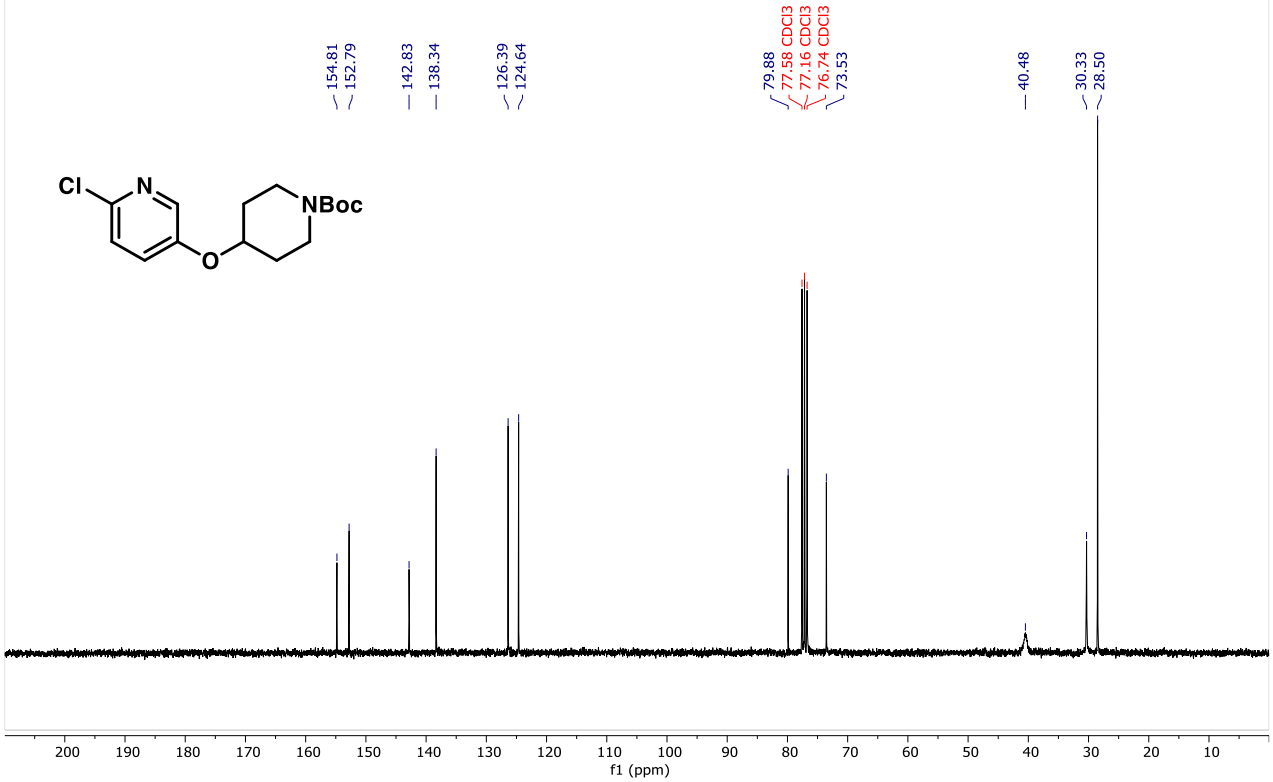

Compound **4k** $^{1}$H NMR (300 MHz, $CDCl_3$)

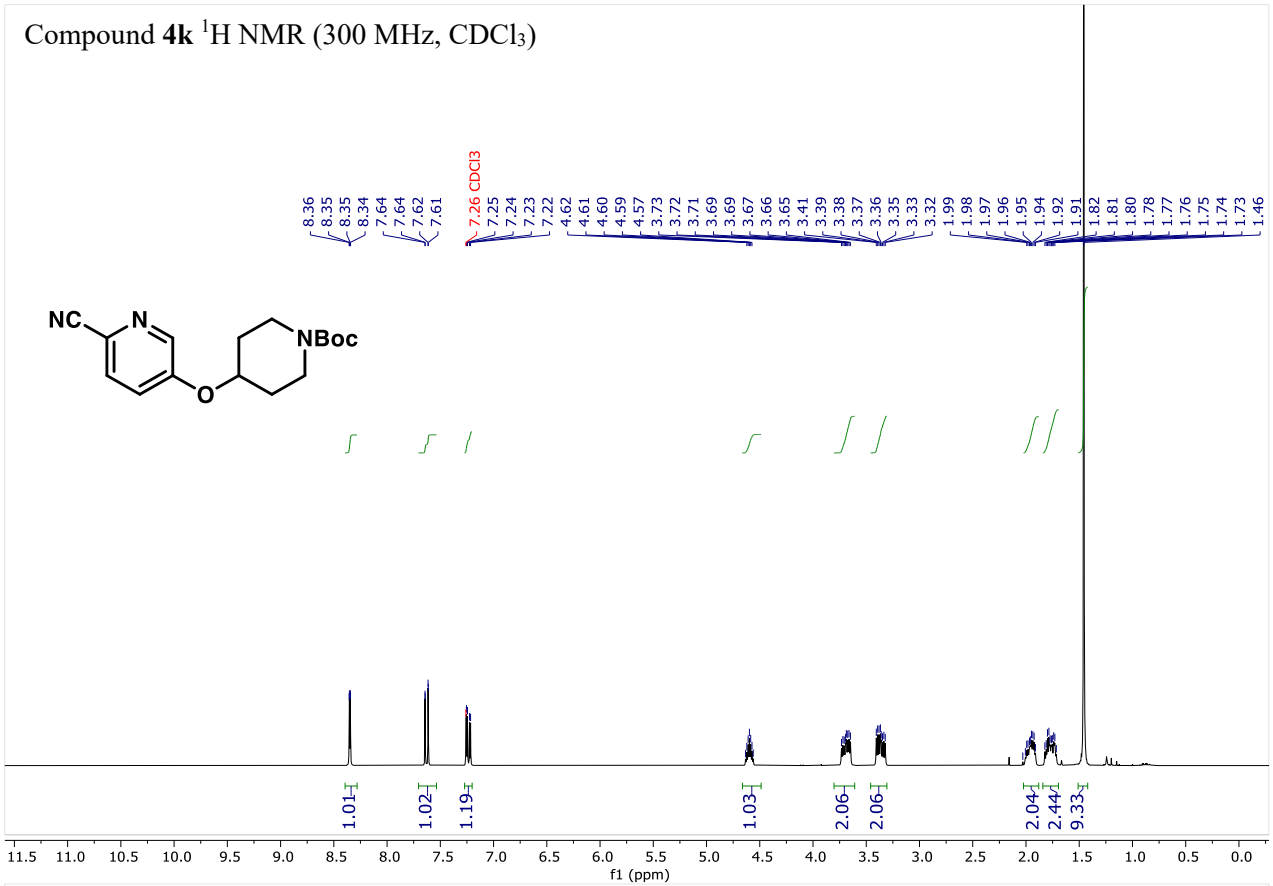


Compound **4k** $^{13}$C NMR (75 MHz, $CDCl_3$)